HEALTH MONITORING OF PRECAST BRIDGE DECK PANELS WITH GLASS FIBER REINFORCED POLYMER BARS

by

Korin McDonald Holden

A dissertation submitted to the faculty of
The University of Utah
in partial fulfillment of the requirements for the degree of

Doctor of Philosophy

Department of Civil and Environmental Engineering

The University of Utah

December 2012

The University of Utah Graduate School

STATEMENT OF DISSERTATION APPROVAL

The dissertation of **Korin McDonald Holden**

has been approved by the following supervisory committee members:

Lawrence Reaveley	, Co-Chair	**July 18, 2012** Date Approved
Chris Pantelides	, Co-Chair	**August 7, 2012** Date Approved
Janice Chambers	, Member	**July 18, 2012** Date Approved
Dan Adams	, Member	**July 18, 2012** Date Approved
Richard Porter	, Member	**July 18, 2012** Date Approved

and by **Chris Pantelides**, Chair of the Department of **Civil and Environmental Engineering**

and by Charles A. Wight, Dean of The Graduate School.

ABSTRACT

Glass fiber reinforced polymer (GFRP) bars are an innovative material that have special properties. One property is their noncorrosive nature that lends itself to being able to replace steel reinforcement in bridge decks; however, GFRP bars have a lower elastic modulus than steel reinforcement contributing to higher deflections unless a greater percentage of reinforcement is utilized. One way to monitor bridge deflections is to instrument the deck panels and check the various measurements. The bridge used in this research was constructed using precast GFRP reinforced deck panels and prestressed concrete girders. The deck panels were monitored throughout the transportation from the precast yard to the bridge by the use of electrical strain gauges. The bridge is instrumented with accelerometers that measure vertical accelerations of the girders, linear variable displacement transducers (LVDT) that measure vertical displacement of the deck panels and vibrating wire strain gauges (VWSG) that measure the strain in the concrete deck panels.

Remote monitoring was done by the use of a secure modem. Data were collected for three purposes. First, lifting strains were measured, analyzed and compared to a finite element model. Collected data from electrical strain gauges were compared to tensile cracking limits. Second, long-term VWSG and LVDT data were recorded and charted to extract strains and deflections. Trucks with a known weight passed over the bridge while strains and displacement data were recorded during testing. Data were interpreted,

analyzed and compared to design requirements. Third, multiple trucks with a known weight and speed passed over the bridge during testing while acceleration data was collected. Research was conducted to determine the impact factor for design, the period of the bridge, structural damping and primary mode shapes.

This research showed that the lifting layout for large GFRP precast panels was successful for crack prevention during transportation and installation. This study recorded a performance history for future use of GFRP bridge decks showing that strain and deflections were well within code limits. Accelerometer data showed that the bridge is dynamically stable and that truck speed and axle weight are the main contributions to the acceleration response of the bridge.

For my Dad

TABLE OF CONTENTS

ACKNOWLEDGEMENTS

The research reported in this dissertation was supported by the Utah Department of Transportation (UDOT). Special thanks to Rebecca Nix at UDOT for providing the research opportunity, information and support. Also, special thanks to Mike Adams of Campbell Scientific and the contributions he has given to this research.

I would like to acknowledge the assistance of Jim Ries and Committee Co-chairs Professors Chris P. Pantelides and Larry D. Reaveley. Additional thanks go to Mark Bryant and the students at the of the University of Utah: Brett Raddon, Erika Weber, Ruifen Liu, Shannon Hansen, Shawn Malan, Zac Jones, Wade Stinson, Dylan Brown, Jonathon Wood and my husband Deric Holden, in the experimental portion of the research. I also would like to acknowledge the contributions of my committee by imparting their knowledge and help: Dr. Porter, Dr. Tikalsky, Dr. Adams and Dr. Chambers.

CHAPTER 1

INTRODUCTION

Utah Department of Transportation would like to be able to design bridges for a 75-year design life, but actual bridge decks have required replacement after 30 to 40 years due to corrosion of the steel reinforcement. These replacements require traffic interruption and great cost. Glass Fiber Reinforced Polymer (GFRP) reinforcing bars are beginning to be used as an alternative to steel rebar in bridge decks because of their noncorrosive characteristics; however there is limited amount of research regarding precast concrete panels for bridge decks fully reinforced with GFRP bars.[1,2]

GFRP bars have not been greatly utilized because there are no long term results on creep, fatigue and long-term loading effects. Additionally, GFRP deck systems will only become more widespread if their long-term performance can be shown to exceed that of conventional materials. Replacing steel reinforcement in bridge decks with GFRP will add sustainability; however, the elastic modulus of GFRP bars is significantly less than that of steel bars which leads to higher deflections and requires a greater percentage of reinforcement. Large deflections lead to cracks and water penetration. In order to determine bridge deflections, monitoring of the dynamic and static loads is required to ascertain the long-term health of the bridge. Because of inadequate information, many States will not use GFRP as a primary reinforcement. Therefore, the need is great to

analyze and test the technology available for increasing the durability of bridge decks and decreasing long term costs in terms of repairs and maintenance.

GFRP bars were used in the building of the Beaver Creek Bridge, located near Price, Utah. The bridge was constructed in two phases. Phase I was completed previously with two lanes, allowing two-way traffic to pass over the bridge while Phase II was being constructed. Phase II construction has two lanes and was instrumented for long term monitoring. This research project specifically focuses on how different loads affect the response and potential long term performance of the bridge constructed in Phase II. The overall span of the bridge is 88 ft-2 in., with an out to out width of 88 ft-10 in. The girders are AASHTO Type IV prestressed beams.[3] The deck was designed in accordance with ACI 440.1 R-06.[4] The design of the deck panels was controlled by estimated crack width and deflection; therefore, bar spacing was reduced by 33% and deck thickness was increased from 8 in. to 9-1/4 in.

In order to reduce construction time and user impacts, this bridge was constructed using 24 precast deck panels with mild longitudinal posttensioning applied transverse to the panel joints to prevent water seepage. Posttensioning consisted of 11 tendons; each tendon is made up of three 0.6 in. Grade 270 low relaxation steel strands that were grouted. In Phase II, two precast panels were instrumented for lifting with electrical strain gauges and with vibrating wire strain gauges for heath monitoring. Additionally, Phase II was instrumented with six linear variable displacement transducers for monitoring static deflections and six accelerometers for monitoring dynamic deflections.

This dissertation presents a performance history for GFRP precast deck panels utilizing long term health monitoring techniques. This should promote the widespread

acceptance of GFRP bars for reinforcing bridge decks; contributions will be explained in the following chapters. Chapter 2 provides a detailed literature review that discusses GFRP bar testing, health monitoring and health monitoring of GFRP deck panels including monitoring of the deck panel lifting.

Next, Chapter 3 discusses monitoring the lifting of the precast panels from the casting yard to the bridge site. Strain data are provided and compared to service limit states as well as a finite element model. The strain data are key to determine if micro-cracking had occurred in the panels while they were being lifted.

Chapter 4 details the loads that were applied to the two precast panels in the bridge that were monitored during posttensioning, truck load testing, and long-term testing using vibrating wire strain gauges. The bridge deck deflections relative to the two diaphragms connecting the prestressed concrete girders were monitored using linear variable differential transformers. The absolute deflection of the girders at midspan was surveyed during a static truck load.

In Chapter 5, the dynamic performance of the girders during a dynamic truck load test are presented. Calculations are preformed to ascertain the structural damping, natural period, dynamic displacement and dynamic allowance limit (impact factor) of the bridge. Lastly, Chapter 6 presents conclusions and suggestions for future research.

1.1 References

1. Benmokrane, B., El-Salakawy, E., El-Ragaby, and A., Lackey, T. 2006. "Designing and Testing of Concrete Bridge Decks Reinforced with Glass FRP Bars." *Journal of Bridge Engineering* 11(2): 217-229.

2. Benmokrane, B., El-Salakawy, E., El-Gamal, and S. Goulet, S. 2007. "Construction and Testing of an Innovative Concrete Bridge Deck Totally Reinforced with Glass FRP Bars: Val-Alain Bridge on Highway 20 East." *Journal of Bridge Engineering* 12(5): 632-645.

3. American Association of State Highway and Transportation Officials. 2009. *AASHTO LRFD Bridge Design Specifications.* 4th Ed.

4. American Concrete Institute. ACI 440.1R-06. 2006. *Guide for the Design and Construction of Structural Concrete Reinforced with FRP Bars*. American Concrete Institute, Farmington Hills, MI.

CHAPTER 2

LITERATURE REVIEW

2.1 Overview

Glass fiber reinforced polymer composites have been used in military and commercial applications since the 1940's.[1] It is only in the last 20 years that GFRP has found its way into civil engineering application in bridges. Testing of concrete members with GFRP bars is ongoing to determine if it is a viable construction material, but there is little long term testing due to the relative "newness" of the product. For civil engineering, electrical glass or E-glass may be used for its nonconductive and noncorrosive properties. Additionally, E-glass is relatively inexpensive. However, GFRP bars using E-glass have a low modulus of elasticity, which may cause concrete members to experience large deflections and require design adjustments. Deflections are a paramount consideration when designing a bridge. This literature review encompasses GFRP bar testing, bridge monitoring techniques and bridge monitoring of GFRP deck panels. The literature will present research on lifting precast panels and dynamic bridge loading; both are important in understanding the health condition of the bridge.

2.2 GFRP Bar Testing

Weber and Baquero[2] simulated long-term strength by aging bars under a wide range of stress levels at elevated temperatures (40°C and 60°C) in a highly alkaline solution for

specific time periods (1000 hours). Bars were then tested in conventional tensile tests. Tests showed that below a 400 MPa threshold stress level, the bars retained about 90% of the virgin strength.

Weber and Baquero also mention that the long-term strength of FRPs depends on the ambient temperature to which the reinforcing bars are exposed and on the number and amplitude of temperature changes over the life of the structure. Therefore, GFRP has been tested for extreme temperatures. Robert and Benmokrane[3] have researched the GFRP matrix and fiber induced to extreme temperatures at a microscopic level. At lower temperatures (0-100°C), the GFRP material properties functioned well; however, at higher temperatures (23°C-315°C) the stiffness and strength properties decreased.

GFRP bond strength to concrete has also been researched under fatigue and freeze/thaw conditions. Pull tests showed that freeze/thaw cycles improved the bond strength by 40%. Fatigue cycles, however, reduced the bond strength by 50%.[4]

2.3 Bridges with Monitoring Instrumentation

Many bridges are monitored for fatigue, cracking, deflection and creep. The Grondals Bridge in Sweden is a concrete box culvert bridge with clear spans of 120 m that experienced cracking. The bridge was strengthened using carbon fiber reinforcement. A linear variable displacement transducer (LVDT) system was installed at that time to assess the integrity of the repaired structure. Readings from the LVDTs were compared to service limit states.[5] Olund and Dewolf[6] monitored three different types of bridges for temperature and vehicle loading using accelerometers, strain gauges, thermocouples and tiltmeters.

In addition to strain gauges, LVDTs and accelerometers, innovative instrumentation that is less evasive is being implemented. Fiber optic sensors (FOS) are suitable for a fully noninvasive method because of their very small dimensions. FOS are used to measurement internal strain, response to thermal variations and static and dynamic loading conditions.[7,8]

Lastly, to health monitor effectively a continuous history has to be recorded. A continuous monitoring system, capable of handling a large number of sensor data channels and video signals would be ideal. Systems can operate online via a high-speed wireless Internet network, allowing real-time data transmission.[9,10]

2.4 GFRP Deck Panels in Bridges with Instrumentation

Bridges in areas with severe climates require deicing salts which, over time, penetrate into the concrete and corrode the steel reinforcement. GFRP bars are useful in bridge decks due to their noncorrosive properties.

El-Salakawy, et al.[11] monitored a bridge deck slab with GFRP bars in Canada; one full span of the bridge reinforced with glass FRP reinforcing bars, while the other span was reinforced with galvanized steel bars. The deck panels were cast-in-place. During construction, a total of 16 fiber optic sensors (FOS) were installed on the top and bottom of the deck in addition to being embedded in the concrete to measure strains. After six months of the bridge in service, the research team positioned two trucks over the girders and measured static strains and displacements. For the single truck load the maximum measured strains in the bottom transverse GFRP and steel bars were 30 and 34 microstrain (με), respectively. For a28-day strength of 4000 psi concrete, the tensile cracking limit is 131 με.

Farhey[12] performed a similar investigation to El-Salakawy using an all-GFRP precast two lane bridge in 1997. Again, stiffness was a critical factor and the code limit used was span/800 for service loads. From a larger set of sensors, a total of 66 monitored continuously: 12 flexural strains at midspan, 12 web vertical compression strains at span ends, 12 bond-line slip at span ends, 18 axial strains at beam bottom flanges, three tilt meters at the deck end, four deck and beam thickness temperature, ambience temperature, and relative humidity sensors. All sensors were slow-response instruments designed to monitor the quasi-static structural state, as opposed to the short-term dynamic response to moving vehicle loads. Data were reported through an automated data acquisition and transmission system since construction began. The data logger was remotely accessed and programmed via a telephone line. The maximum average daily strain oscillations were up to 150 με for most sensors.

Alkhrdaji and Nanni[13] led an investigation of the Walker Avenue Bridge in Rolla, Missouri, a 7.9 m concrete box culvert bridge reinforced entirely with GFRP bars. The bridge was instrumented utilizing three LVDTs. Measured deflections were small, indicating no significant loss of stiffness and minimal cracking. Maximum deflection utilizing a 30.2 kip rear axle load was 0.92 in. Similar studies were modeled using finite elements.[14]

The Canadian Ministry of Transportation[15] has sponsored extensive research into the behavior of composite bridges. In 1997, the Crowchild Trail Bridge in Calgary, Alberta, became the first in the world to have a continuous span steel-free bridge deck. Steel reinforcement was only used at the regions of interior piers and overhanging cantilevers due to evenly spaced transverse steel straps placed across the top of adjacent girders for

lateral restraint to the girders. A total of 103 electrical strain gages, two fiber optic strain sensors, and five thermistors were installed with the new deck in 1997. 20 electrical resistance type strain gages and two Fabry-Perot FOS were installed on the GFRP bars to compare the technologies. In 1997 and 1998, static tests were conducted utilizing nine load cases of two nominally 79.8 kip trucks. 42 girder strains were found to be below 80 με and steel strap strains were below 40 με. Total rebar strain due to mechanical and thermally induced deformation during a 23ºF ambient temperature change was 140 με as measured by the non-temperature compensated FOS, which is comparable to the strain measured during the static load test in the present research. A dynamic amplification factor of 1.15 was observed during dynamic tests conducted under passing truck traffic in the 1998 test.

Similar studies have been conducted using dynamic truck testing and finite element modeling.[16,17,18] Additionally, research has been done for impact factors and girder distribution factors for GFRP precast deck panels.[19,20]

2.5 Lifting Strains

Iowa State University evaluated lifting strains for steel reinforced deck panels on the 24th Street Bridge.[21] The precast deck panels measure 10 ft long x 52 ft-4 in. wide x 8 in. thick. Each of the two steel reinforced deck panels were instrumented with 16 BDI strain gauges. Panel 1 was fully lifted after 40 seconds; as the crane lifted and swung the panel over to the bridge, the strain peaked (68 με) at about 240 seconds. The transverse strain in the center line of the panel, showed the highest strain readings varied from 55 με to 68 με all in tension. The longitudinal gauges varied between 3 με to 40 με all in compression

during the placement of the panel. In general, the strain decreases at locations away from the center of the panels.

Panel No. 2 was monitored and at approximately 63 seconds the panel was fully picked up and the strain at centerline of the panel was at approximately 130 με. At time 441 seconds, Panel No. 2 reached a maximum strain of approximately 230 με and the strain in all the gauges varied from 48 με to 230 με. At approximately 1150 seconds, the panel's leveling bolts were fully resting on the girders.

In Canada, precast concrete GFRP deck panels are being used in forestry bridges; precast saves construction time.[22] The deck panels, composed of random glass fibers, were made stiff at the edges by using an internal arching system to decrease tensile forces. As well as stiffening the panel's edge or including extra reinforcing steel, moving the lift points inward and away from the end of the panel reduce cracking during transportation.[23] In 1989, Mast also addressed the issue of lifting points, suggesting moving them in, a short distance from the ends, thereby increasing lateral stability.[24] It has been noted that shifting the lift points inward increases concrete strength and decreases concrete stresses at prestressing harp points.[25]

Lifting strains are important to monitor because lifting induces cracks in the panels. A cracked panel can still transfer truck loads if the cracks are the size of a hairline. In addition, cracks lead to reinforcement corrosion.[26] Although GFRP bars are non-corrosive, cracks in the concrete are not desirable since they can reduce aggregate interlock and the shear capacity of the deck panels. Lab tests have been conducted with Aslan 100 GFRP No. 5 bars to investigate cracks in concrete beams.[27,28] Under 40% overload conditions, no crack opening behavior was observed.

2.6 References

1. Tang, B., 1997. DOT - Federal Highway Administration Fiber Reinforced Polymer Composites Applications in the USA, Hng-32, Bridge Specialist Group 400 Seventh Street, S.W. Rm. 3203 Washington, D.C.

2. Weber, A., and Baquero, C. W. 2010. "New Durability Concept for FRP Reinforcing Bars Combined durability and creep rupture testing allows for realistic design values." *Concrete International* 31(7): 49.

3. Robert, M., and Benmokrane, B. 2010. "Behavior of GFRP Reinforcing Bars Subjected to Extreme Temperatures." *Journal of Composites for Construction* 14(4): 353-360.

4. Alves, J., El-Ragaby, A., and El-Salakawy, E. 2011. "Durability of GFRP Bars' Bond to Concrete under Different Loading and Environmental Conditions." *Journal of Composites for Construction* 15(3): 249-262.

5. Täljsten, B., Hejll, A. and James, G. 2007. "Carbon Fiber-Reinforced Polymer Strengthening and Monitoring of the Gröndals Bridge in Sweden." *Journal of Composites for Construction* 9(2): 227-235.

6. Olund, J., and DeWolf, J. 2007. "Passive Structural Health Monitoring of Connecticut's Bridge Infrastructure." *Journal of Infrastructure Systems* 13(4): 330-339.

7. Bonfiglioli, B., and Pascale, G. 2003. "Internal Strain Measurements in Concrete Elements by Fiber Optic Sensors." *Journal of Materials in Civil Engineering* 15(2): 125-133.

8. Zhang, B., Benmokrane, B., and Nicole, J. 2003. "Laboratory Evaluation of Fiber-Optic Sensors for Strain Monitoring." *Journal of Materials in Civil Engineering* 15(4): 381-390.

9. Fraser, M., Elgamal, A., He, X., and Conte, J. 2010. "Sensor Network for Structural Health Monitoring of a Highway Bridge." *Journal of Computing In Civil Engineering* 24(1): 11-24.

10. Helmicki, A., Hunt, V., and Nims, D. 2012. "Instrumentation of the Maumee River Crossing." Ohio Department of Transportation Office of Research and Development and the Federal Highway Administration State Job Number 426354

11. El-Salakawy, E., Benmokrane, B., El-Ragaby, A., and Nadeau, D. 2006. "Field Investigation on the First Bridge Deck Slab Reinforced with Glass FRP Bars Constructed in Canada." *Journal of Bridge Engineering* 11(3): 470-479.

12. Farhey, D. 2005. "Long-Term Performance Monitoring of the Tech 21 All-Composite Bridge." *Journal of Composites for Construction* 9(3): 22

13. Alkhrdaji, T., and Nanni, A. 2001. "Construction and Long-Term Monitoring of a Concrete Box Culvert Bridge Reinforced with GFRP Bars." RDT01-016, Center for Infrastructure Engineering Studies, University of Missouri-Rolla.

14. Coogler, K., Harries, K., Wan, B., Rizos, D., and Petrou, M. 2005. "Critical Evaluation of Strain Measurements in Glass Fiber-Reinforced Polymer Bridge Decks." *Journal of Bridge Engineering* 10(6): 704-712.

15. Cheng, J.J., and Van Zwol, T. "Steel Free Bridge Deck: Field Performance and Evaluation." Department of Civil and Environmental Engineering, University of Alberta.

16. P. Alagusundaramoorthy and R. Veera Sudarsana 2008. "Reddy Testing and Evaluation of GFRP Composite Deck Panels." *Ocean Engineering* 35: 287–293.

17. Phillips, K., Harlan, M., Roberts-Wollmann, C., and Cousins, T. "Performance Of A Bridge Deck With Glass Fiber Reinforced Polymer Bars As The Top Mat Of Reinforcement." Department of Civil and Environmental Engineering Virginia Polytechnic Institute & State University.

18. Fu, C., AlAyed, H., Made, A., and Robert, J. 2007. "Field Performance of the Fiber-Reinforced Polymer Deck of a Truss Bridge." *Journal of Performance of Constructed Facilities* 21(1): 53-60.

19. Restrepo, E., Cousins, T., Lesko, J. 2005. "Determination of Bridge Design Parameters through Field Evaluation of the Route 601 Bridge Utilizing Fiber-Reinforced Polymer Girders." *Journal of Performance of Constructed Facilities* 19(1): 17-27.

20. Benmokrane, B., El-Salakawy, E., El-Gamal, and Goulet, S. 2007. "Construction and Testing of an Innovative Concrete Bridge Deck Totally Reinforced with Glass FRP Bars: Val-Alain Bridge on Highway 20 East." *Journal of Bridge Engineering* 12(5): 632-645.

21. Wipf, T., Phares, B., Bigelow, J., Hosteng, T., and Nadermann, A. 2010. "Evaluation of the 24th Street Bridge Institute for Transportation." Iowa State University, IA.

22. Laszlo, G., and Imper, R. 1989. "Handling and Shipping of Long Span Bridge Beams." *PCI Journal* 34(6): 86-101.

23. Seguirant, S. 1998. "New Deep WSDOT Standard Sections Extends Spans of Prestressed Concrete Girders." *PCI Journal* 43(4): 92-119.

24. Mast, R. F. 1989. “Lateral Stability of Lone Prestressed Concrete Beams.” *PCI Journal* 34(1): 35-53.

25. Mufti, A., Bakht, B., and Newhook, J. 2004. “Precast Concrete Deck Slabs for Slab-on-Girder System: A New Approach.” *ACI Structural Journal* 101(3): 395-402.

26. Benmokrane, B., El-Salakawy, E., Desgagné, G., and Lackey, T. 2004. “FRP Bars for Bridges.” *Concrete International* 26(8): 84-90.

27. Zou,Y., and Huckelbridge, A. 2007. “Experimental Crack Growth in GFRP Reinforced Concrete.” *Journal of Bridge Engineering* 12(2): 246-255.

28. Benmokrane, B., El-Salakawy, E., El-Ragaby, A., and Lackey, T. 2006. “Designing and Testing of Concrete Bridge Decks Reinforced with Glass FRP Bars.” *Journal of Bridge Engineering* 11(2): 217-229.

CHAPTER 3

LIFTING STRAINS IN PRECAST CONCRETE GLASS FIBER REINFORCED POLYMER DECK PANELS

3.1 Abstract

The Beaver Creek Bridge on US Highway 6 is a pilot project for Glass Fiber Reinforced Polymer (GFRP) posttensioned bridge decks in the State of Utah. The Utah Department of Transportation has decided to evaluate GFRP reinforcing bars as an alternative to steel rebar in this bridge deck to increase their lifespan. The precast deck panels were posttensioned in the longitudinal direction to reduce water penetration into the deck panel joints and lifted from below at four points using straps and cables instead of embedded anchors. The panels were lifted in three stages to transport them from the precast yard to the bridge: (i) lifting out of the formwork, (ii) lifting onto the truck, and (iii) lifting onto the bridge. Two concrete panels were instrumented with 28 electrical gauges. Strain data was compared to theoretical ultimate concrete strains to determine whether tensile cracking had occurred. Deflections of the panel were calculated using the finite element model. During all lifting stages, the panels exhibited acceptable levels of deflections and strains, and there was no cracking observed. Experimental strain measurements showed that they were below cracking limits. The lifting method was successful and is recommended for precast panels constructed with GFRP bars.

3.2 Introduction

The Utah Department of Transportation (UDOT) has the goal of increasing the lifespan of bridges as well as to decrease user delays with the use of accelerated bridge construction. In addition, research utilizing corrosion resistant materials which decrease scheduled maintenance, is currently being carried out. Construction of the Beaver Creek Bridge, approximately 20 miles north of Price, Utah on US-6 was completed in 2009. The precast bridge deck was constructed using Glass Fiber Reinforced Polymer (GFRP) bars instead of traditional steel reinforcing bars. The GFRP bars have a lower elastic modulus than steel bars which leads to larger deflections and possible cracking. The single span bridge is composed of 12 AASHTO Type IV prestressed girders.[1] The bridge has an overall span length of 88 ft-2 in. and an out-to-out width of 88 ft-10 in.

The deck was designed in accordance with ACI 440.1 R-06[2], and constructed using 24 precast bridge deck panels in two phases. Phase I was constructed previous to 2009 with two lanes, one lane each way. Phase II construction began in July, 2009 using pre-cast girders and deck panels. The construction was completed with a cast-in-place, three-foot closure pour; the closure pour couples both sections thereby creating a more stable bridge which links the 12 panels of Phase I to the 12 panels of Phase II. The closure pour couples the deck response due to traffic and reduces the dynamic response. Phase II bridge deck panels measure 41 ft-5 in. long, 6 ft-10 in. wide and 9¼ in. thick, as shown in Figures 3.1 and 3.2. The design 28-day concrete compressive strength was to be 4000 psi; at the time of lifting, the concrete deck panel strength had increased to 6200 psi.

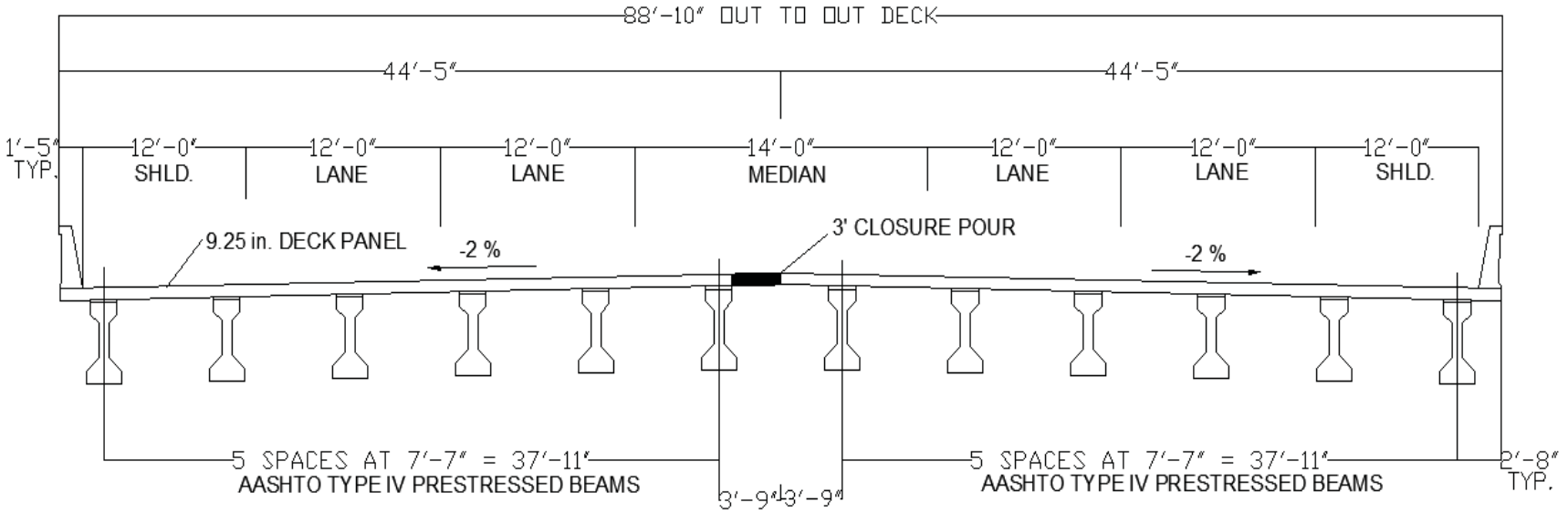

Figure 3.1. Elevation of Beaver Creek Bridge showing deck and girders

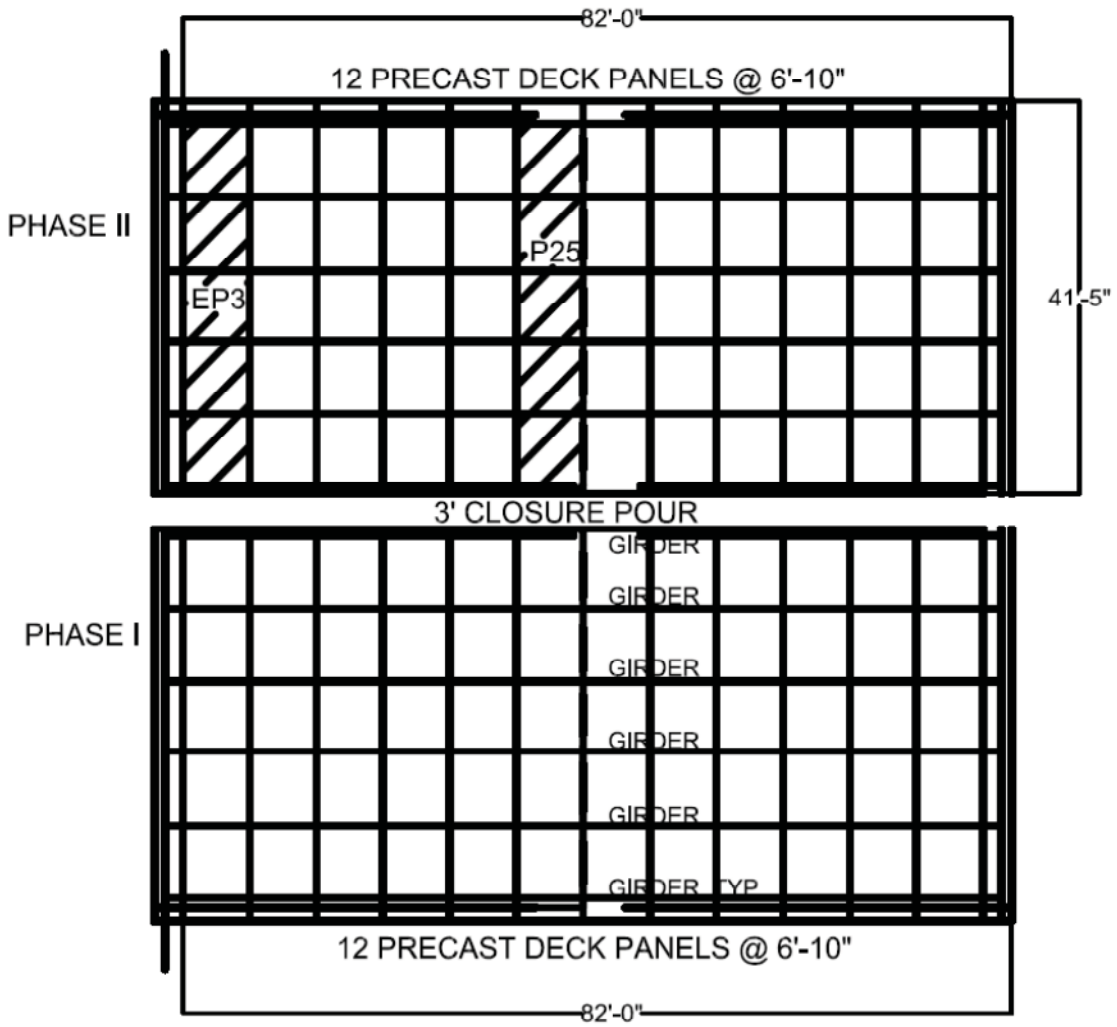

Figure 3.2. Plan view of Beaver Creek Bridge showing prestressed girders and deck panel

Figure 3.3 shows the double mat of #5 GFRP bars with a spacing of 4 in. in the longitudinal direction; matching bars were used for the closure pour. Figure 3.4 shows panel EP3 before the parapet was cast and the GFRP bars extending from the concrete for three feet to construct the closure pour between the bridge deck and the approach slab.

The panels were cast in Pleasant Grove, Utah, transported 64 miles to the bridge site and lifted into place. Each panel was lifted a total of three times. In the first lift the deck panel was removed from the formwork; at this time the panel did not have a parapet. A second lift placed the panel with the parapet on the truck trailer that transported it to the bridge. The final lift placed the panel and parapet on top of the girders at the bridge site.

Traditionally, embedded anchors are attached to reinforcing bars. The deck was lifted using straps instead of embedded anchors to decrease the shear forces transferred to the GFRP bars.[3] Additionally, GFRP was used to resist corrosion; steel coils and embeds would allow a potential path for corrosion. Lastly, these precast panels were the longest UDOT had used and wanted to add precautionary measures by lifting from below. From a construction point of view, lifting from below takes the same effort and time as lifting from embeds or steel coils. However, there was a learning curve for maneuverability of the panels. Lifting was monitored by strain gauges located at 46 in. and 202 in. from the back of the parapet, represented by arrows in Figure 3.5. For each lift, the panels were lifted at four points from below with cables attached to steel HSS 4 in.x4 in. tube sections and straps, as shown in Figures 3.6-3.8. The PCI Handbook was referenced for lifting point locations; however, there is currently no requirement for lifting from below a GFRP reinforced panel.[4] This is a new lifting procedure for panels reinforced with GFRP bars;

Figure 3.3. GFRP bar layout with bars extended for the closure pour

Figure 3.4. Panel EP3 at the precast yard with approach slab reinforcement on the right

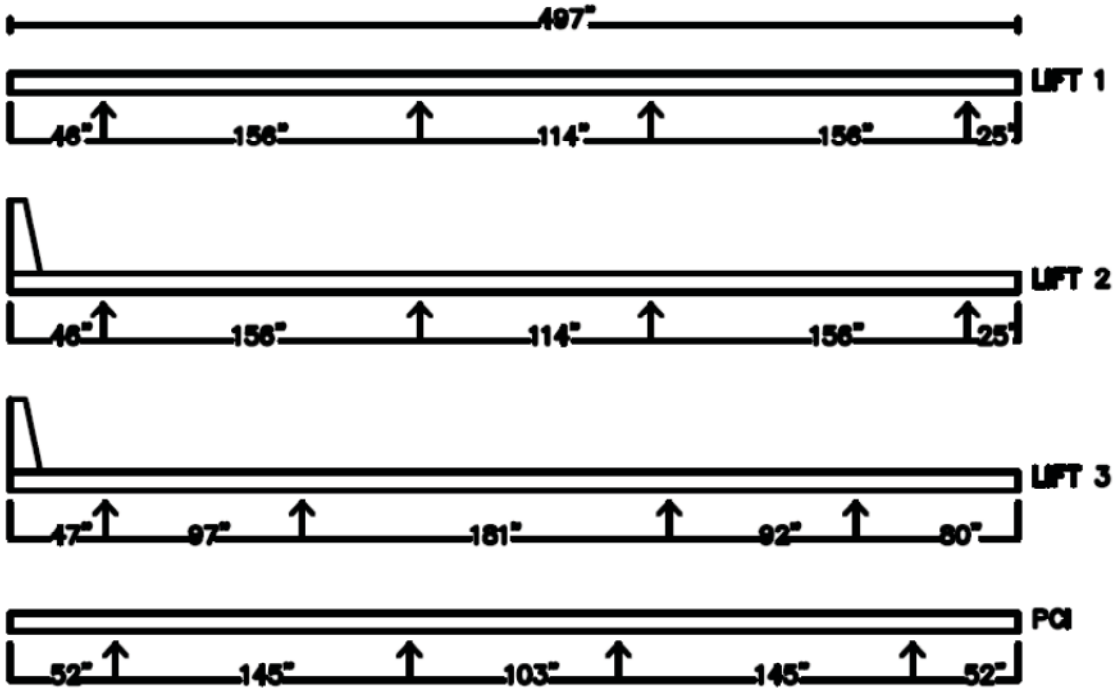

Figure 3.5. Lifting point diagram

Figure 3.6. Panel lifting using HSS 4x4 steel tubing attached to 1” diameter steel cables

Figure 3.7. First lift out of the forms at the casting yard

Figure 3.8. Third and last lift at the bridge including parapet

hence, strains of the panels for various lifting arrangements were studied. Lifting strains are important to monitor because the process of lifting may induce large deflections and cracks in the panels. Cracks may lead to reinforcement corrosion.[5] Although GFRP bars are noncorrosive, cracks in the concrete are not desirable since they can reduce aggregate interlock and the shear capacity of the deck panels.

3.3 Experimental Data

Panels EP3 and P25, shown in Figure 3.2, were instrumented with 28 electrical strain gauges during lifting and transportation. These gauges were attached directly to both the top and bottom GFRP reinforcing mats and recorded the strains in the bars; strain data was collected using dataloggers. Of the 28 gauges, 20 were placed in the transverse direction of the bridge (longitudinal direction of the panel) to record strains in the long dimension of the panel during lifting. The remaining eight gauges were placed in the span direction of the bridge to record posttensioning strains in the short dimension of the panel. For crack monitoring, the 20 gauges placed in the transverse direction of the bridge are used for the analyses presented in this research. Figure 3.9 provides a more detailed sketch of the locations of the strain gauges. Electrical strain gauges were chosen due to their high sampling rate potential, relatively low cost and overall simplicity.

3.3.1 First Lift

Panels P25 and EP3 were lifted out of the forms on July 27th and August 6th 2009, respectively. The lifts occurred before the parapets had been cast. The maximum strain profile for half of the length of panel P25 is shown in Figure 3.10 with tension taken as positive; strain gauge pair distances are measured from the back of the parapet (Figure

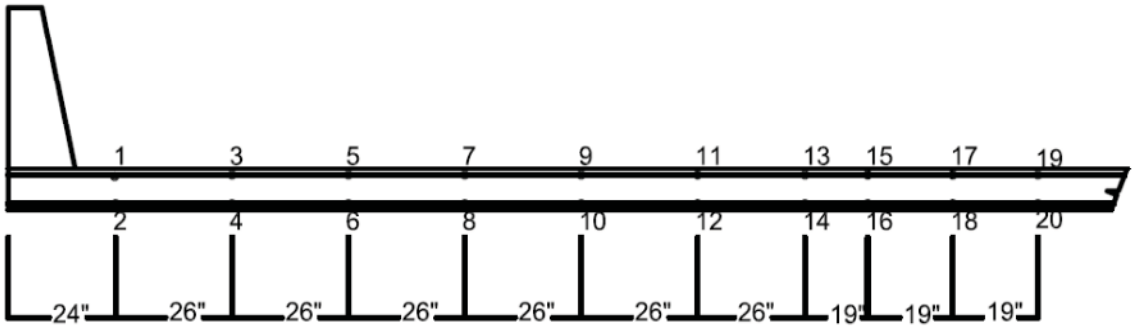

Figure 3.9. Electrical gauge locations for both panels and lift points

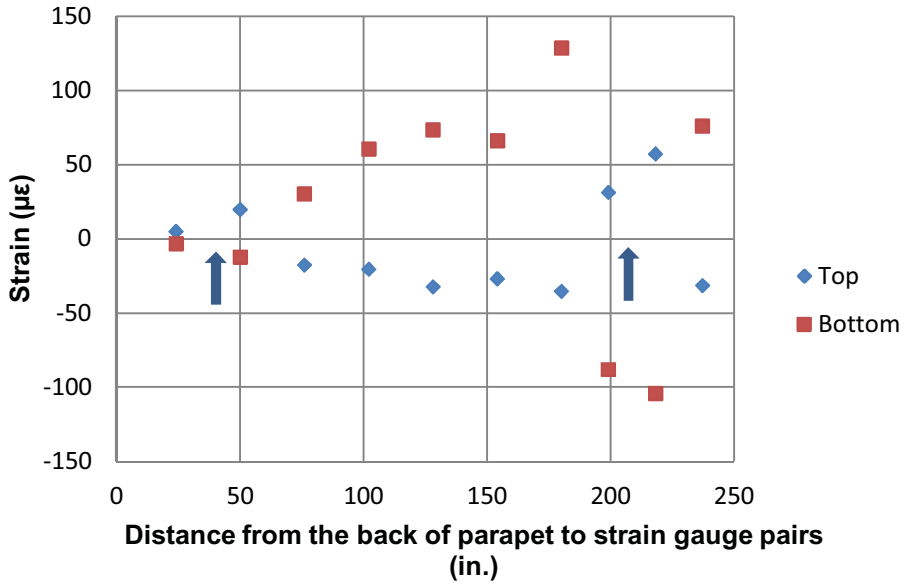

Figure 3.10. Strain Profile for P25 during its first lift removing it from the formwork

3.9). From the graph, the maximum tensile strain in the bottom mat is 128 microstrain (με) while the maximum tensile strain in the top mat is 57 με. These strains are smaller than the theoretical tensile strain of 138 με that would cause cracking. The tensile cracking limit is obtained by using Equations (3.1-3.3), where f_r represents the modulus of rupture[6], and E_c represents the elastic modulus of concrete. The lifting points are located at 46 in. and 202 in. from the back of the parapet, and are represented by arrows. Panels were notched at 47 in., 144 in., 325 in. and 417 in. to allow for strap removal for Lift 3 after the panel was located at its permanent position on the bridge deck.

$$f_r = 7.5\sqrt{f_c'} \tag{3.1}$$

$$E_c = 57000\sqrt{f_c'} \tag{3.2}$$

$$\varepsilon_{cr} = \frac{f_r}{E_c} \tag{3.3}$$

3.3.2 Second Lift

The panels were transported from the precast yard to the bridge site on September 3rd, 2009. The transportation process involved two lifts (referred to as Lifts 2 and 3), and a 64 mile journey on a flatbed trailer. Before the second lift, the parapets had been cast. The collected data from this day are limited to the first thirteen strain gauges from each panel (Figure 3.9). The maximum strain profile during the second lift for half the panel is shown in Figure 3.11; the maximum tensile strain in the bottom mat was 5 με while the maximum tensile strain in the top mat was approximately 15 με. These strains are significantly lower than the tensile cracking strain.

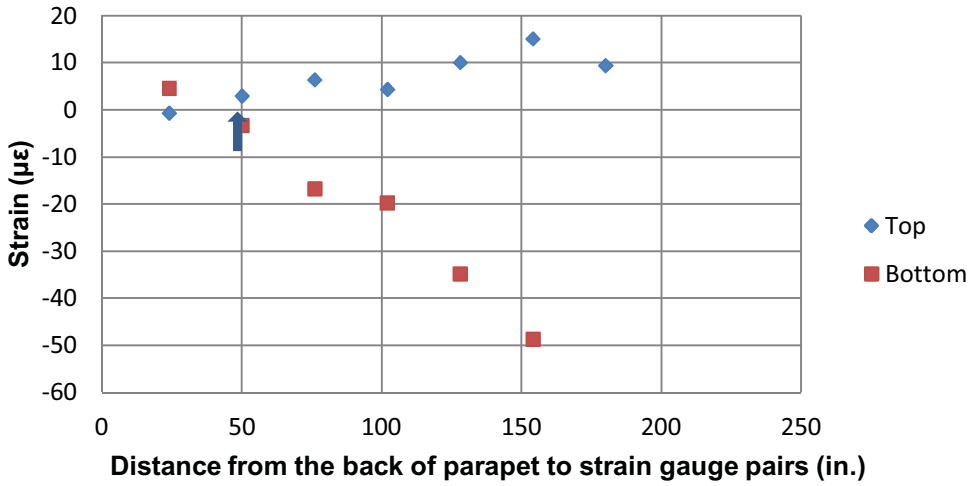

Figure 3.11. Strain Profile for panel EP3 during its second lift

3.3.3 Transportation

The panels were placed on trucks for a 64-mile journey to the bridge site. The maximum and minimum of all strains during transport are shown in Figure 3.12. During transport of panel EP3, careful observations were made and correlated to the strains on the graph.

The maximum strain for the entire day did not surpass 60 με in either tension or compression. Observations made during the day panel EP3 was moved to the bridge site are shown in Figure 3.12 and the following stages are noted: (1) The second lift, placing the panel on the truck; (2) Truck is stationary while panel is strapped down and straps are tightened resulting in slight increase in strain; (3) Truck begins to move through the precast yard; (4) Truck is stationary while waiting to get on the freeway; (5) Truck travels the 64 miles to the bridge site and vibration is evident; (6) Truck arrives at the bridge site and remains stationary until it is unloaded; (7) Truck maneuvers the construction site and moves into position; (8) Tie-downs are removed and (9) Panel is lifted onto the bridge and into place with straps.

3.3.4 Third Lift

The maximum strain profile during the third lift is shown in Figure 3.13. The third lift occurred directly after the transportation of the panel. The straps were slipped out after the panels were placed on the girders. From Figure 3.13, one can see that the maximum tensile strain in the bottom mat is 37 με while the maximum tensile strain in the top mat is 18 με.

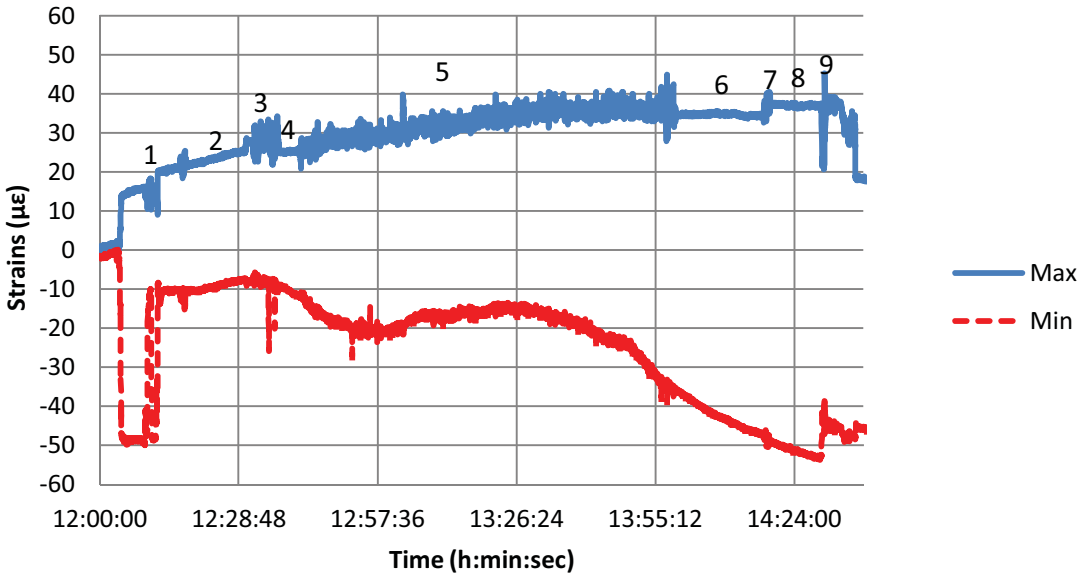

Figure 3.12. Maximum and minimum of all gauges during transport of panel EP3

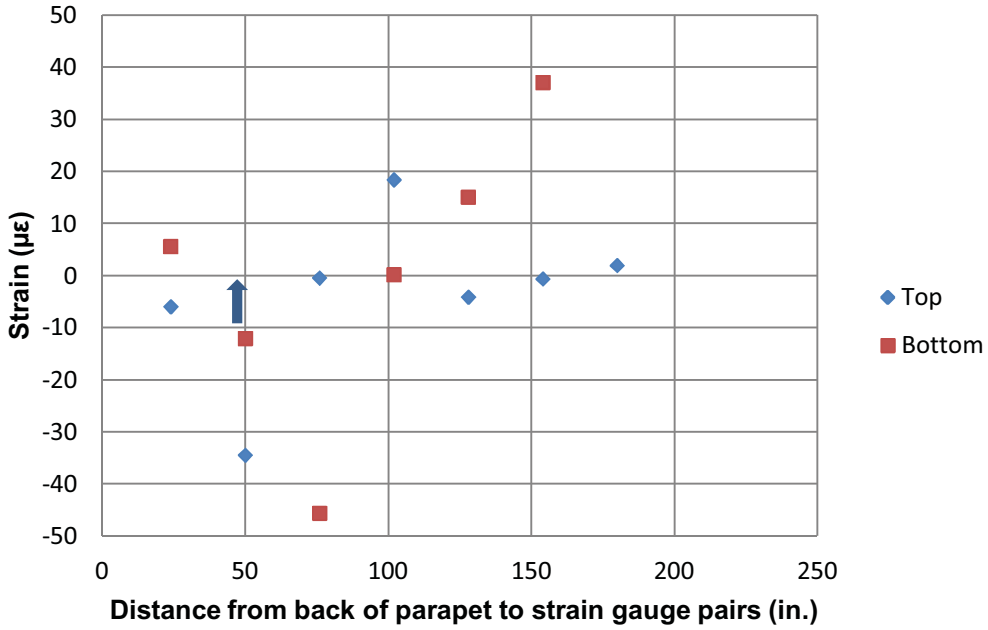

Figure 3.13. Strain profile for EP3 during its third lift

3.4 Analytical Results

From the recorded strains during lifting, the curvature of the panel was determined using Equation (3.4), where "ε" is the strain recorded and "$|d - d'|$" is the distance between the top and bottom reinforcement mats.

$$\varphi_{measured} = \frac{\varepsilon_{top} - \varepsilon_{bottom}}{|d - d'|} \quad (3.4)$$

The measured curvature diagram from the first lift of EP3 is shown in Figure 3.14. Instrumentation was only attached to half the panel; therefore, only two of the four lifting points are included in the curvature diagram. The curvature under the first lifting point at 46 in. is 1.2×10^{-6} /in. The curvature under the second lifting point at 202 in. is 2.5×10^{-5} /in.

3.5 Finite Element Modeling

The three panel lifts, shown in Figure 3.5 marked Lifts 1-3, were modeled as five-layer composite area elements of concrete and GFRP reinforcement in the finite element program.[7] The GFRP was modeled as extruded area shell elements and made up two of the five layers. Lifting devices were modeled as undeformed cables and supporting frame elements. Deflections obtained from the FEM analysis are compared to the AASHTO code limit of span/800 or 0.62 in.; the span for the deck panels is 479 in. The AASHTO code limit was used for lifting because the panels would later be monitored continuously for more than two years in service at the bridge; the code limit needed to be consistent throughout the entire research. The calculated deflection of the panel while it was resting on the ground supported by four HSS pipes was a maximum of 1.66×10^{-3} in. as shown in

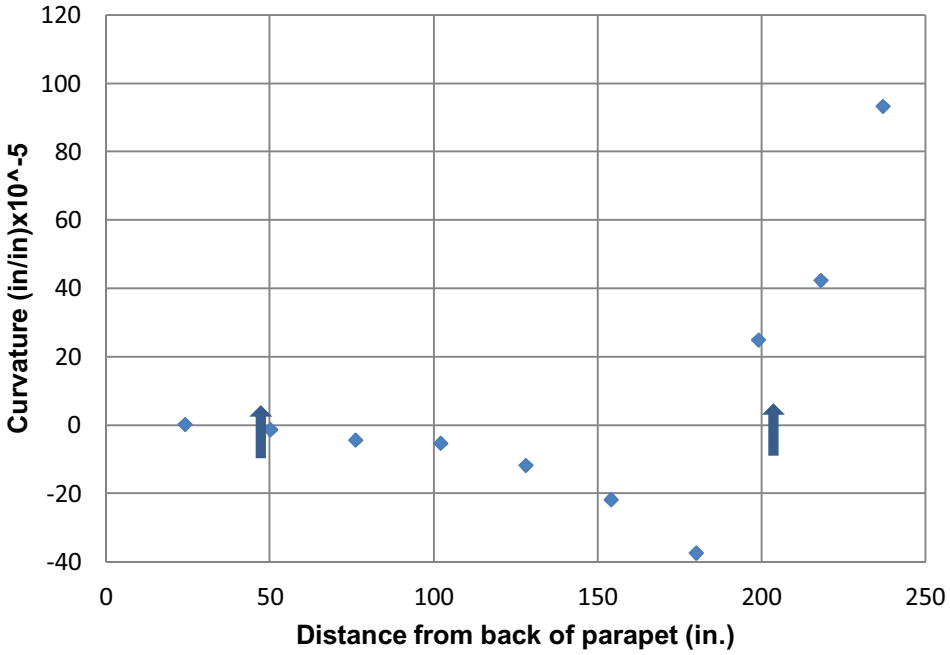

Figure 3.14. Curvature diagram for Lift 1 of EP3

Figures 3.15-3.16. Maximum tensile strains are also reported from the FEM analysis to compare with the tensile cracking limit in the deck panels of 138 με, per ACI 318 and Equation (3.3). Stresses were modeled at the top and bottom surface of the concrete; stresses were then converted to strains by dividing by the elastic modulus of the concrete. However, the gauges measuring the strain data were located on the GFRP bars, 1.5 in. below the top and bottom surface of the panels. Therefore, a more accurate bottom tensile strain of 12 με at the gauges is shown in Figure 3.17 and Figure 3.18. The calculated top and bottom maximum tensile stresses of the panel on the ground were 43 psi and 79 psi as shown in Figure 3.17 with tensile strains also shown in Figure 3.18 for comparison with experimental data.

In Lift 1, the panel system was modeled with four, 1- in. diameter A990 grade steel cables lifting the panel without the parapet from the formwork using two steel beams, as shown in Figure 3.5. The connections from the cables to the frame that was used to lift the panels were modeled as pins, free to rotate. The maximum tensile stress on the top of the slab while in air was 19 psi with a corresponding strain of 4 με shown in Figures 3.19-3.20. The maximum tensile stress on the bottom of the slab while in air was 129 psi with a corresponding strain of 29 με shown in Figures 3.21-3.22.The maximum deflection in air was 0.035 inches, shown in Figures 3.23-3.24. The curvature was plotted with a maximum of 6.18×10^{-5} in./in. as shown in Figure 3.25. The model did not correlate well with collected data shown in Figure 3.14 because it is difficult to simulate in the finite element model the bond between the panel and the bottom of the formwork being broken prior to total panel weight distribution to the lifting cables.

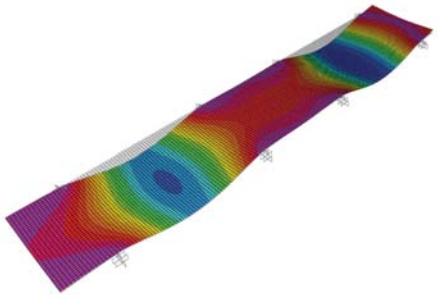

Figure 3.15. Deflected panel with a maximum deflection of 0.00166 in.

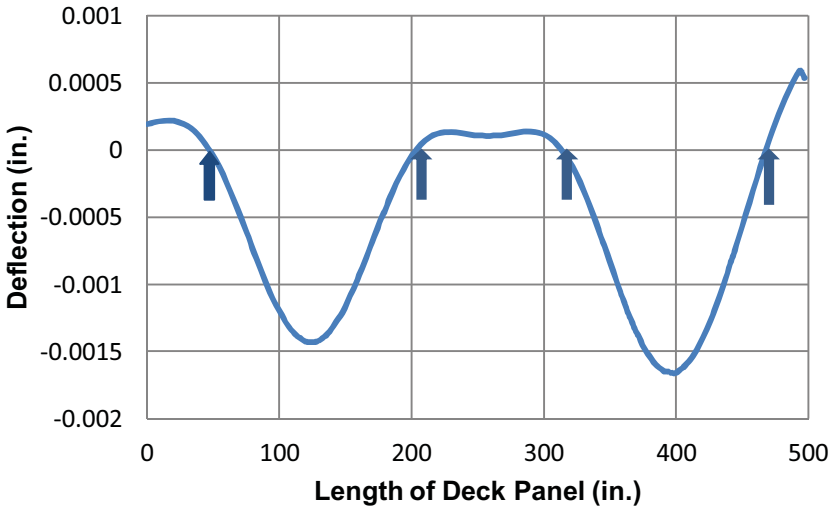

Figure 3.16. Midline displacement for panel sitting on the ground

Figure 3.17. Maximum bottom tensile panel stress of
79 psi in the panel and 217 psi at supports

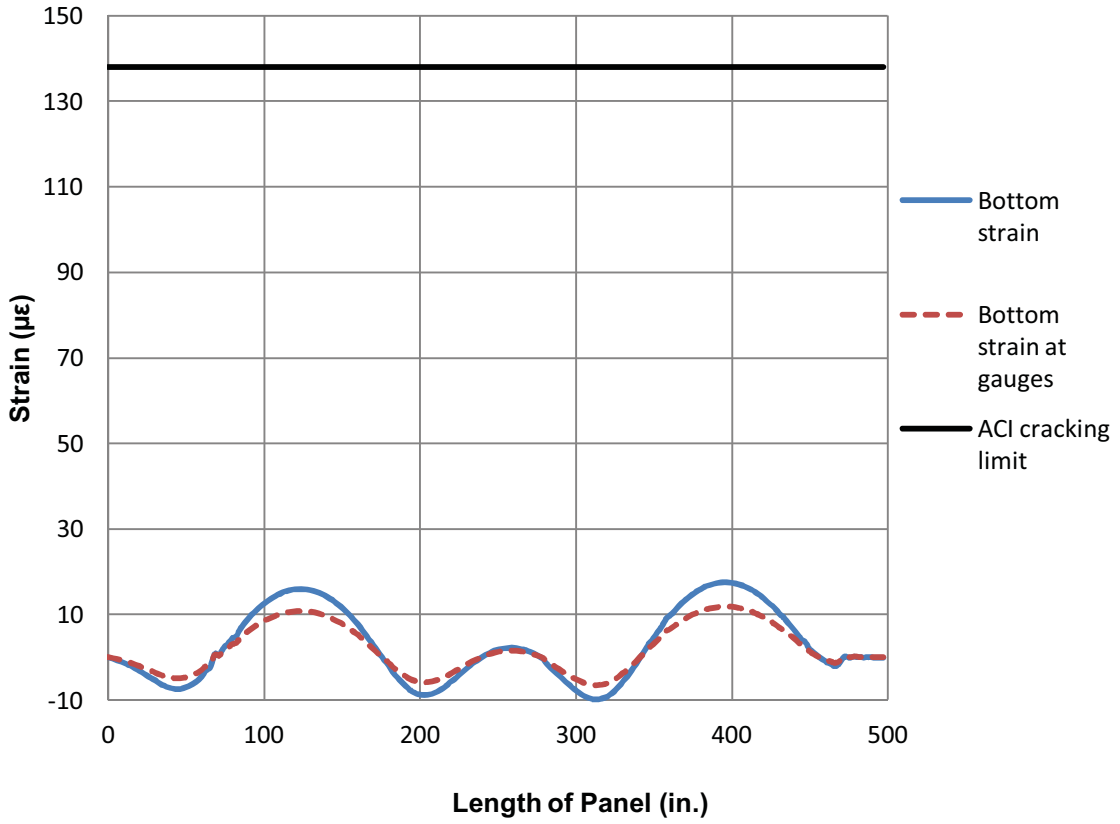

Figure 3.18. Mid-line bottom tensile strains of panel while on ground

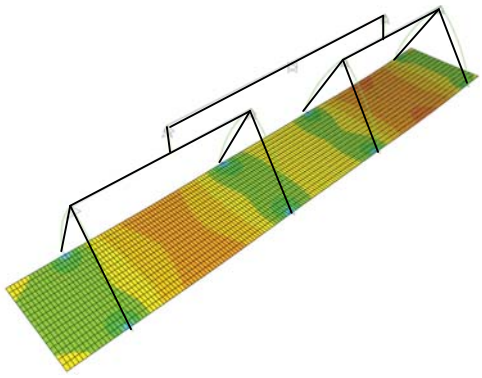

Figure 3.19. Maximum tensile stress of 19 psi at the top of deck panel while lifting-Lift 1

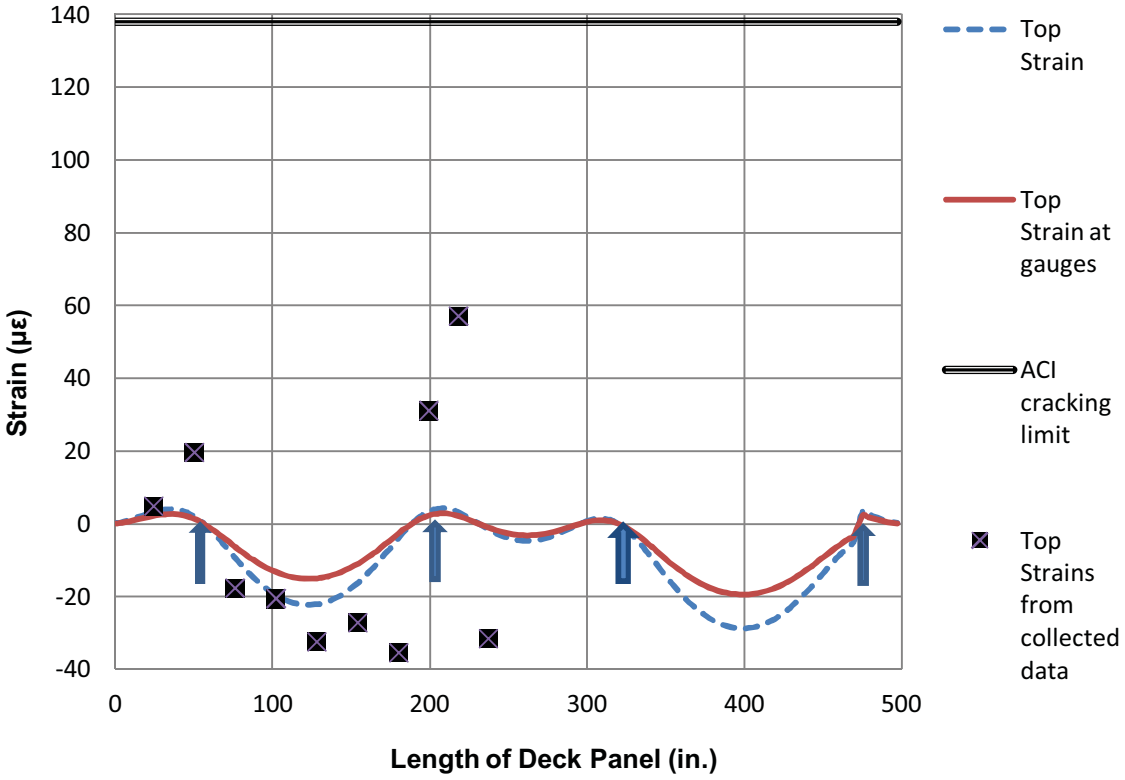

Figure 3.20. Mid-line top strain without parapet- Lift 1

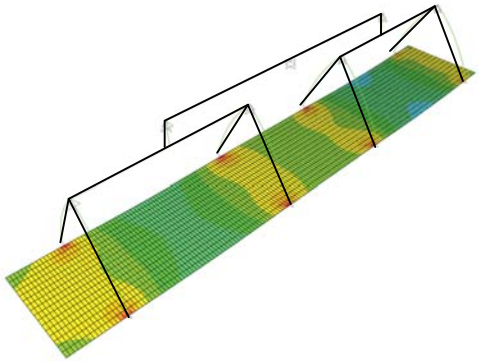

Figure 3.21. Maximum tensile stress of 129 psi at the bottom of deck panel while lifting- Lift 1

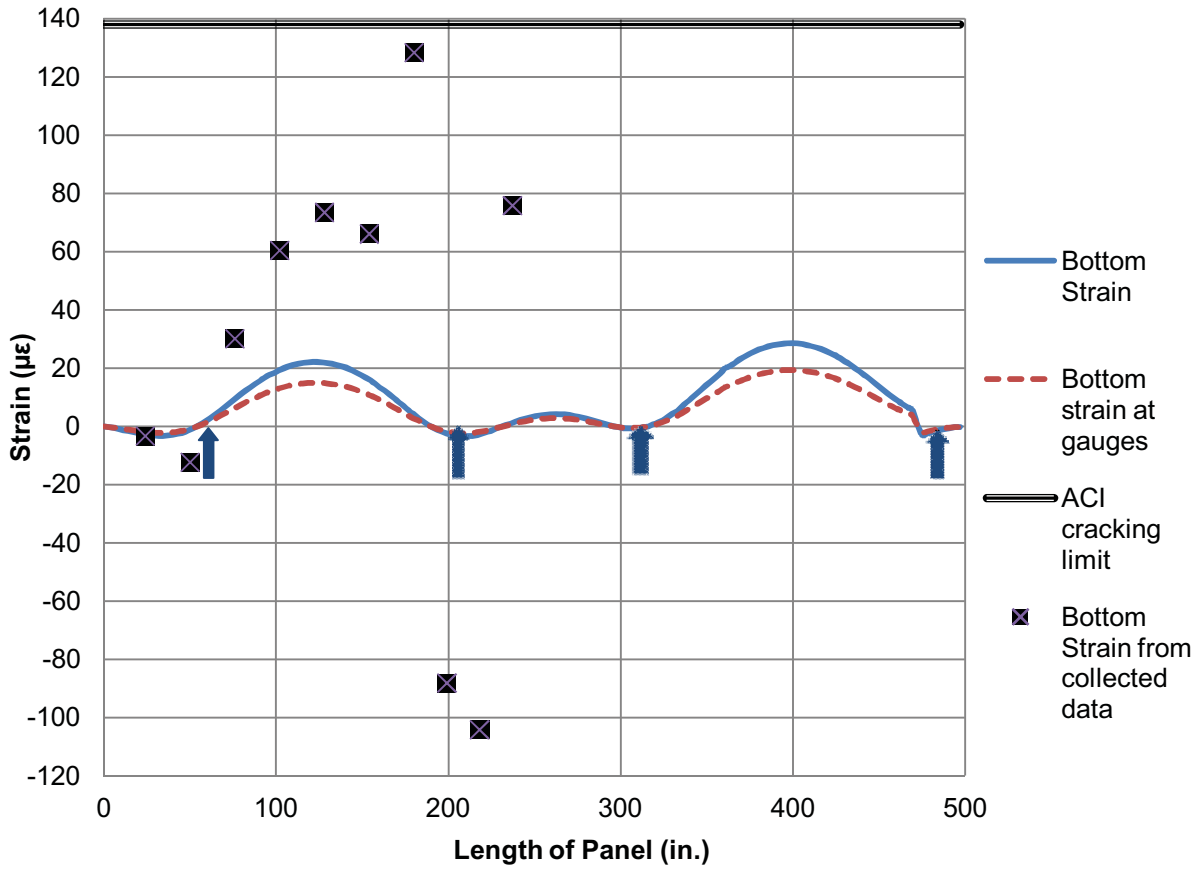

Figure 3.22. Mid-line bottom strain without parapet- Lift 1

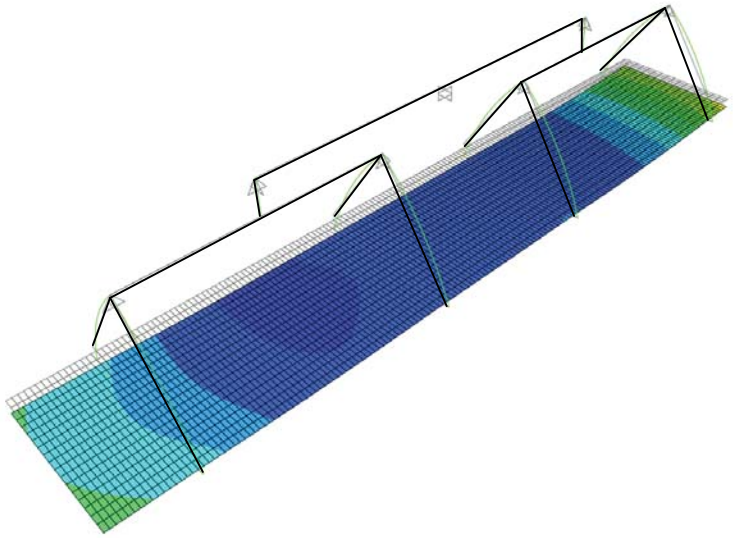

Figure 3.23. Deflected panel with a maximum midline deflection of 0.035 in.- Lift 1

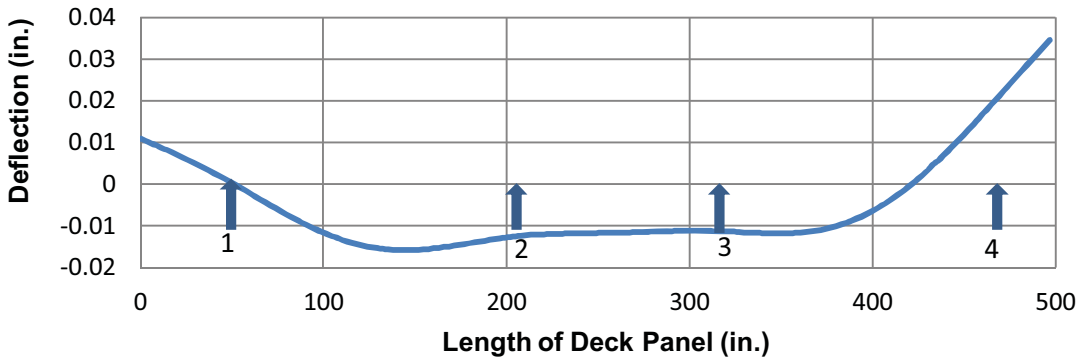

Figure 3.24. Midline displacement for panel lifting without the parapet- Lift 1

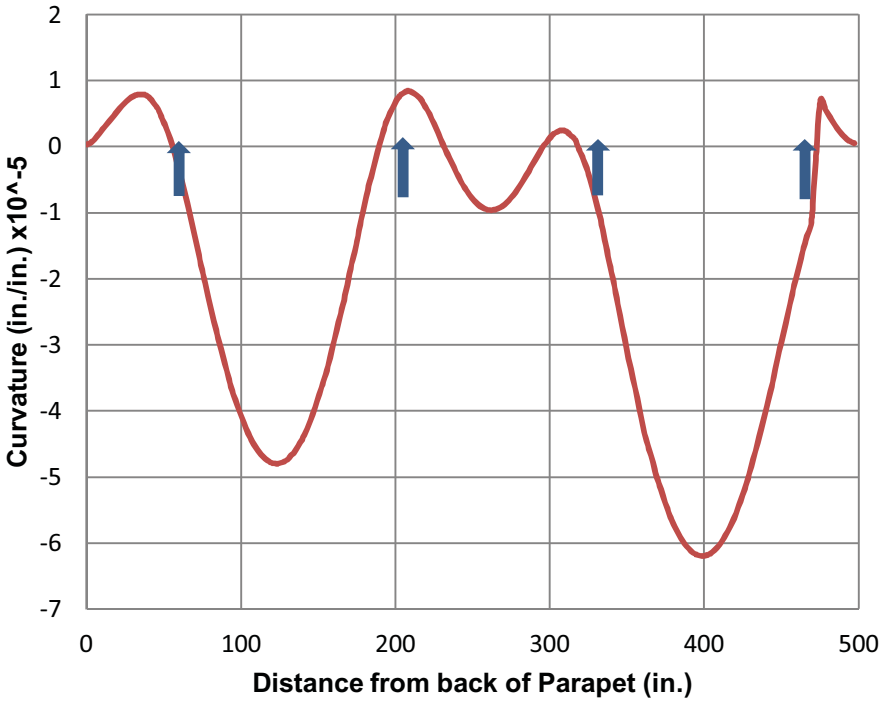

Figure 3.25. Curvature for panel lifting without the parapet- Lift 1

Lift 2 was modeled with cables lifting the panel with the parapet on the left side of the panel, as shown in Figure 3.5. The parapet was modeled as an equivalent distributed load placed at the end of the panel. The maximum tensile stress on the top of the slab while in air was 125 psi with a corresponding midline strain of 28 με, as shown in Figures 3.26-3.27. The maximum tensile stress on the bottom of the slab while in air was 127 psi with a corresponding midline strain of 28 με, as shown in Figures 3.28-3.29. The maximum deflection in air was -0.12 inches, as shown in Figures 3.30-3.31.

Lift 3 was modeled with straps lifting at the revised pick point locations and the parapet, as shown in Figure 3.5. The parapet was modeled as an equivalent distributed load placed at the end of the panel. The connections from the straps to the truss were modeled as pins, free to rotate. The maximum tensile stress on top of the slab while in air was 146 psi with a corresponding midline strain of 33 με shown in Figures 3.32-3.33. The maximum tensile stress on the bottom of the slab while in air was 61 psi with a corresponding midline strain of 14 με shown in Figures 3.34-3.35. The maximum deflection in air was -0.10 in. shown in Figures 3.36-3.37; the AASHTO design limit for deflection is 0.62 inches.

In the design of the bridge, the deflection of the panel relative to the girders was calculated using the HL-93 truck load and the deflection equation from ACI 440.1R-06. The deflection of the deck relative to the girders due to positive live load moment was calculated as 0.10 in. The AASHTO design limit is 0.625 in. of deflection and a tensile cracking strain of 138 με.

Lift 3 was modeled for a parametric study of lifting points, investigating if fewer pick points would have met the AASHTO design requirements. Strains and deflections were

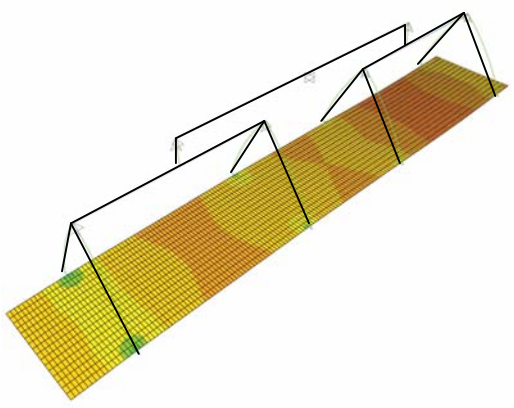

Figure 3.26. Maximum tensile stress of 128 psi at the top of deck panel while lifting- Lift 2

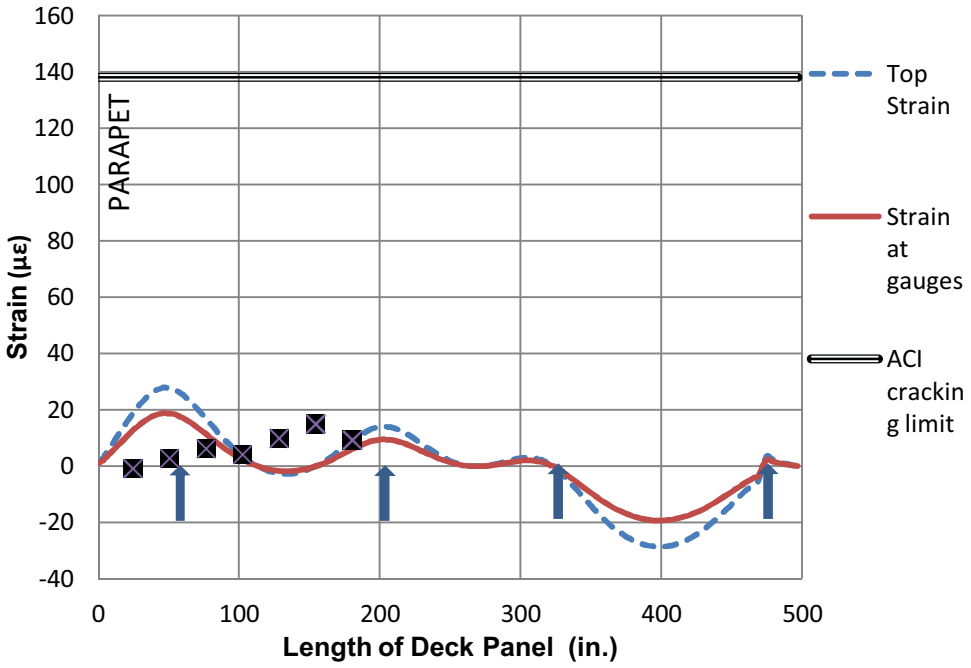

Figure 3.27. Midline strains of top of deck panel while lifting- Lift 2

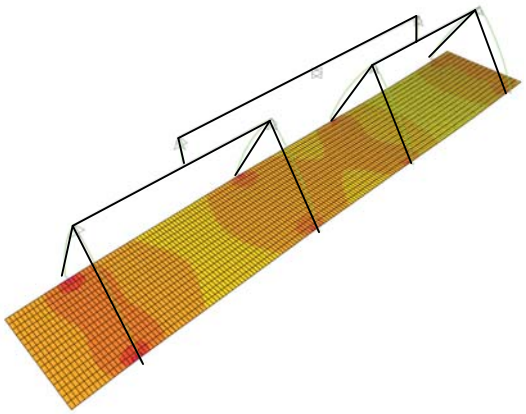

Figure 3.28. Maximum stress of 127 psi (tension) at the bottom of deck panel while lifting- Lift 2

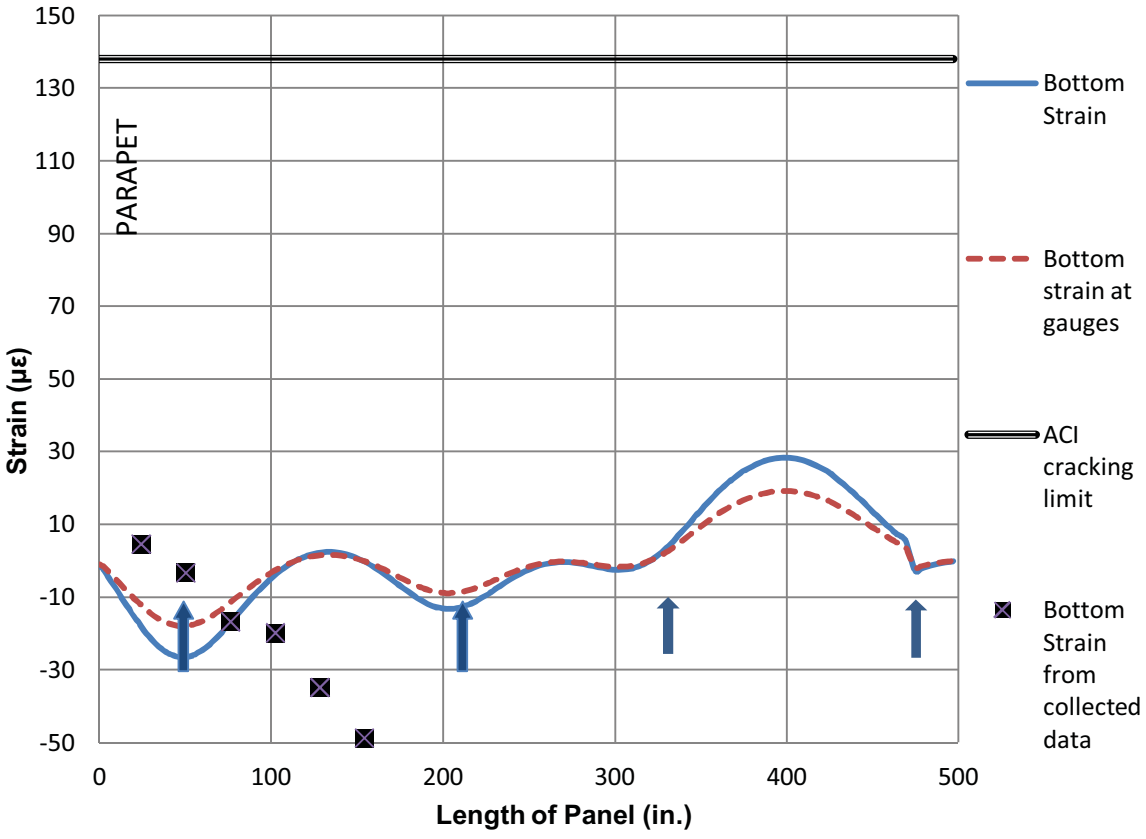

Figure 3.29. Midline strains of bottom of deck panel while lifting- Lift 2

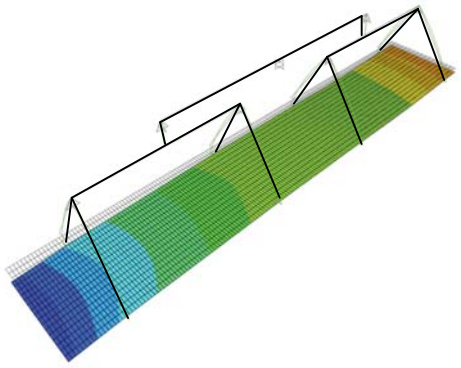

Figure 3.30. Deflected panel with a maximum midline deflection of -0.12 in.-Lift 2

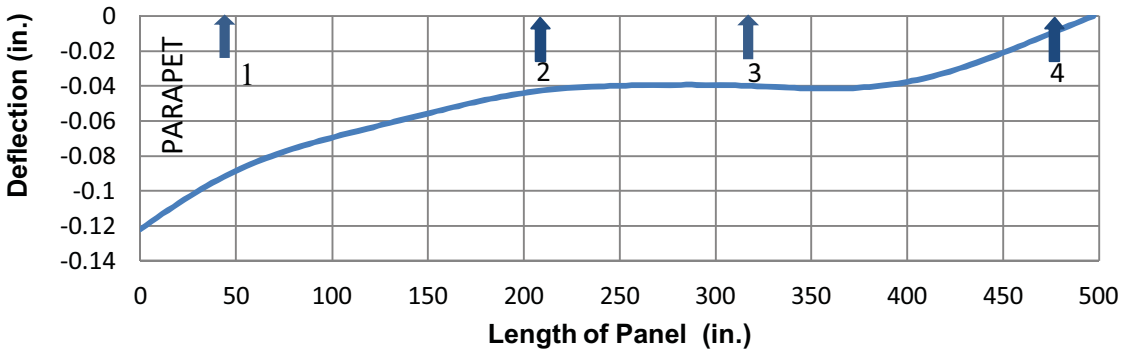

Figure 3.31. Midline displacement for panel lifting with the parapet-Lift 2

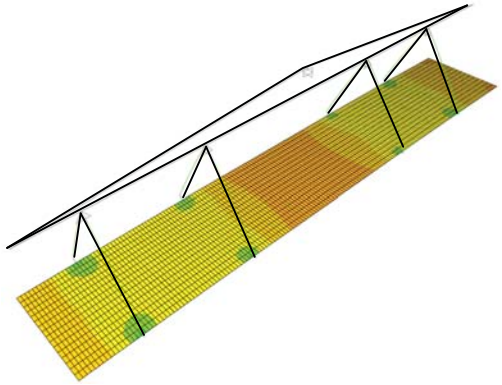

Figure 3.32. Maximum tensile top stress of panel with parapet
while lifting is 146 psi- Lift 3

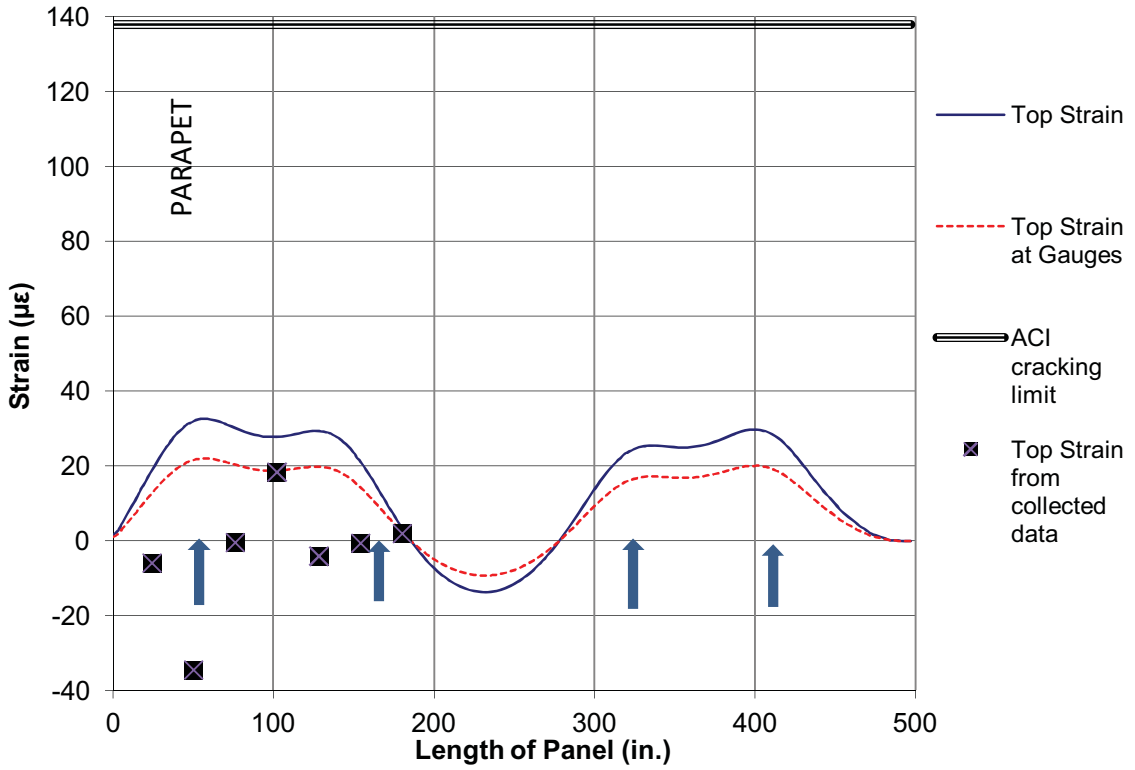

Figure 3.33. Mid-line top strain with parapet- Lift 3

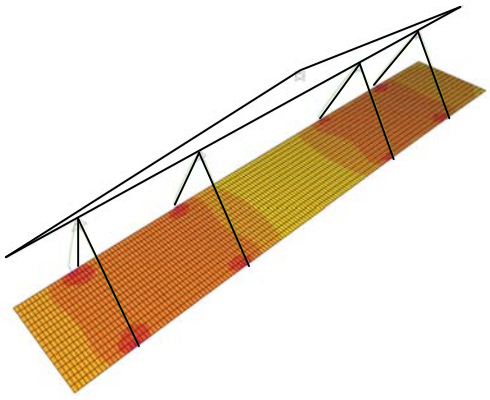

Figure 3.34. Maximum Bottom Stress panel with parapet is -144 psi (compression)-Lift 3

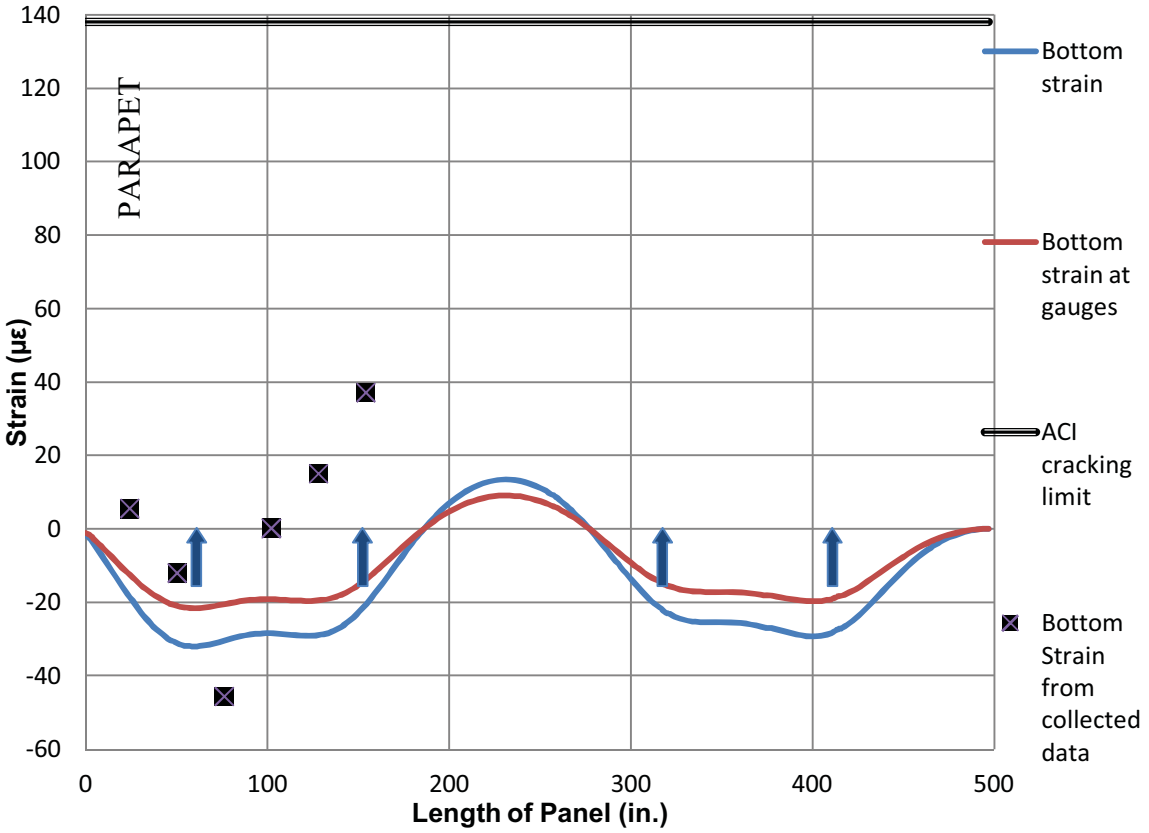

Figure 3.35. Mid-line bottom strain with parapet- Lift 3

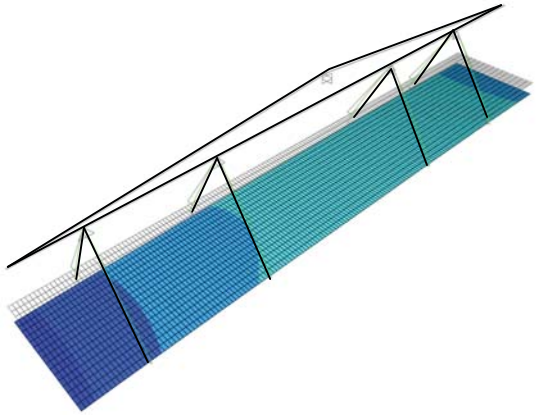

Figure 3.36. Deflected panel with a maximum midline deflection of -0.11 in.-Lift 3

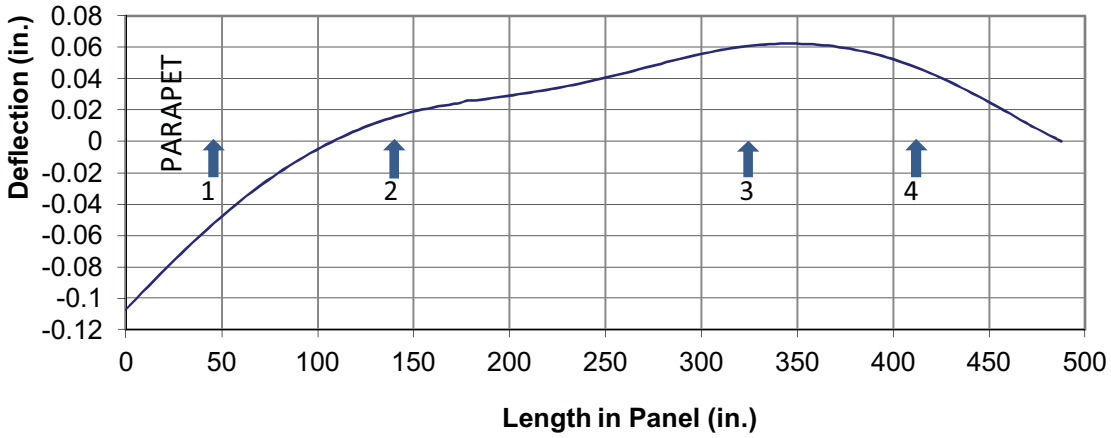

Figure 3.37. Deflected panel with a maximum midline deflection of -0.11 in.- Lift 3

modeled to compare to code limits as shown in Figures 3.38-3.46. Pick points 1 and 3 were modeled for top and bottom strains; midline deflections were plotted. Similarly, pick points 1 and 4 as well as pick points 2 and 3 were modeled. A table of comparisons between the collected data and the finite element model displaying maximum tensile strain and deflection is shown in Table 3.1.

3.6 Conclusions

Because GFRP has a low elastic modulus, large deflections which lead to cracking are a concern. GFRP panels were constructed and placed without damaging them in a way that would compromise their integrity and functionality in-service at the bridge. Instead of lifting by embeds attached to the bars, lifting the deck panels from below decreased stress concentrations in the panel and shear stresses in the bars; this is a viable lifting method for such precast deck panels. Monitoring the panels during lifting and transportation gave a strain history to check against the tensile cracking limit. The strains for all three lifts were in the same range and never exceeded 128 με; the tensile limit of the concrete used for the precast deck panels is 138 με. There were no visible signs of cracking.

The finite element model predicted a maximum deflection of 0.12 in. (Lift 2, with parapet) which is within the AASHTO design limit for service loads of span/800 or 0.62 in. Furthermore, the collected data compared well with the model. Curvature results from the finite element model did not correlate well with the collected data due to the bond stresses from the panel being lifted out of formwork that were not modeled in the finite element analysis. All two-point hypothetical lifting scenarios violate AASHTO's deflection limit and displayed tensile cracking. The four point lifting method displayed

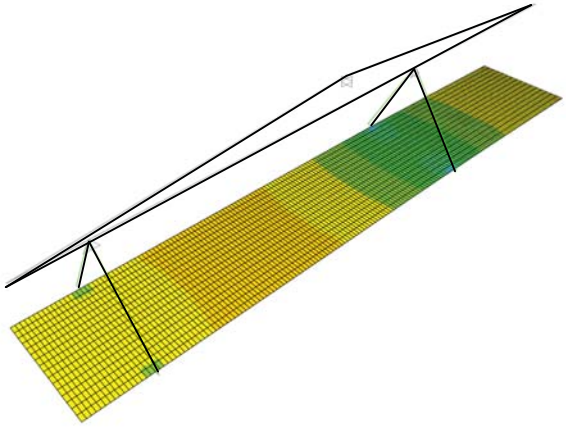

Figure 3.38. Hypothetical pick points 1 and 3 top strain

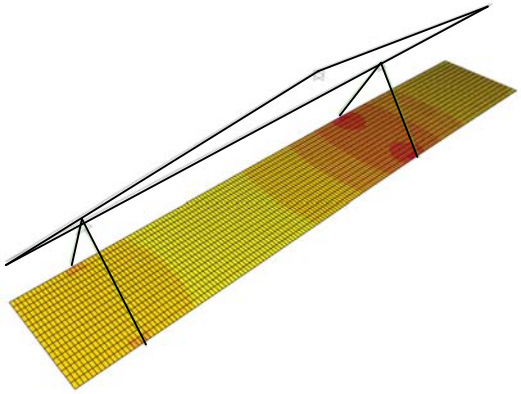

Figure 3.39. Hypothetical pick points 1 and 3 bottom strain

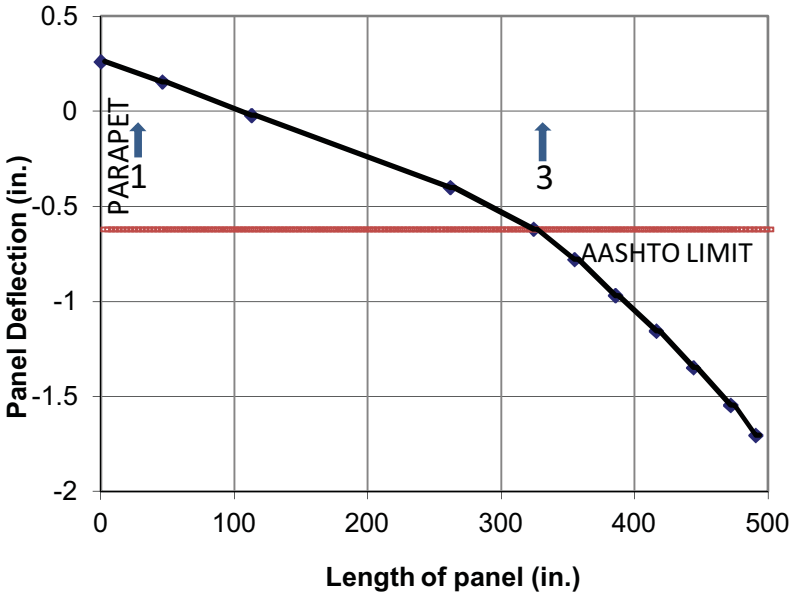

Figure 3.40. Pick points 1 and 3 deflected panel

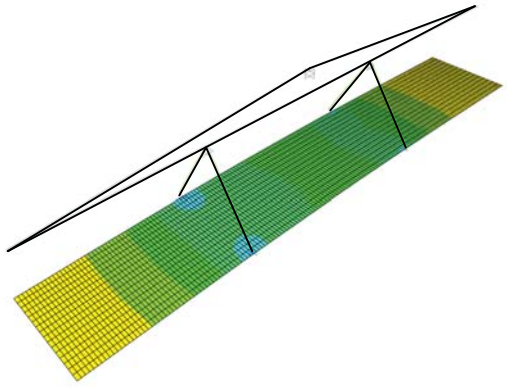

Figure 3.41. Hypothetical pick points 2 and 3 top strain

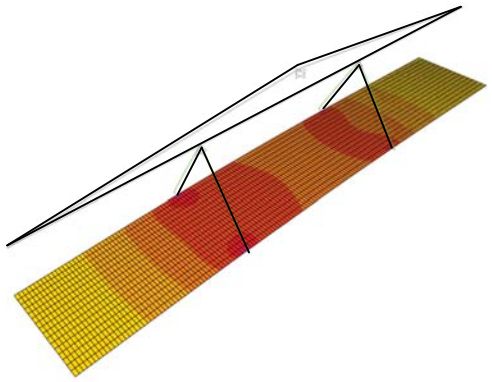

Figure 3.42. Hypothetical pick points 2 and 3 bottom strain

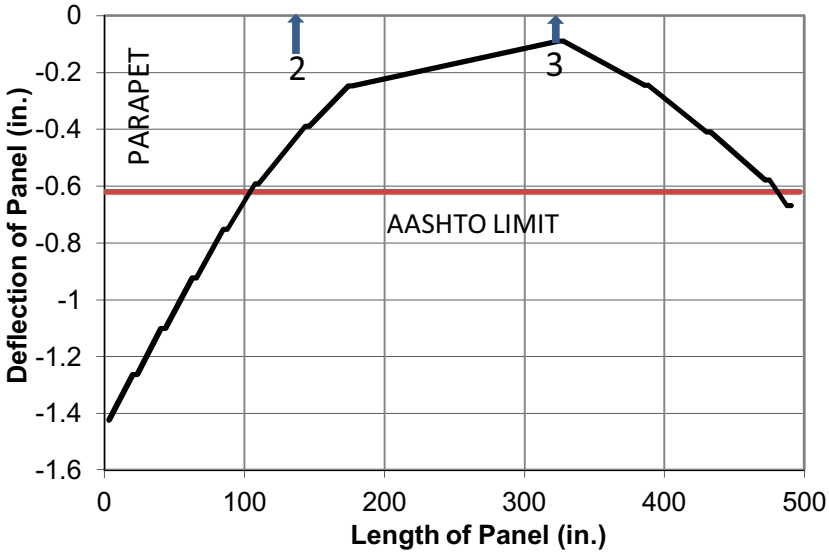

Figure 3.43. Pick points 2 and 3 deflected panel

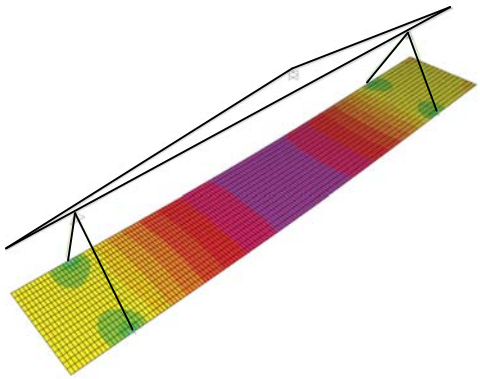

Figure 3.44. Hypothetical pick points 1 and 4 top strain

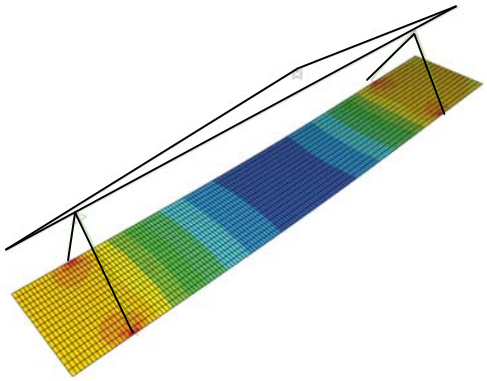

Figure 3.45. Hypothetical pick points 1 and 4 Bottom strain

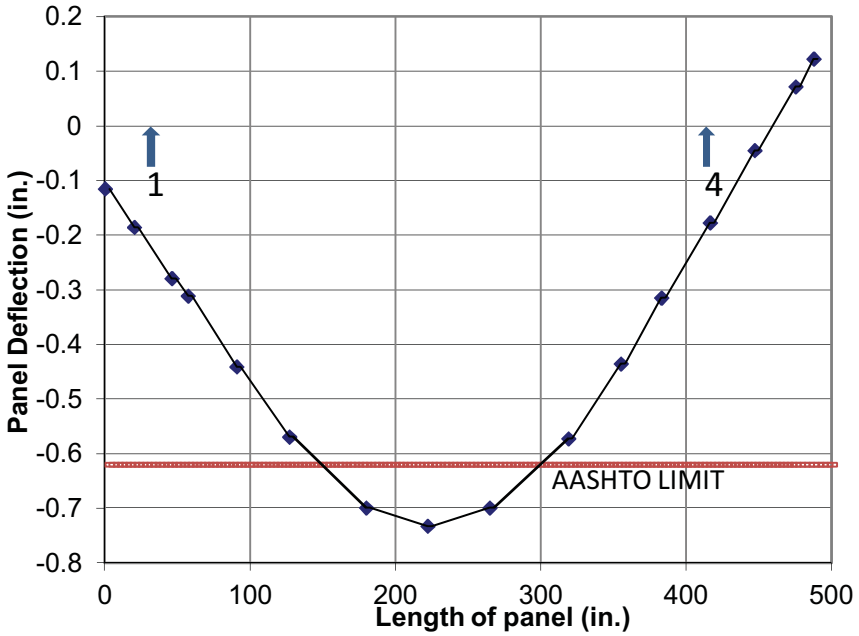

Figure 3.46. Pick points 1 and 4 deflected panel

Table 3.1. Comparison between collected data and model

	Collected Data		Finite Element Model			% Difference
	Tensile Strain at gauge, με	Curvature EP3	Maximum deflection, in.	Tensile Strain at gauge, με	Curvature Panel EP3	Tensile Strain
Lift 1	50	$2.5x10^{-5}$	0.035	19	$6.18x10^{-5}$	62%
Lift 2	15	$9.8x10^{-6}$	-0.12	19	$8.7x10^{-5}$	26%
Lift 3	18	$8.6x10^{-6}$	-0.11	22	$9.9x10^{-5}$	22%
Points 1,3	N/A	-	-1.7	154	-	-
Points 2,3	N/A	-	-1.4	201	-	-
Points 1,4	N/A	-	-0.73	173	-	-

good results and is recommended for precast panels constructed with GFRP bars as well as traditionally reinforced deck panels. The deck panels were monitored at the bridge for three years; recorded strains never exceeded the lifting strains.[8]

3.7 Acknowledgments

This research would not have been possible without the help from UDOT, especially Becky Nix, and Mike Adams from Campbell Scientific. Additional thanks are due to the students, faculty and staff of the University of Utah civil engineering department.

3.8 References

1. American Association of State and Highway Transportation Officials 2009. *AASHTO LRFD Bridge Design Guide Specifications for GFRP Reinforced Concrete Bridge Decks and Traffic Railings*. 1st Ed. American Association of State Highway Transportation Officials, Washington, DC.

2. American Concrete Institute Committee 440. 2006. *Guide for the Design and Construction of Structural Concrete Reinforced with FRP Bars (ACI 440.1R-06)*. American Concrete Institute, Farmington Hills, MI.

3. Nix, R. Personal Communication. 2010.

4. Precast/Prestressed Concrete Institute. 1999. *PCI Design Handbook,* Fifth Ed.

5. Benmokrane, B., El-Salakawy, E., Desgagné, G., and Lackey, T. 2004. "FRP Bars for Bridges." *Concrete International* 26(8): 84-90.

6. American Concrete Institute Committee 318, 2005. *Building Code Requirements for Structural Concrete (ACI 318-05).* American Concrete Institute, Farmington Hills, MI.

7. *CSiBridge SAP 2000*. 2011. Computer software. Vers. 14.1. Computers and Structures Inc. Web.

8. Pantelides, C.P., Holden, K.M., and Ries, J.M. 2012. "Health Monitoring Of Precast Bridge Deck Panels Reinforced With Glass Fiber Reinforced Polymer (GFRP) Bars." Utah Department of Transportation Research Division Report No. UT-12.03.

CHAPTER 4

PERFORMANCE OF BRIDGE CONSTRUCTED WITH GFRP REINFORCED PRECAST CONCRETE DECK PANELS

4.1 Abstract

The Utah Department of Transportation is trying to increase the life of bridge decks by using glass fiber reinforced polymer (GFRP) bars. GFRP bars do not corrode and therefore are a good alternative to steel reinforcement. The Beaver Creek Bridge was constructed using prestressed concrete girders and precast concrete panels reinforced with GFRP bars that were attached to the girders and posttensioned in the direction of traffic. Long-term monitoring of two precast deck panels and six girders is reported. Static truckload test results are discussed and observations are made regarding the overall response of the bridge. The deflections of the girders to known static loads and distribution factors are evaluated. Data from loads applied to the bridge were collected remotely for approximately 3 years and analyzed. Collected data also include concrete strains in the deck panels and relative displacements of the panels with respect to the girders. The response of the girders and bridge deck is evaluated by comparing test results to design requirements as well as finite element analyses from computer generated models. It is shown that after 3 years in service, the performance of the bridge including the precast concrete deck is well within design requirements.

4.2 Introduction

Currently, Utah bridges are engineered for a 75-year design life, but the decks require replacement after 30 to 40 years due to corrosion of steel reinforcement. These replacements require time and money; there is currently an alternative solution in the form of GFRP reinforcement of the bridge decks. Glass Fiber Reinforced Polymer (GFRP) reinforcing bars may be used as an alternative to steel rebar because of their non-corrosive characteristics and their high strength-to-weight ratio. Consequently, GFRP has a much lower elastic modulus than steel reinforcement and large deflections may occur. There is little research regarding precast concrete panels for bridge decks reinforced with GFRP bars.[1,2] GFRP reinforcement has not been utilized until recently, which indicates there is no long-term data for creep, fatigue and long term loading effects. Therefore, many states have not used GFRP as primary reinforcement.[3] There is a great need to evaluate the use of GFRP reinforcement in actual bridges. Phillips and Harlem stated in 2005 that "(t)here is no conclusive research on the extent of deflection and cracking that would occur in an all GFRP-reinforced concrete deck." Philip and Harlan instrumented one of three spans of a bridge with GFRP as the top mat reinforcement and steel as the bottom mat reinforcement. The other two spans were constructed with traditional steel reinforcement. There were no significant differences in the behavior and performance of the total deck after 2 years of monitoring. The present research aims to contribute to the knowledge base by monitoring deflections and strains due to loads applied to the precast GFRP bridge deck panels.

The monitored bridge is the Beaver Creek Bridge on US-Route 6 near Price, Utah. The overall span of the bridge is 88 ft-2 in., with an out-to-out width of 88 ft-10 in. as

shown in Figures 4.1-4.2. The girders are AASHTO Type IV prestressed beams.[4] The deck was designed in accordance with the requirements of the ACI 440.1 R-06 Guidelines.[5] The bridge was constructed in two phases; this research is focused on Phase II. A precast three-foot closure pour with GFRP bars was constructed between the two phases to couple the two bridges and emulate cast-in-place construction. The closure pour was not designed for shear loading or fatigue. This is a construction issue that influences the bridge as a whole and is checked by the mode shapes proving that the composite action between both phases is working and acts as one bridge not two phases.

The design of the deck panels was controlled by crack width and deflection for service loads. The lower modulus of elasticity of GFRP bars (5920 ksi) leads to wider crack widths than with traditional steel reinforcing, and a higher panel deflection. Therefore, more GFRP bars and a greater deck thickness were used. In order to reduce construction time and user impacts, this bridge was constructed using 24 precast deck panels with longitudinal post-tensioning transverse to the joints to prevent leaking. Posttensioning consisted of low relaxation steel strands that were grouted after post tensioning. The individual deck panels had a length of 41ft-5in., a width of 6ft-10in., and a thickness of 9-1/4in. as shown in Figure 4.2.

The research is focused on how different loads affect the bridge to determine performance. Load effects are monitored by instrumentation at the bridge and collected remotely. Two bridge deck panels were monitored during posttensioning, truck load testing, and long-term testing using vibrating wire strain gauges (VWSG). The bridge deck deflections are relative to the two diaphragms connecting the prestressed concrete girders and were monitored using linear variable differential transformers (LVDT), as

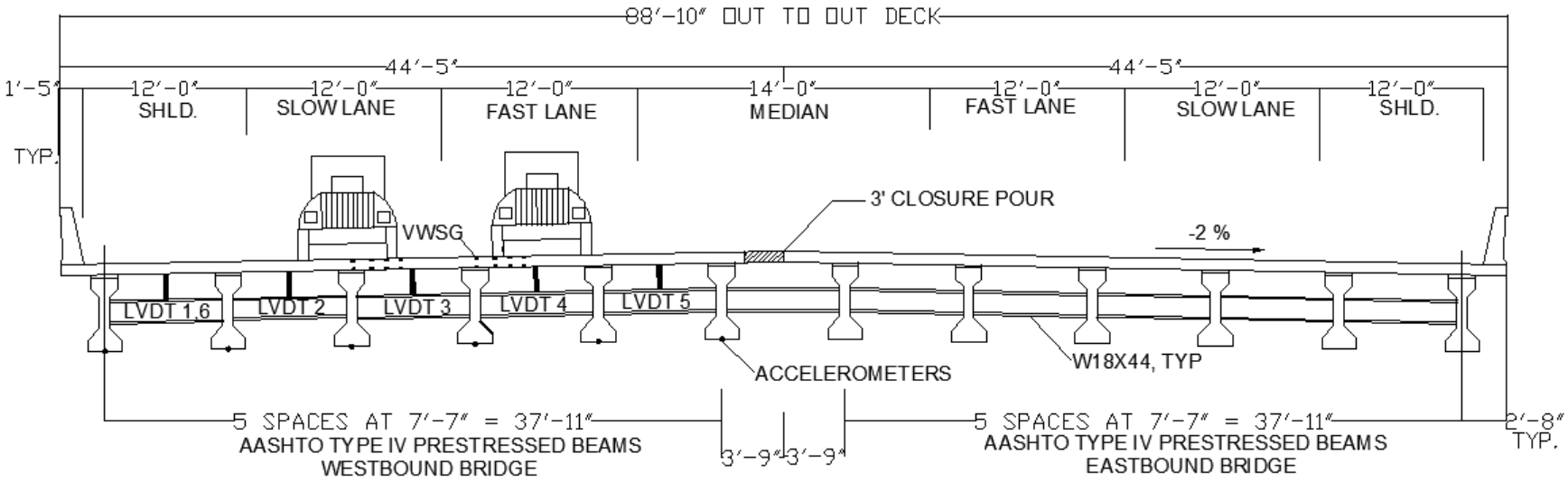

Figure 4.1. Elevation of Beaver Creek Bridge showing deck, girders and instrumentation

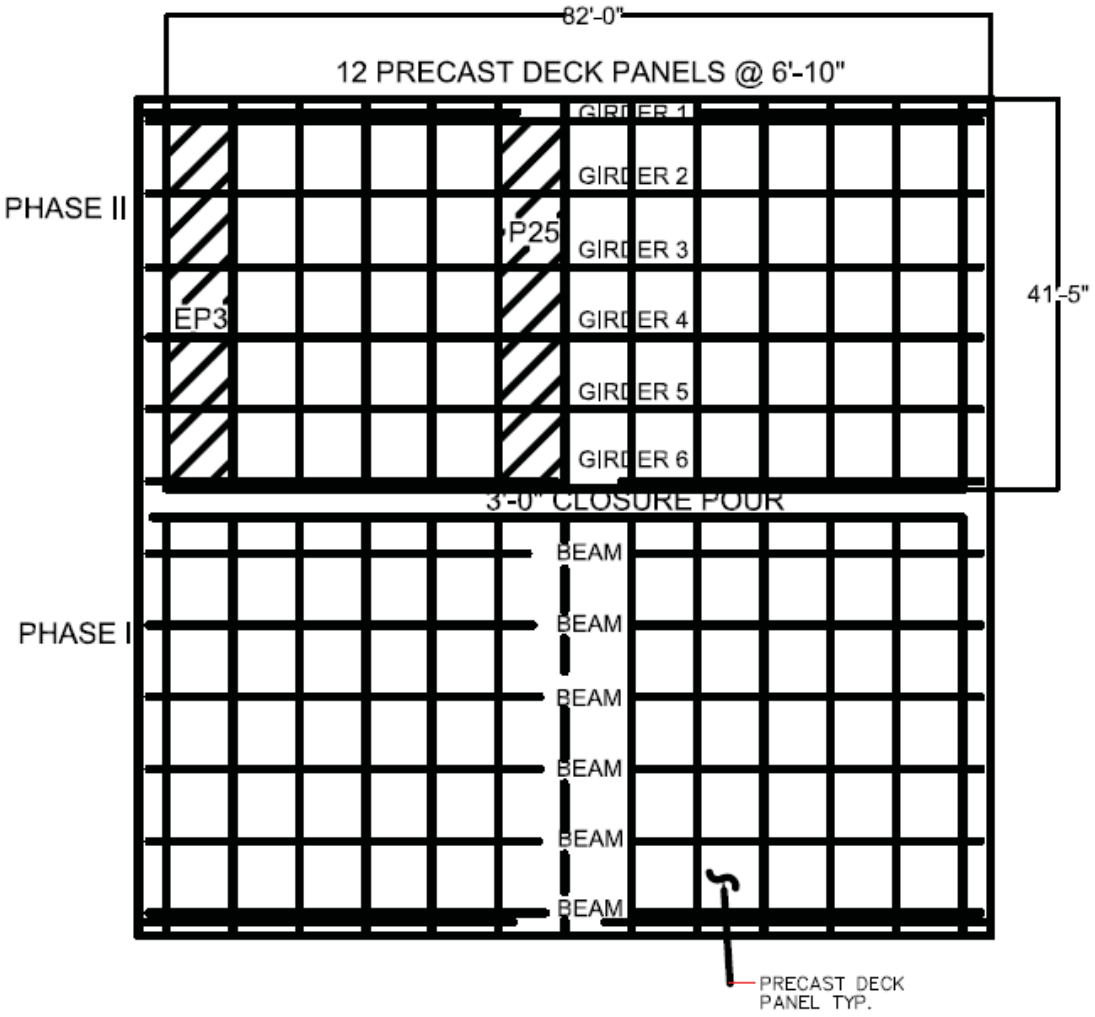

Figure 4.2. Plan view of Beaver Creek Bridge

shown in Figure 4.1. Accelerometers were also instrumented at midspan of the girders to monitor vertical accelerations. From accelerometer data, dynamic displacements were found.

4.3 Instrumentation of Precast Panels

Data from in-situ instrumentation is remotely collected through a secure wireless modem to the University of Utah. Instrumentation is connected to three Campbell Scientific dataloggers. The dataloggers are able to transmit real time data remotely through a secure IP address to the project laptop.

Twenty-four Geokon 4200™ VWSG monitored the static strain in the deck panels for long-term monitoring. These gauges were also used to record strains induced by posttensioning, as well as the change in strain due to creep and shrinkage and for long-term monitoring. Gauges were placed parallel and transverse to the direction of traffic. The parallel to traffic gauges monitored the posttensioning at the panel joints. Gauges in the deck panels were placed at selected locations on the top and bottom rebar mat, 6.5 in. apart over several girders and operate at 500 Hz with a sampling rate of 2 seconds. The maximum strain in the panel was plotted and the curvature calculated at midspan of the deck thickness.

Six LIPS®P101 displacement sensors were attached to the diaphragm and the deck between the west bound girders and operate at 13 V with a sampling rate of 1 Hz. These sensors record relative static displacement measurements of the deck to the diaphragm. This is a key measurement to determine if the design requirement of span/800 is satisfied. Collected data were also compared to a computer generated model.

Six accelerometers were instrumented at midspan with a sampling rate of 300 records at 50 Hz to record vertical accelerations for long-term monitoring. An event triggering camera was connected to one of the accelerometers to record large accelerations from trucks passing over the bridge. Vertical accelerations are an important design consideration due to their influence on the integrity of the prestressed concrete girders.[6]

4.4 Design Requirements and Values

The overall bridge design was a HL-93 in accordance with 2007 AASHTO LRFD Bridge Design Specification 4th Edition and 2008 Interim Specification. The deck was designed according to ACI 440.1R-06. Precast handling was in accordance with the PCI Handbook 5th Edition.[7]

The allowable deflection of a typical girder is specified to be span/800, or 1.32 in. The maximum design tensile strength in the GFRP bars of the bridge deck panels is 95 ksi. The modulus of elasticity in the GFRP bars of the bridge deck panels is 5.92×10^6 psi. The design speed is 65 mph. Additional design requirements are provided by Pantelides et al.[8]

4.5 Data Analysis and Measurements

4.5.1 Strains and Curvature

The VWSG for long-term monitoring have a mechanical component that measures the change in strain in the concrete and a temperature component that records the diurnal strain from morning to night. These two components are combined in one output. Separating out the thermal effects gives a maximum mechanical, or true, strain. Figure 4.3 shows a graphical representation of 3 years of true strain of the concrete for VWSG 2

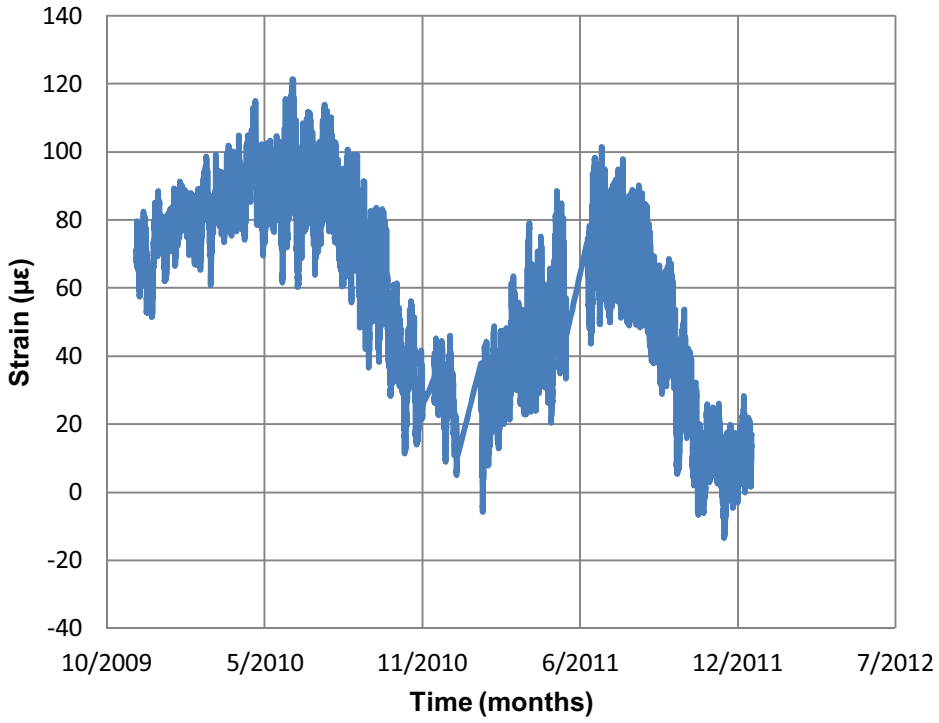

Figure 4.3. Three-year concrete strain record

which is located at the bottom mat of bars, of 121 microstrain (με) in tension and a minimum of 13 με in compression. These are within the design constraints of 16,000 με tension for the GFRP bars and the concrete tensile cracking limit of 138 με. The corresponding stresses to the measured strains are, respectively, 3.7 MPa and -0.4 MPa. These points correlate well with the field investigation on the first bridge deck reinforced with GFRP bars by El-Salakawy and Benmokrane [9] with values of 62 με and -125 με in the bars and concrete, respectively, with corresponding stresses of 2.60 MPa and -3.56 MPa.

With a known distance and recorded top and bottom strains, curvature is then calculated by:

$$\Phi=(\varepsilon_{top}+\varepsilon_{bottom})/y \tag{4.1}$$

where Φ = curvature in 1/in.; ε_{top} = top strain gauge measured in με; ε_{bottom} = bottom strain gauge measured in με; y = seperation distance. These strains in the concrete are within the limits of 138 με in tension at which concrete theoretically would crack and -3000 με at which concrete fails in compression. As shown in Figure 4.4, the absolute maximum curvature is $3.3x10^{-5}$ 1/in.; ambient temperature and relative humidity were also monitored for 2 years for concrete conditions, as shown in Figure 4.5.

4.5.2 Long-Term Bridge Deflections

On September 29, 2009 several truck load tests were conducted before the bridge was opened to traffic; these consisted of nine static tests and the weights of the trucks are noted in Table 4.1. The static tests are broken down into three groups depending on the

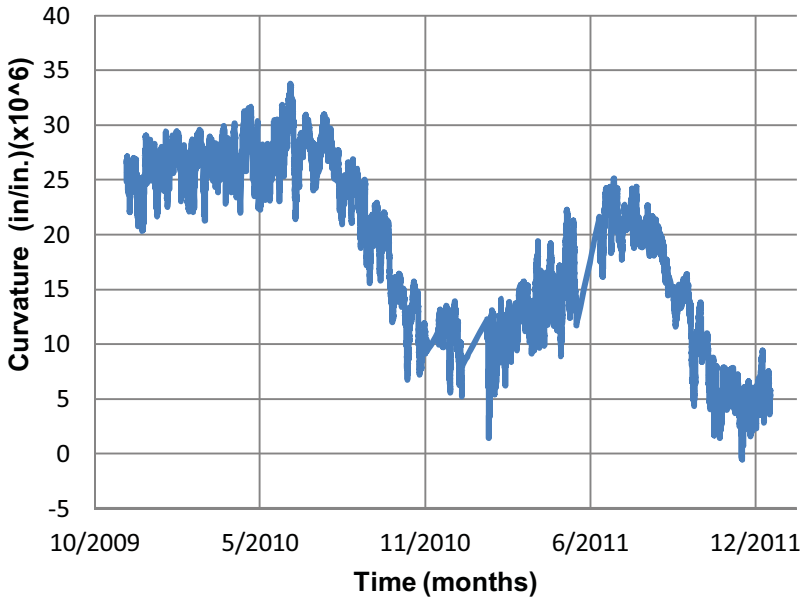

Figure 4.4. Curvature over a 2-year period from Nov. 2009 to Jan. 2012

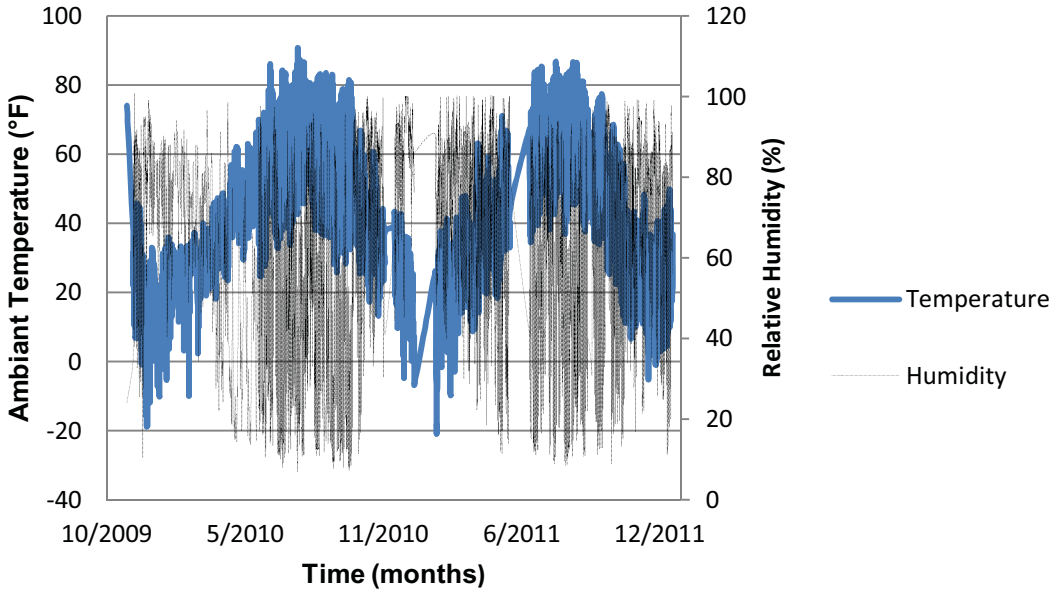

Figure 4.5. Ambiant temperature and relative humidity over a 2-year period

Table 4.1. Truck weight and distribution for testing

Truck	Weight-kips	Rear Axle-kips	Front Axle-kips
A, 2009	43.88	14.78	29.10
B, 2009	43.16	14.48	28.68
A, 2010	37.94	14.5	23.44
B, 2010	45.68	17.48	28.2

lanes being loaded. Using Truck "A", Tests 1-3 were performed on the slow lane; using truck "B", tests 4-6 were performed on the fast lane; both trucks "A" and "B" were used in tests 7-9 in their respective lanes. These measurements were made using LVDTs at the two W18x44 steel diaphragms shown in Figure 4.1. The three tests for each case were obtained by centering the rear axle of the truck over the east diaphragm, midspan and west diaphragm, respectively; the deck deflections are from the 2009 tests shown in Figures 4.6-4.8. These deflections represent the maximum relative movement of the deck with respect to the prestressed girders, at the diaphragm of the deck. Single trucks produce an unbalanced load condition that results in relative uplift elsewhere in the deck as shown in Figures 4.6-4.7 (LVDT 3 and LVDT 4); this is a good indication that the deck is composite with the girders.

From the September 29, 2009 test, the highest relative deflections were found to be 0.007 in. in the fast lane between girders 4 and 5 during Test 8 and Test 9 as shown in Figure 4.8; this is reasonable since both trucks "A" and "B" are parked between the midspan and the west diaphragm during Test 8 and are parked on the west diaphragm during Test 9. The magnitude of the relative deflection is very small, which shows that the bridge deck and the girders have good composite action.

On September 1, 2010, both "A" and "B" trucks sat simultaneously over the girders in 5 different stations: beginning abutment (1), east diaphragm (2), midspan (3), west diaphragm (4) and ending abutment (5). The deck deflections were very similar to previous results with a maximum of 0.003 in**.** LVDT 3 and LVDT 4 are shown in Figure 4.9; other LVDT's read 0.001 in. or below. The 2010 results are smaller than the 2009 results due to a lighter truck.

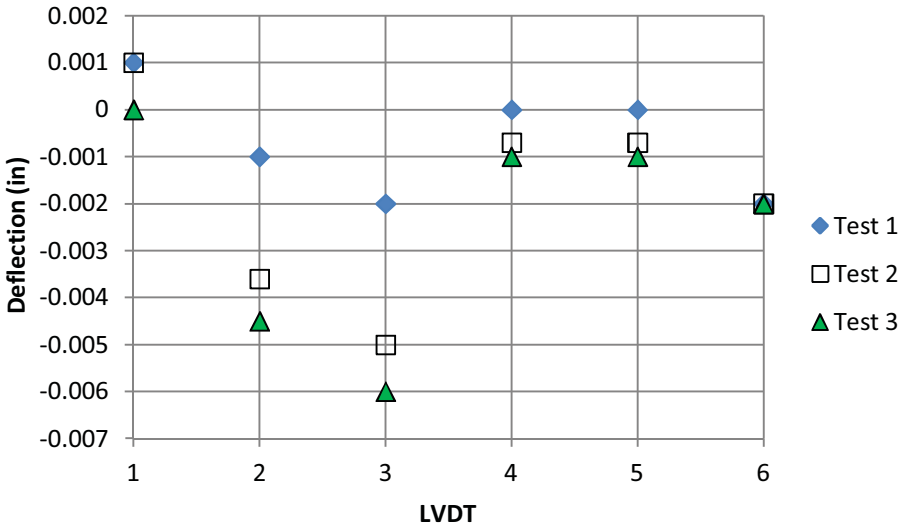

Figure 4.6. Deck deflections from testing for Truck A, Sept. 29, 2009

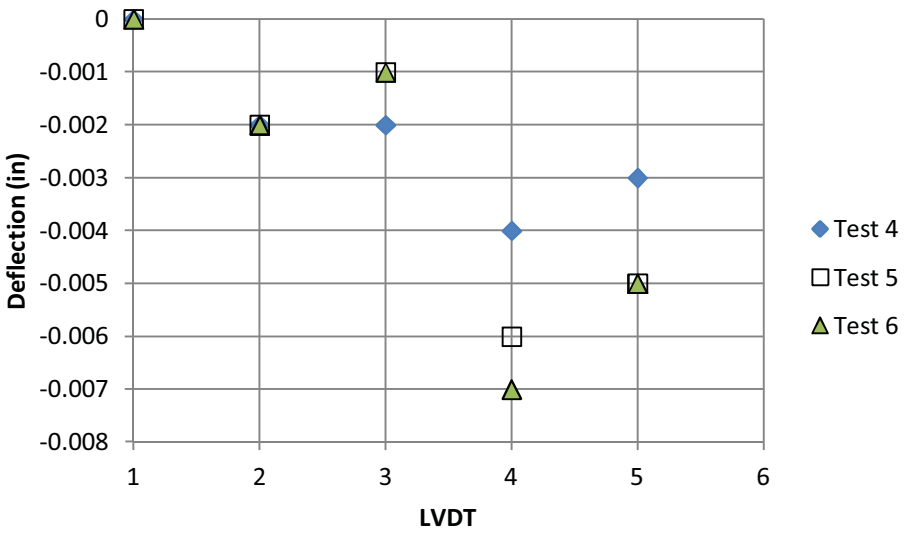

Figure 4.7. Deck deflections from testing for Truck B, Sept. 29, 2009

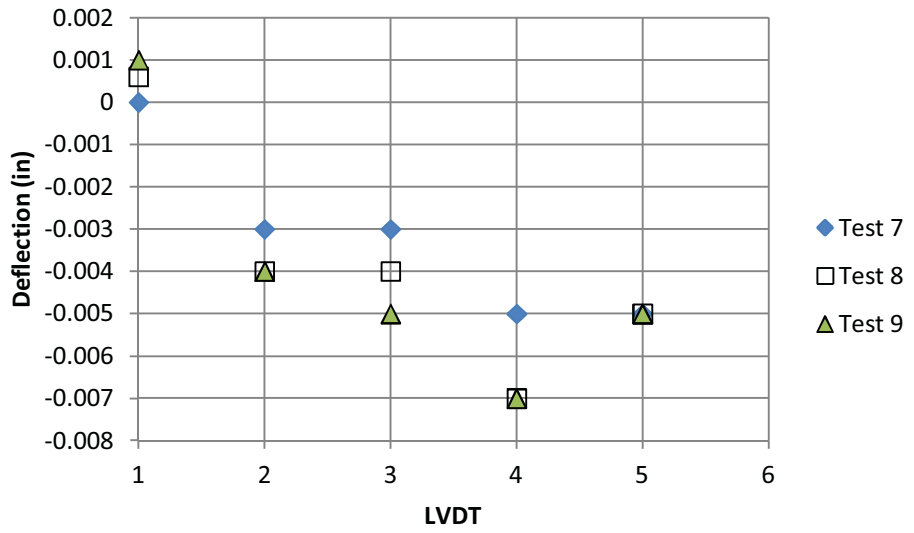

Figure 4.8. Deck deflections from testing for Truck A and Truck B, Sept. 29, 2009

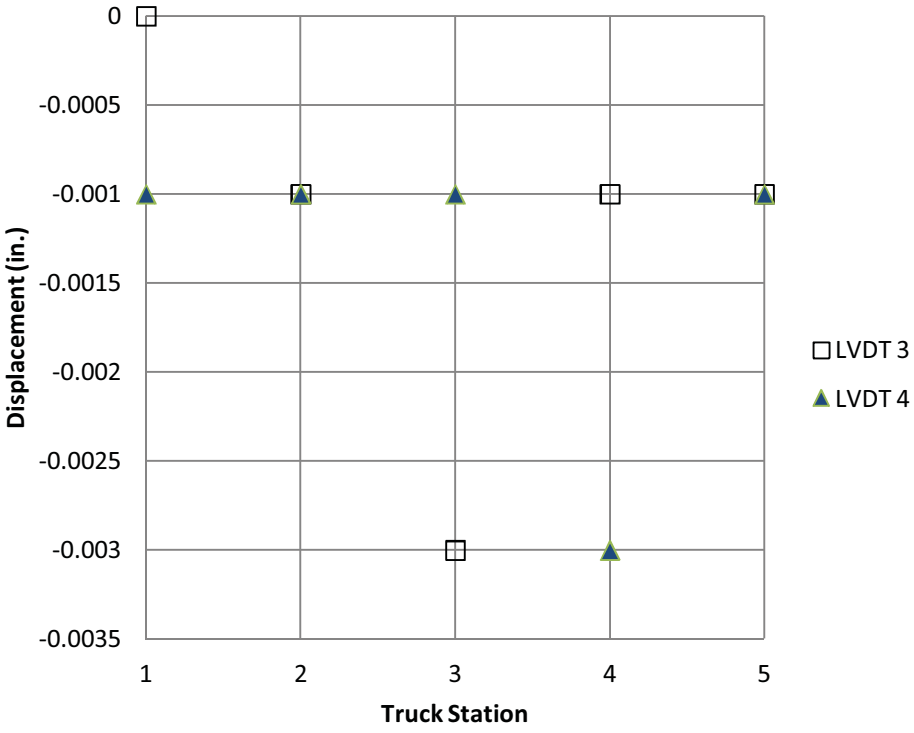

Figure 4.9. Deck deflections from testing for Truck A and Truck B, Sept. 1, 2010

Over the course of a year, the LVDT's have recorded various maximum displacements, as shown in Table 4.2. The October 8, 2010 deflections of 0.15 in. and 0.14 in. were the highest deflections recorded due to an overloaded truck during construction time that month. The event triggering camera confirmed the construction on the bridge. Service deflection limits for the panels were span/800 or 0.11 in. The October deflections exceed the limit, however the deflections are dynamic deflections and not static so it is reasonable that they are higher.

4.5.3 Girder Deflections

As expected, the maximum deflection of the girders occurred during Truck Load Test #8 which was conducted on September 29, 2009 when both trucks were parked at the bridge midspan. The maximum deflection was 0.13 in. as shown in Figure 4.10, recorded in girder 4 located between the two trucks. The peak deflection of 0.13 in. was well below the AASHTO limit of L/800, or in this case 1.32 in.

During truck load test 9, additional girder displacements were measured above the west diaphragm. This was done to correlate girder deflections and panel deflections at the same point. Additional deflection data were taken for girders two and three, as seen in Figure 4.11. The displacement of the diaphragm at midspan between girders two and three was calculated to be 0.06 in. Combining this with the panel deflection from LVDT #2 for the same test, the total deflection of the panel located above LVDT #2 has been calculated to be 0.064 in. The relative deflection of the panel with respect to the least deflected girder can be determined using half the difference between the two girders and deflections data from LVDT #2. This results in a deflection of 0.016 in. relative to girder

Table 4.2. Deck deflections relative to girders (in.)

	LVDT 2	LVDT 3	LVDT 4	LVDT 5
9/2009	0.003	0.004	0.006	0
5/2010	0.002	0.006	0.008	0.005
8/2010	0.014	0.004	0.005	0.015
9/2010	0.001	0.003	0.003	0.001
10/2010	0.15	0.14	0.017	0.027
11/2010	0.001	0.001	0.001	0.004
3/2011	0.001	0.002	0.002	0.003

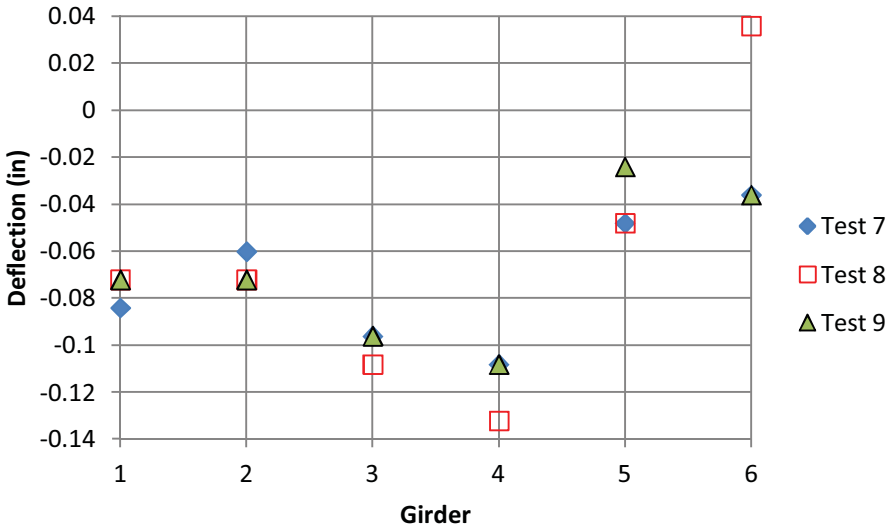

Figure 4.10. Midspan Girder Deflections for tests 7 through 9 in Girder #4

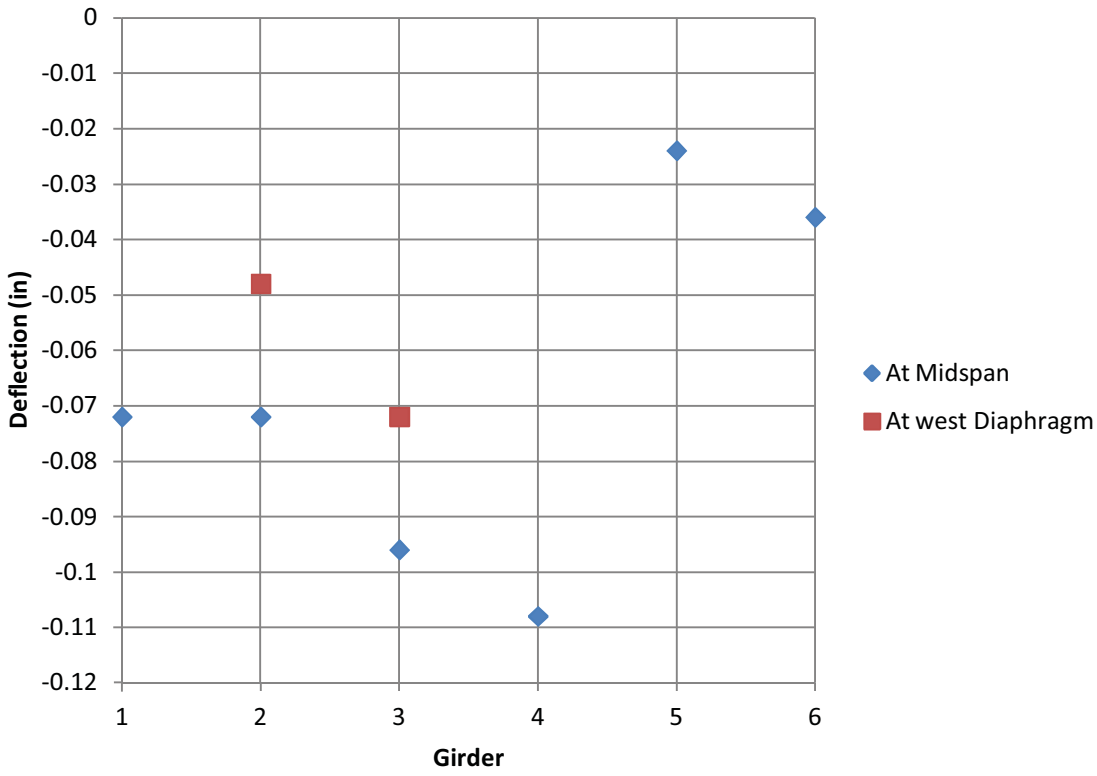

Figure 4.11. Girder deflections for truck load test 9

3. Both these values are below the predicted design limit of 0.101 in. by the use of beam theory and superposition.

With girder deflections known, live load distribution factors can be calculated using the AASHTO-LRFD Specification S.4.6.2.2. Distribution factors show how the load from one girder transfers to the deck and in turn to other girders. Live load distribution factors are shown for girders 3 and 4 in Table 4.3; these girders showed the highest deflections in the data set. The data set values in Table 4.3 are significantly smaller than the AASHTO specification, indicating that the girder design is conservative.

4.5.4 Long-Term Bridge Accelerations

The accelerometers were placed at midspan to recorded vertical accelerations of truck traffic as an indication of the health of the bridge. Annual truck tests were performed using trucks with a known weight and speed. Truck test data were then analyzed and a time history is made of the vertical accelerations in the girders. Figure 4.12 depicts vertical accelerations in girder 2 caused by two similar weight of truck (43 kips) traveling at similar speeds (65 mph), two years apart. From vertical acceleration data, the period and dynamic displacement can be calculated. The dynamic displacement caused by the vertical accelerations from the truck in 2009 was 0.015 inches; dynamic displacement from the truck in 2011 was 0.017 inches. Both truck records have a period of 0.125 seconds. If the period does not change over time, it is an indication that the material properties of the girders have not changed and are maintaining their structural integrity.

4.6 Finite Element Modeling

SAP 2000[10] was used to generate finite element models of the bridge. The deck, girders, abutment springs and prestressed tendons were analyzed; area elements were

Table 4.3. Live load distribution factors for one and two lanes loaded

Girder	Truck A	Truck B	AASHTO one lane loaded	Truck A and B	AASHTO two lanes loaded
3	0.24	0.22	0.45	0.27	0.63
4	0.24	0.30	0.45	0.33	0.63

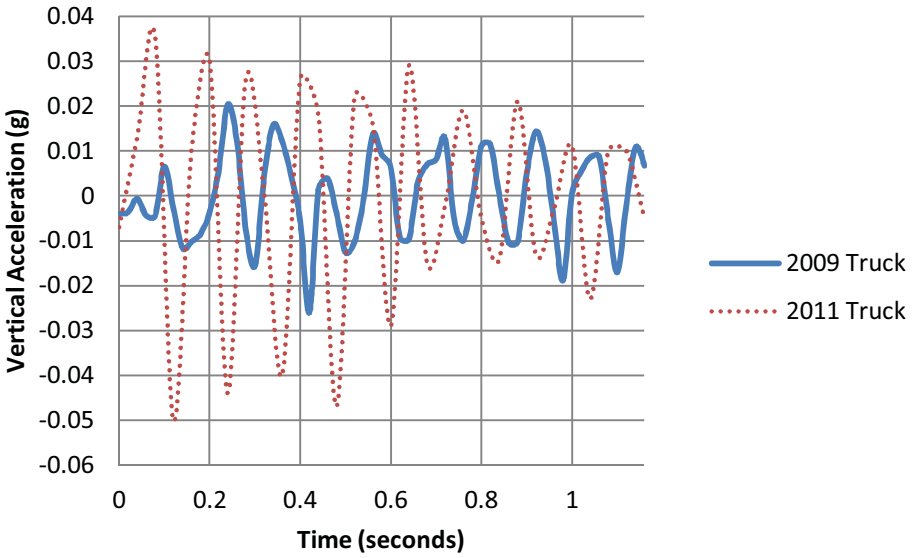

Figure 4.12. Vertical acceleration monitoring in girder 2

used for the deck and girders, line elements for the prestressed tendons in the girders and spring elements for the abutments as shown in Figure 4.13. The model contains 52 area elements and 1251 nodes. The abutments were modeled as a fixed-fixed integral abutment condition with rotational springs and the deck-to-girder condition was modeled as fixed connection. Material properties used in the model for the compressive concrete strength of the deck and girders were 6200 psi and 7000 psi, respectively. Tendons for the prestressing were modeled as Grade 270 steel and GFRP reinforcement was modeled using #5 bars with an elastic modulus of 5920 ksi and tensile yield strength of 95 ksi. A time history loading case was used to capture the dynamic truck loading on the bridge. Linear static load cases were used for the dead, prestressed and total service load conditions. The modeled bridge was compared to collected data.

Dead load, prestress load, and a dynamic truck load using a 44 kip truck traveling at 65 mph were analyzed. The maximum deflections for the three loads were -0.201 in., $+3.03 \times 10^{-4}$ in., and -0.003 in., respectively, which are shown in Figures 4.14-4.16. Using an AASHTO Service I case load combination, the bridge was analyzed with all three loads applied. This gave a maximum displacement of -0.203 in. as shown in Figure 4.17, which is still within the span/800 design limit which is 1.32 in.

The bridge was also analyzed for stress, as shown in Figure 4.18, to compare strain data. The maximum bridge stress was 913 psi (tension) at the prestressed girders at the abutments and the minimum was -393 psi (compression) at the deck midspan. Dividing by the elastic modulus of the concrete, 4506 ksi, gives a strain of 203 με (tension) and -87 με (compression). The maximum stress in the deck was -235 psi (compression) at

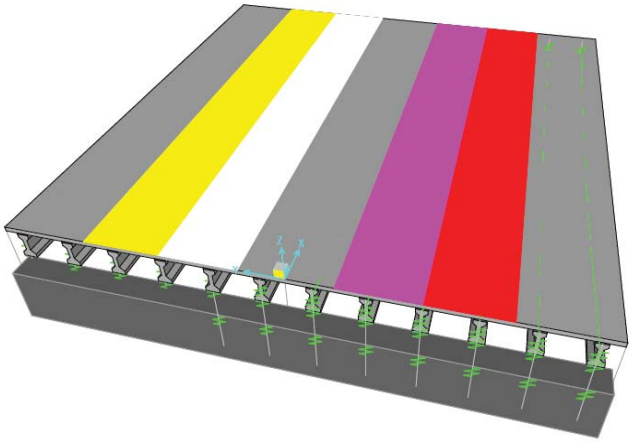

Figure 4.13. Model showing lanes, girders and abutments

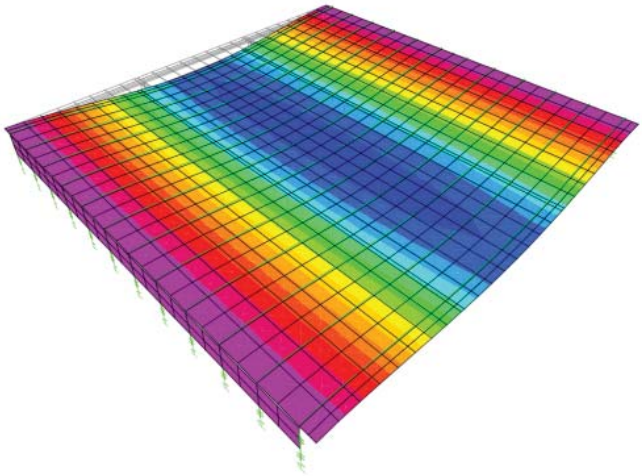

Figure 4.14. Finite Element model of the dead loads; maximum deflection is -0.201 in.

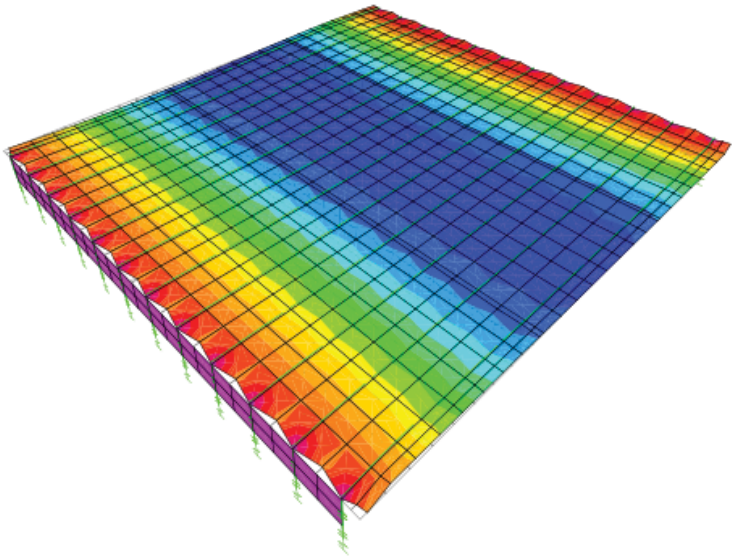

Figure 4.15. Finite Element model of the prestress loads;
maximum deflection is +0.0003 in.

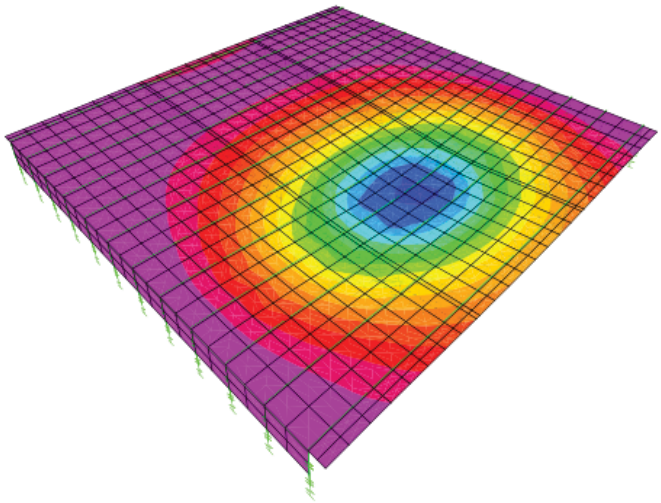

Figure 4.16. Finite Element model of the truck loads at midspan in
the inside lane; maximum deflection is -0.003 in.

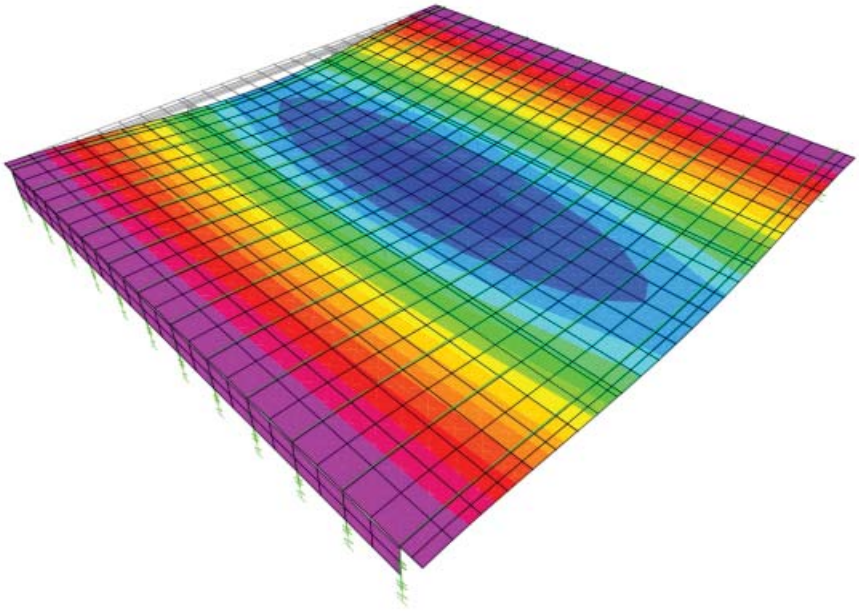

Figure 4.17. Total bridge deflection of -0.203 in.

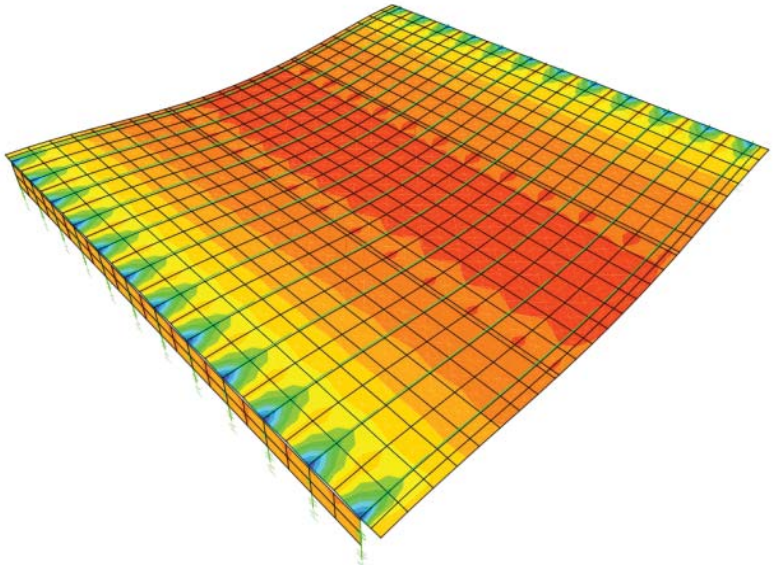

Figure 4.18. Stress on bridge with a maximum of 913 psi and a minimum of -393 psi

midspan, giving a strain of -52 με (compression). This compares to the collected deck strain data of 121 με (tension) and –13 με (compression).

A static model of two trucks, one in each lane, parked at midspan was analyzed. The truck load shown in Figure 4.19 gives a truck live load deflection of 0.003 in. in the deck; the total bridge deflection including dead load and prestressing was 0.17 in. This compares with the maximum total static measured deflection of 0.15 in. in the girders shown in Figure 4.11, and is well within the allowable limit of span/800 or 1.32 in.

A comparison of experimental data with modeled data is shown in Table 4.4. The model is conservative and predicts on average 25% higher values than the collected data. The collected data are in raw form, whereas the model applies inherent code corrections and phi factors. Additionally, the software does not allow a steel diaphragm between concrete girders; a modular ratio was used for the steel diaphragms to model concrete diaphragms.

A parametric study was conducted using the finite element model. An unbalanced load condition was modeled with two 44 kip trucks positioned in the westbound lanes. Girder type and number were varied with deck thickness, as shown in Table 4.5. All configurations meet the design requirements of span/800 (1.32 in.), 618 psi tensile stress in the deck for cracking and 175 ksi at the prestressed tendons.

Twelve bridge vibration modes were analyzed and the three significant ones (mode 1, mode 2 and mode 4) are shown below in Figures 4.20 to 4.22. The fundamental period for mode 1 is 0.125 seconds; the period for mode 2 is 0.123 seconds. Table 4.6 shows modal mass participation ratios; mode 1 governs in the vertical direction Z, whereas

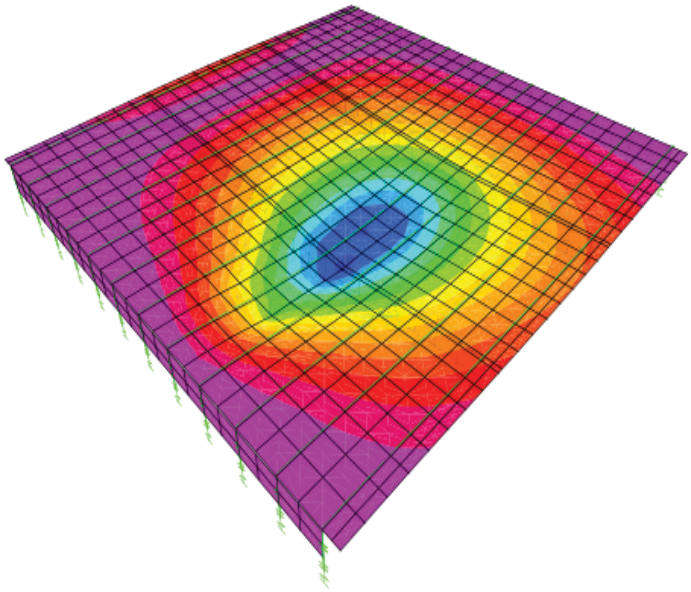

Figure 4.19. Static truck load at midspan in inside lane; deflection of -0.003 in.

Table 4.4. Comparison of collected data to computer generated model

	Model	Collected Data	% diff
Maximum Strain in Deck	207 με (tension)	119 με (tension)	42%
Minimum Strain in Deck	89 με (compression)	139 με (compression)	56%
Maximum Static Bridge Deflection in Girders	0.201 in.	0.15 in.	25%
Deck Deflections Due To Trucks	0.003 in.	0.007 in.	133%

Table 4.5. Parametric Bridge Study

Deck Thickness	FEM Deflection (girder midspan) (in)	FEM Stress (tendon ends) (psi)	FEM Stress (deck midspan) (psi)
8"	0.203	862	234
AASHTO III Girder	0.297	1043	274
AASHTO III, 2 less Girders	0.453	-12267	431
AASHTO IV, 2 less Girders	0.312	-12187	367
8.5"	0.203	882	234
AASHTO III Girder	0.295	1058	273
AASHTO III, 2 less Girders	0.421	-11689	429
AASHTO IV, 2 less Girders	0.291	-11593	365
9.25"	0.203	913	235
AASHTO III Girder	0.296	1099	274
AASHTO III, 2 less Girders	0.448	-10929	427
AASHTO IV, 2 less Girders	0.309	-10836	362

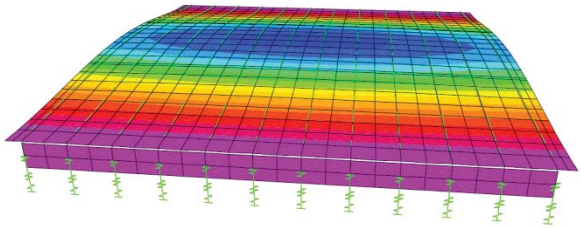

Figure 4.20. Mode 1, period of 0.125 sec.

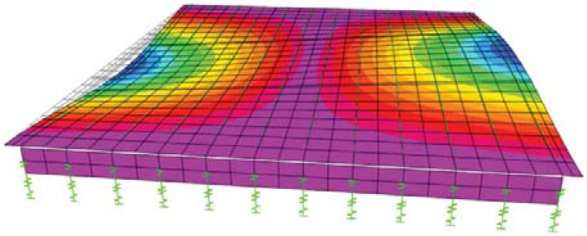

Figure 4.21. Mode 2, period of 0.123 sec.

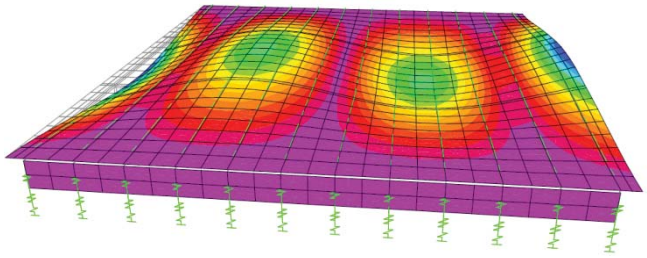

Figure 4.22. Mode 4, period of 0.076 sec.

Table 4.6. Modal Mass Participation Ratios

Mode	**Period** Sec	**Frequency** Hz	**X** **%**	**Y** **%**	**Z** **%**
Mode 1	0.13	7.98	1.46E-07	7.65E-11	**99.74444**
Mode 2	0.12	8.12	8.22E-14	**59.17984**	6.48E-16
Mode 3	0.11	9.51	9.55E-09	3.17E-12	0.19679
Mode 4	0.08	13.11	0	**40.81368**	8.45E-17
Mode 5	0.06	16.61	18.66468	7.58E-09	0.004128
Mode 6	0.06	16.61	11.30396	8.18E-10	0.006864
Mode 7	0.06	16.61	69.92683	1.81E-10	4.76E-06
Mode 8	0.06	16.63	0.094401	1.27E-10	0.047764
Mode 9	0.06	16.65	0.010129	3.28E-10	3.21E-07
Mode 10	0.06	16.65	3.81E-06	2.17E-11	1.4E-05
Mode 11	0.06	16.94	1.13E-12	0.001833	1.22E-13
Mode 12	0.06	16.94	2.19E-10	0.004645	3.93E-12

mode 2 and mode 4 govern in the direction transverse to traffic, Y. Mode 1 displays good composite action between the deck and the girders. Mode 2 and 4 show strong activity at the closure pour linking Phase I and Phase II together. It is imperative to note that the closure pour transfers forces to both sides of the bridge for dynamic stability.

4.7 Conclusion

Monitoring the Beaver Creek Bridge for three years provided a performance history for the precast GFRP deck panels. The bridge deck, which was constructed using GFRP reinforced precast panels, showed good composite action with the prestressed girders. The relative deflections between the bridge deck and the girders were monitored; the low modulus of the GFRP was a concern due to the possibility of incurring large deflections. Over a three-year period, the deck deflections were within the code design limits of 0.62 in. and the highest recorded deflection was 0.15 in. The highest recorded strain in the deck was 121 με and was within code design limits of 138 με and the curvature was small. During construction times where large trucks were utilized, the relative displacements were the maximum points in the data set. Vertical accelerations in the girders showed dynamic stability and the dynamic deflections were significantly less than the recorded static deflections. The live load distribution factors showed even load sharing between the girders and were below the AASHTO code limits. The collected VWSG and LVDT data were well below the design limits and showed no cracking in the deck panels.

The computer generated bridge model showed that deck deflections and deck stresses were within the code and the design limits. The model correlated with collected data from the field. The finite element model captured mode shapes that gave insight into bridge

properties. Significant modes showed good composite action between the GFRP deck panels and the precast girders as well as illustrating the load transfer at the cast-in-place closure pour. The parametric study of the bridge showed that deck thickness and girder number could be reduced; however, only deck deflection limits and deck stresses were checked for each scenario. From the tests carried out for the precast concrete bridge deck panels reinforced with GFRP bars, it is clear that this is a viable construction method.

4.8 Acknowledgments

The author acknowledges the financial assistance of the Utah Department of Transportation, especially Becky Nix. In addition, the author acknowledges Mike Adams from Campbell Scientific. Additional thanks are due to the students, faculty and staff of the University of Utah civil engineering department, especially Jim Ries.

4.9 References

1. Benmokrane, B., El-Salakawy, E., El-Ragaby, A., and Lackey, T. 2006. "Designing and Testing of Concrete Bridge Decks Reinforced with Glass FRP Bars." *Journal of Bridge Engineering* 11(2): 217-229.

2. Benmokrane, B., El-Salakawy, E., El-Gamal, S., and Goulet, S. 2007. "Construction and Testing of an Innovative Concrete Bridge Deck Totally Reinforced with Glass FRP Bars: Val-Alain Bridge on Highway 20 East." *Journal of Bridge Engineering* 12(5): 632-645.

3. Phillips, K., Harlan, M.; Roberts-Wollmann, C., and Cousins, T. 2005. "Performance of a Bridge Deck with Glass Fiber Reinforced Polymer Bars as the Top Mat of Reinforcement." Virginia Polytechnic Institute and State University.

4. American Association of State Highway and Transportation Officials. 2009. *AASHTO LRFD Bridge Design Specifications.* 4th Ed.

5. American Concrete Institute. 2006. *Guide for the Design and Construction of Structural Concrete Reinforced with FRP Bars ACI 440.1R-06*. American Concrete Institute, Farmington Hills, MI.

6. Broekhuizen, D., 1996. “Effects of Vertical Accelerations on Prestressed Concrete Bridges.” Thesis. University of Texas at Austin.

7. Precast/Prestressed Concrete Institute. 1999. *PCI Design Handbook,* Fifth Ed.

8. Pantelides, C., Ries, J., and Nix, R. 2011. “Precast GFRP Reinforced Bridge Deck Panels.” PCI/NBC Conference, Salt Lake City, UT.

9. El-Salakawy, E., Benmokrane, B., El-Ragaby, A., and Nadeau, D. 2006. “Field Investigation on the First Bridge Deck Slab Reinforced with Glass FRP Bars Constructed in Canada.” *Journal of Bridge Engineering* 11(3): 470-479.

10. *CSi Bridge SAP 2000*. 2011. Computer software. Vers. 14.1. Computers and Structures Inc. Web.

CHAPTER 5

DYNAMIC RESPONSE OF PRECAST BRIDGE SYSTEM

5.1 Abstract

The Beaver Creek Bridge on US Highway 6 in Utah was built in 2009 and has a span of 88 ft. Bridge elements included prestressed concrete girders and posttensioned precast concrete deck panels reinforced with Glass Fiber Reinforced Polymer (GFRP) bars. Some of the deck panels and the girders were instrumented for strain and deflection. The response of the bridge to traffic loads was collected remotely and continuously for 3 years. Collected data include vertical accelerations of the girders measured at midspan through accelerometers from truck loads. Testing of the bridge included five truck load tests that were carried out at various times. Collected dynamic truck load data were analyzed to provide dynamic deflections, structural damping and impact factors. The response of the girders is compared to design recommendations, as well as calculated responses from computer generated finite element models. It was determined that there is a correlation between truck axle weight and maximum girder acceleration at midspan. In addition, the results from the finite element model correlated well with the period of the bridge, dynamic displacements and magnitude of girder accelerations.

5.2 Introduction

In recent years the Utah Department of Transportation (UDOT) has taken proactive measures to increase the lifespan of its bridges as well as to decrease user delays. These measures include accelerated bridge construction (ABC) and the exploration of materials which decrease scheduled maintenance resulting from corrosion. UDOT decided to evaluate Glass Fiber Reinforced Polymer (GFRP) reinforcing bars as an alternative to steel rebar in bridge decks, to determine whether they could increase the lifespan of bridge decks, enough to match the service life of the entire bridge. The elastic modulus of GFRP bars is significantly lower than that of traditional steel reinforcing; the lower modulus leads to greater deflections. One way to check for serviceability is to monitor vertical accelerations in the girders, check for changes in deflections and the fundamental period of the bridge and compare the data to AASHTO's specification for dynamic load allowance of 1.33.[1]

Vertical accelerations are an important design consideration due to their influence on the integrity of the prestressed concrete girders. The accelerations may offset the maximum ductility requirements and the potential slippage and displacement at the seats of the girders.[2] Monitoring of vertical accelerations has been carried out for seismic loads, but less research has been conducted for truck traffic. The Geumdang 122 meter box girder bridge in Korea was instrumented with 16 piezoelectric accelerometers. Two sets of load tests were carried out using three trucks with three different weights (15, 30, and 40 tons) and three different velocities (40, 60, and 80 km/h).[3] The 40 ton test truck traveling at 80 km/h gave a 0.08 g response. Using a Fourier transform, the natural period of the bridge was found to be 0.33 seconds.

In 1997, the multiple span Confederation Bridge in Canada was configured with over 100 channels of sensors including accelerometers for dynamic behavior due to the elements[4]; 13 sections of the main girders were configured with accelerometers on the interior surface near the box girder web. Two accelerometers were configured at the pile shafts in addition to tri-axle accelerometers submerged at the pier base. The accelerometers had a sampling rate of 50 Hz and recorded natural events for 60 seconds. Collected data showed peak accelerations of 0.06g from wind loads. A finite element model produced eight significant mode shapes and correlated well with collected data set.

The University of Connecticut monitored a large continuous 170 ft four span bridge crossing the Connecticut River in Hartford.[5] Twelve accelerometers were used and data were collected for normal traffic loading. A finite element analysis was used to correlate the field data with the actual vibration modes. A fast Fourier transform was used to obtain peak acceleration levels, natural frequencies and mode shapes. The main activity occurred at the lowest natural frequency, of approximately 2.0 Hz. Testing showed that lower natural frequencies were unchanged when test vehicles crossed at different speeds and in different lanes. However, there were large variations in the acceleration levels. This was also the case when further testing was carried out with normal traffic. Acceleration data were used to estimate the displacement; the maximum displacement was estimated at less than 1.0 in.

Wireless Sensor System (WSS) is being implemented for GFRP bridge decks in New York.[6] A total of 30 wireless dual-axis accelerometers were configured at the steel girders and GFRP deck panels; peak accelerations from traffic testing did not exceed 0.010 g. However, eight clear mode shapes were obtained through analysis.

The Beaver Creek Bridge is a single span bridge composed of 12 AASHTO Type IV prestressed girders with two sets of precast panels lying perpendicular to the girders, 12 panels for each direction of traffic. The bridge has an overall span length of 88 ft-2 in. and an out to out width of 88 ft-10 in., as shown in Figures 5.1 and 5.2. The deck was designed in accordance with ACI 440.1 R-06[7], and constructed using a total of 24 precast deck panels. The bridge was constructed in two phases; a three-foot cast-in-place closure pour joins the two phases. This research focuses on Phase II of the Beaver Creek Bridge project. In Phase II, the west-bound bridge was constructed; its deck was composed of 12 similar precast panels each measuring 41ft-5 in. long, 6 ft-10 in. wide, and 9¼ in thick.

The bridge was configured with six single-axis accelerometers, noted as 'ACC' in Figure 5.1. The accelerometers were attached to the bottoms of girders 1-6 at midspan of the bridge to measure vertical accelerations as shown in Figure 5.1. The sensors were connected to a datalogger that was used during truck load tests to obtain peak accelerations. In addition, the accelerometers were used during long term monitoring for the collection of acceleration signatures and the triggering of a fixed camera at the site that was used to take pictures of the trucks causing the accelerations. The accelerometers have a sampling rate of 50 Hertz and a sensitivity of 0.001g; the event trigger for long term monitoring was set at 0.025 g. The accelerometers record 300 records per trigger at a time step of 0.02 seconds for truck load testing and 0.04 seconds for ambient/ long term monitoring.

A still camera was mounted on a 15 ft post located approximately 30 ft north of the west abutment as shown in Figure 5.3. The purpose of the camera was to obtain a visual

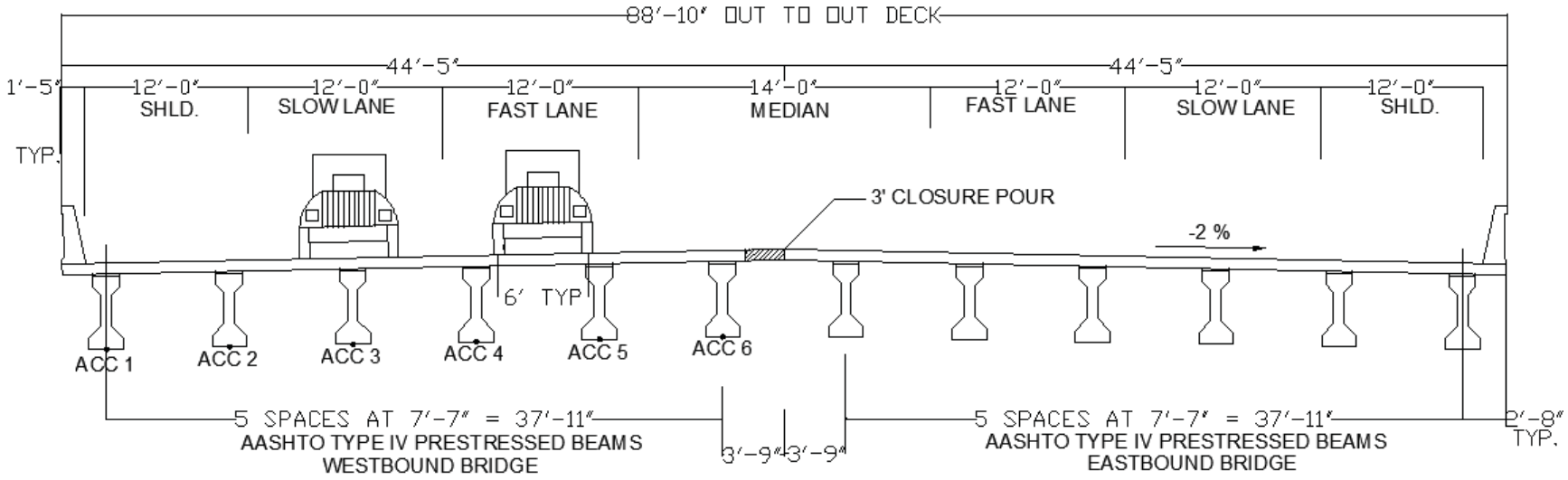

Figure 5.1. Elevation of Beaver Creek Bridge showing deck and girder

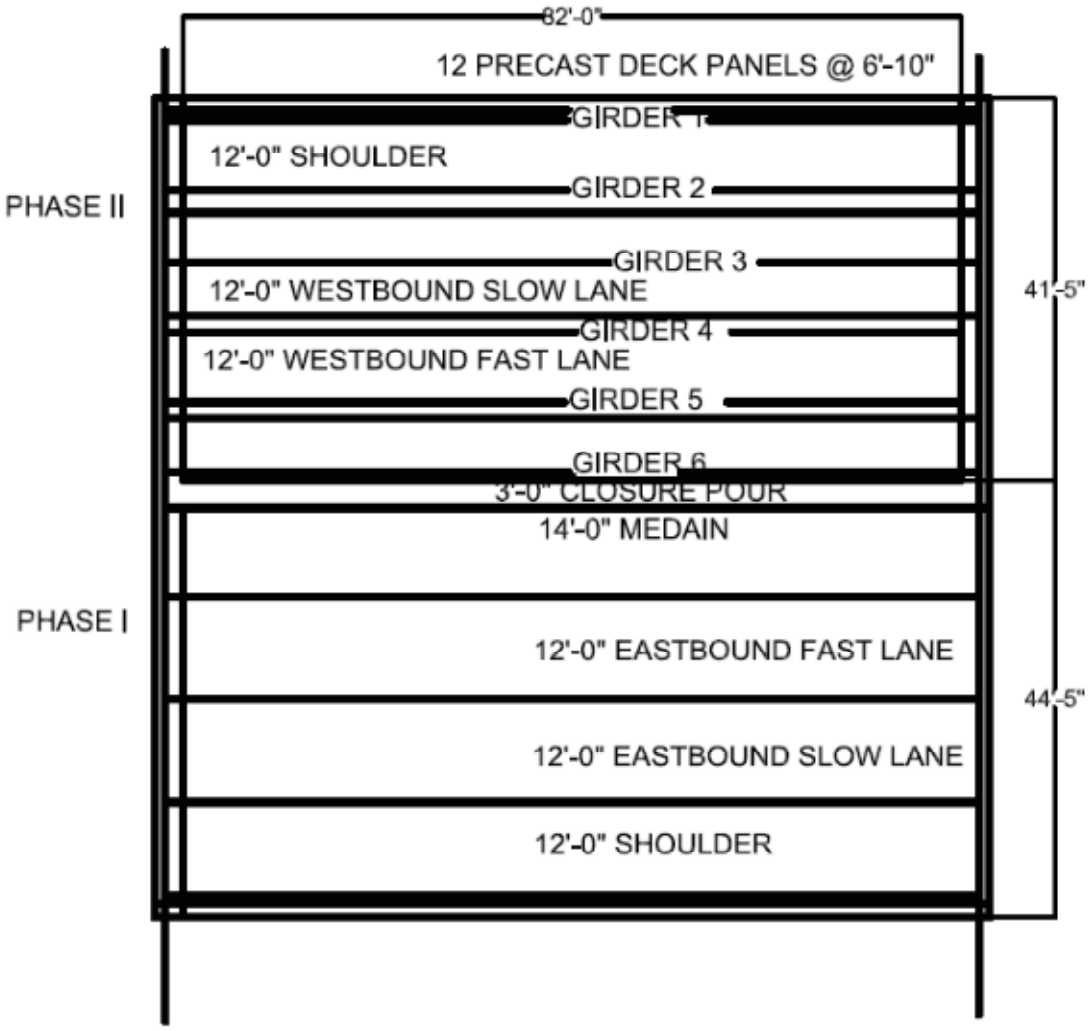

Figure 5.2. Plan view of Beaver Creek Bridge showing prestressed girders and traffic lanes

Figure 5.3. Still camera used for visual record of trucks causing large accelerations

record of the vehicle that caused large accelerations. The camera is triggered whenever ACC 2 at midspan of the second girder exceeds the threshold of 0.025g.

5.3 Truck Load Testing

Truck load testing was carried out for this research at the opening of the bridge and a year later with known truck weights and a range of test speeds. Table 5.1 shows truck load test data for September 29, 2009, September 1, 2010 and November 19, 2010. Figure 5.4 shows typical truck test dimensions during 2009 and 2010.

For the September 29, 2009, Tests 1 and 2 were conducted at 40 miles per hour (mph) with each truck in its respected lane, one at a time. Test 3 was performed with both trucks simultaneously traveling at a speed of 35 mph. Tests 4 and 5 were faster versions of tests 1 and 2 and were conducted at 65 mph. Truck load tests carried out September 1, 2010 were of a similar fashion. A 37.94 kips truck was positioned in the slow lane, a 45.68 kip truck was in the fast lane. A third truck load test was performed on November 19, 2010 with a truck weighing 65.9 kips; this truck was positioned in the slow lane and, due to the type of truck, could only reach a maximum speed of 55 mph. The heavier truck is used to observe how the bridge responds to a heavier load and whether there was a relationship between girder response and truck weight. A fourth and fifth test were conducted on November 21, 2011 and December 5, 2011, which were ambient traffic tests with trucks of a known weight and truck speeds collected from a Lidar gun.

5.4 Truck Load Test Observations

The first truck load test was carried out on September 29, 2009 just before the bridge was opened to traffic. The second truck load test was carried out on September 1, 2010 while the bridge was closed to traffic for maintenance operations. All six accelerometers

Table 5.1. Truck Load Test Data

Date	Test	Lane	Weight, kips	Speed, mph	Maximum response, g
Sept. 29, 2009	1	Slow	43.88	40	0.0156
	2	Fast	43.16	40	0.0262
	3	Both	43.88, 43.16	35	0.021
	4	Slow	43.88	65	0.024
	5	Fast	43.16	65	0.026
Sept. 1, 2010	1	Slow	37.94	10	0.0019
		Fast	45.68	10	0.0019
	2	Slow	37.94	20	0.00696
		Fast	45.68	20	0.00323
	3	Slow	37.94	30	0.00408
		Fast	45.68	30	0.0027
	4	Slow	37.94	40	0.00614
		Fast	45.68	40	0.00746
	5	Slow	37.94	50	0.00867
		Fast	45.68	50	0.0048
	6	Slow	37.94	57	0.0096
		Fast	45.68	58	0.0128
	7	Slow	37.94	70	0.0142
		Fast	45.68	60	0.011
Nov. 19, 2011	1	Slow	65.9	10	0.0034
	2	Slow	65.9	20	0.0036
	3	Slow	65.9	30	0.0075
	4	Slow	65.9	40	0.0035
	5	Slow	65.9	50	0.016
	6	Slow	65.9	55	0.0093

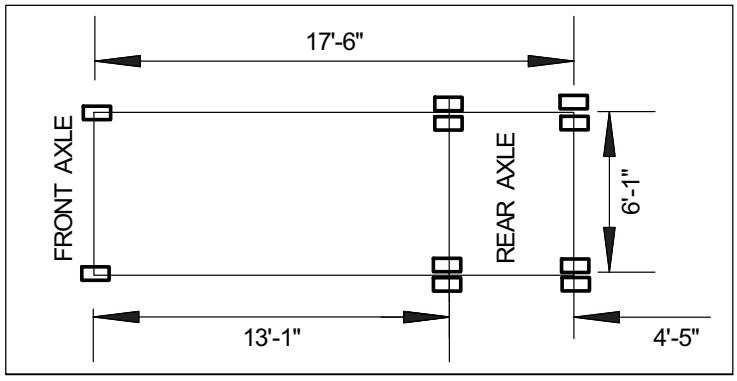

Figure 5.4. Test Truck Dimensions

measured data as shown in Figure 5.5. During the first truck load test, accelerations measured at midspan of the prestressed girders for the 43.16 kips truck traveling in the fast lane at 40 mph showed that the maximum vertical acceleration recorded was 0.015g at midspan of girder 2 (Test 1 in Figure 5.6). By comparison, the maximum acceleration for the truck traveling at 65 mph was 0.026g at midspan of girder 4 (Test 5 in Figure 5.7). Dynamic truck load tests, carried out during the second truck load test of September 1, 2010, showed a maximum overall vertical acceleration of 0.014 g, as shown in Figure 5.8.

A third dynamic truck load test was performed on November 19, 2010 with a truck weighing 65.9 kips. The truck was positioned in the slow westbound lane and, due to the type of the truck used, could reach a maximum speed of only 55 mph. The maximum acceleration was 0.016 g at 50 mph as shown in Figure 5.9. From Table 5.1, there is a trend relating a higher speed to a larger response. Additionally, the heavier truck produced a larger acceleration than the lighter trucks in previous tests. This lead to the collection of ambient data which were known to be heavier trucks.

Truck load tests were carried out in ideal weather conditions and the weight and speed of the truck were known. However, some of the higher acceleration data measured from long term monitoring comes from continuous monitoring and capturing “snapshots” of real life conditions at the bridge. The data and picture below in Figures 5.10-5.11 is a representation of such events; the event triggering the fixed camera’s clock is synchronized 1 min. different than the datalogger’s clock. The particular truck in Figure 5.11 gave a maximum acceleration of 0.032 g as shown in Figure 5.10. The weight and

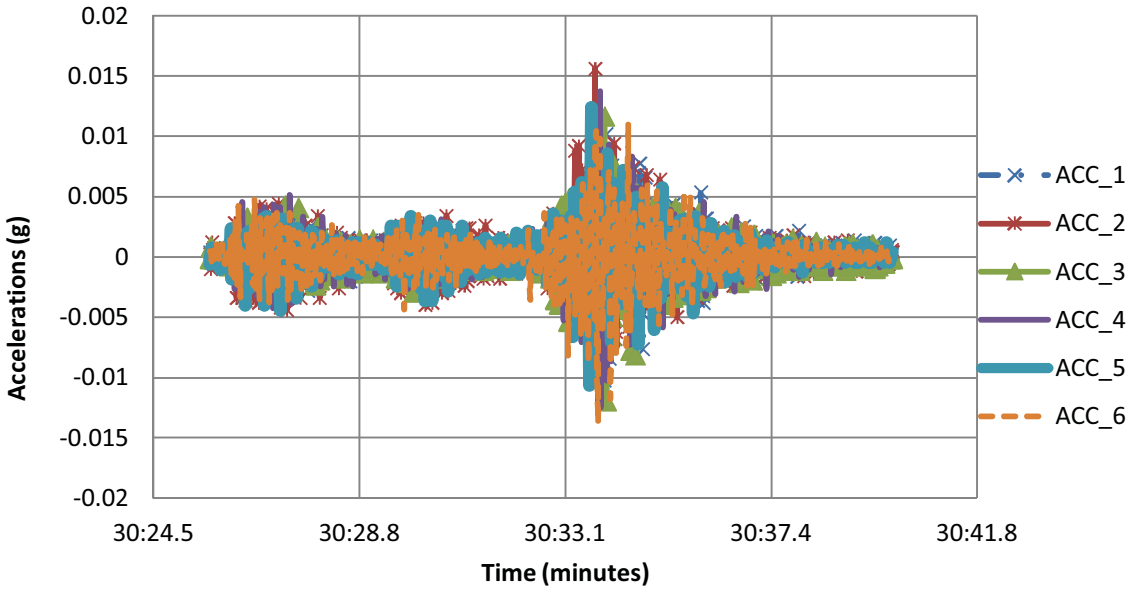

Figure 5.5. Acceleration record for 43.88 truck traveling at 40 mph for Test 1.

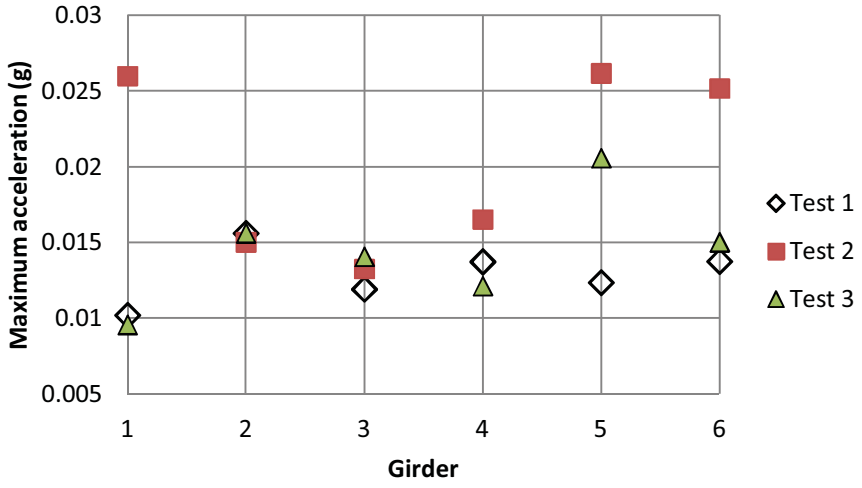

Figure 5.6. Maximum accelerations for trucks traveling at 40 mph.

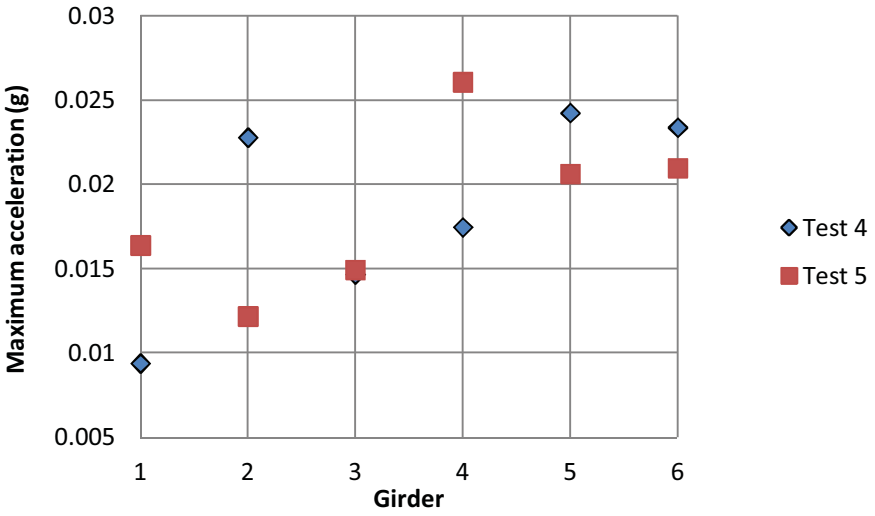

Figure 5.7. Maximum accelerations for trucks traveling at 65 mph

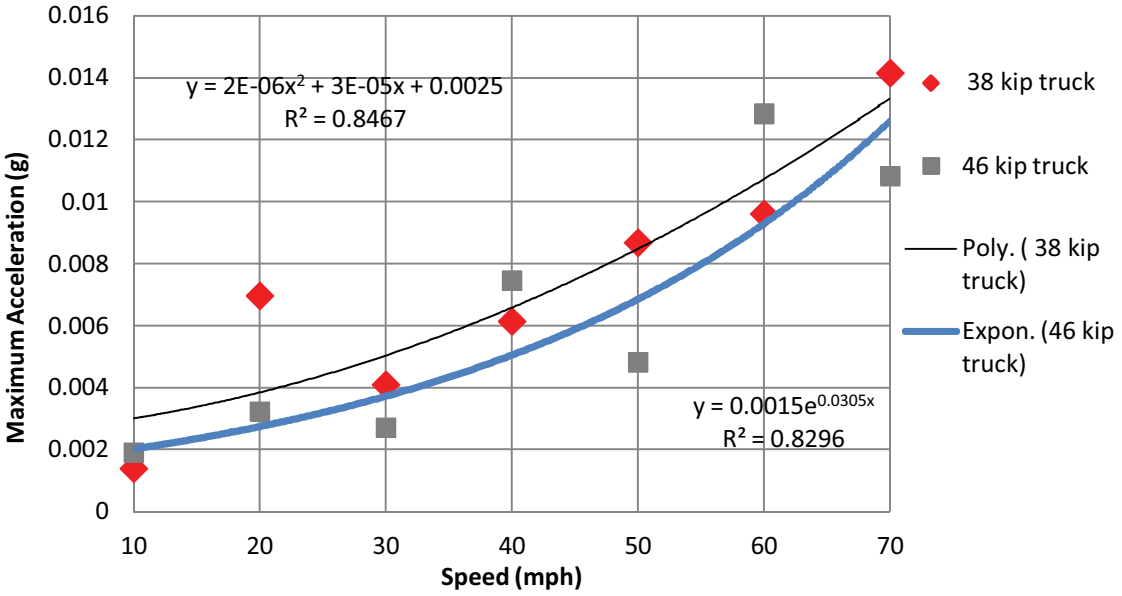

Figure 5.8. Maximum accelerations from second truck load test performed Sept. 1, 2010, as a function of truck speed.

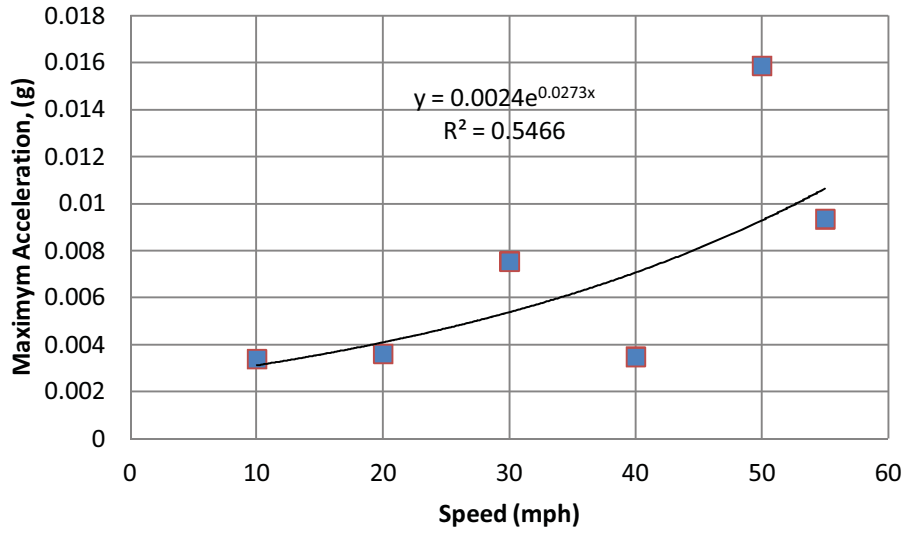

Figure 5.9. Maximum acceleration from third truck load test performed Nov. 19, 2010, as a function of truck speed

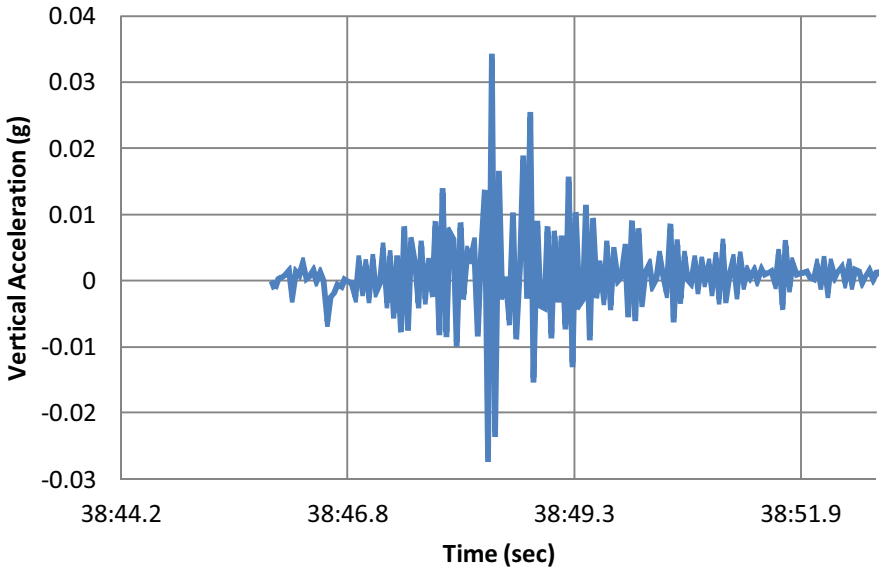

Figure 5.10. Acceleration record for Oct. 15, 2010 during a construction period near the bridge

Figure 5.11. Picture of truck for acceleration of Figure 5.10

speed of the truck are not known. However, the event triggering camera shows construction activity in the vicinity of the bridge for that month.

5.5 Ambient Truck Observations

In addition to special events and planned testing, real time accelerations were captured using accelerometers 2 and 3. These responses were significantly larger than what was observed with controlled annual truck tests, with accelerometer 3 peaking at -0.074g to -0.078g. The trucks from ambient data represent the traffic actually on the bridge. Over the course of three days, representative screen shots with live feed were captured; the highest daily response measured by accelerometers 2 and 3 (represented by two lines) is shown in Figures 5.12-5.14, with vertical acceleration measured in g's versus real time.

As observed in Figures 5.12-5.14, ambient data show accelerations without the knowledge of the truck weight or speed. On November 21, 2011 a fourth truck load test was carried out. A continuous sample of 90 trucks traveling westbound were weighed at the UDOT Peerless Port of Entry No.8037 Highway 6. The port of entry is approximately 10 miles from the bridge. The research team collected truck speeds using a Pro Laser III LiDAR gun; thus, both the truck weight and speed were known. The sample set included trailers, tankers, flatbeds, cabs and small trucks. The times were recorded as the trucks passed over the bridge at midspan, making it possible to match the truck with the accelerometer data recorded. Accelerometers 2 and 3, positioned at midspan of girders 2 and 3 in the slow lane, were used for ambient data collection. Sample pictures and acceleration records of trucks in the data set are shown in Figure 5.15. There is a trend showing that the larger truck weight, the larger the vertical response.

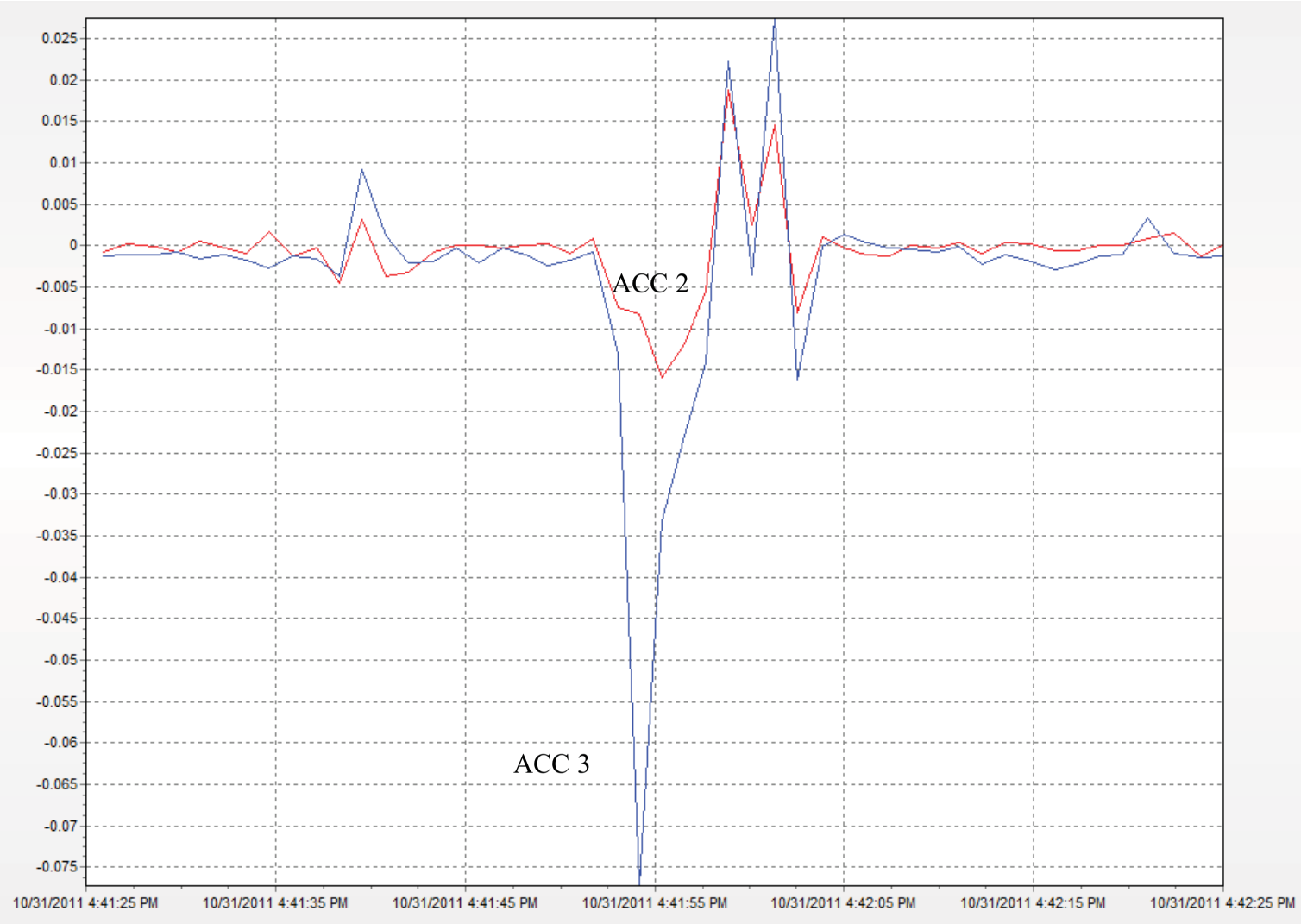

Figure 5.12.Acceleration of -0.075 g at midspan of girder 2 on October 31, 2011

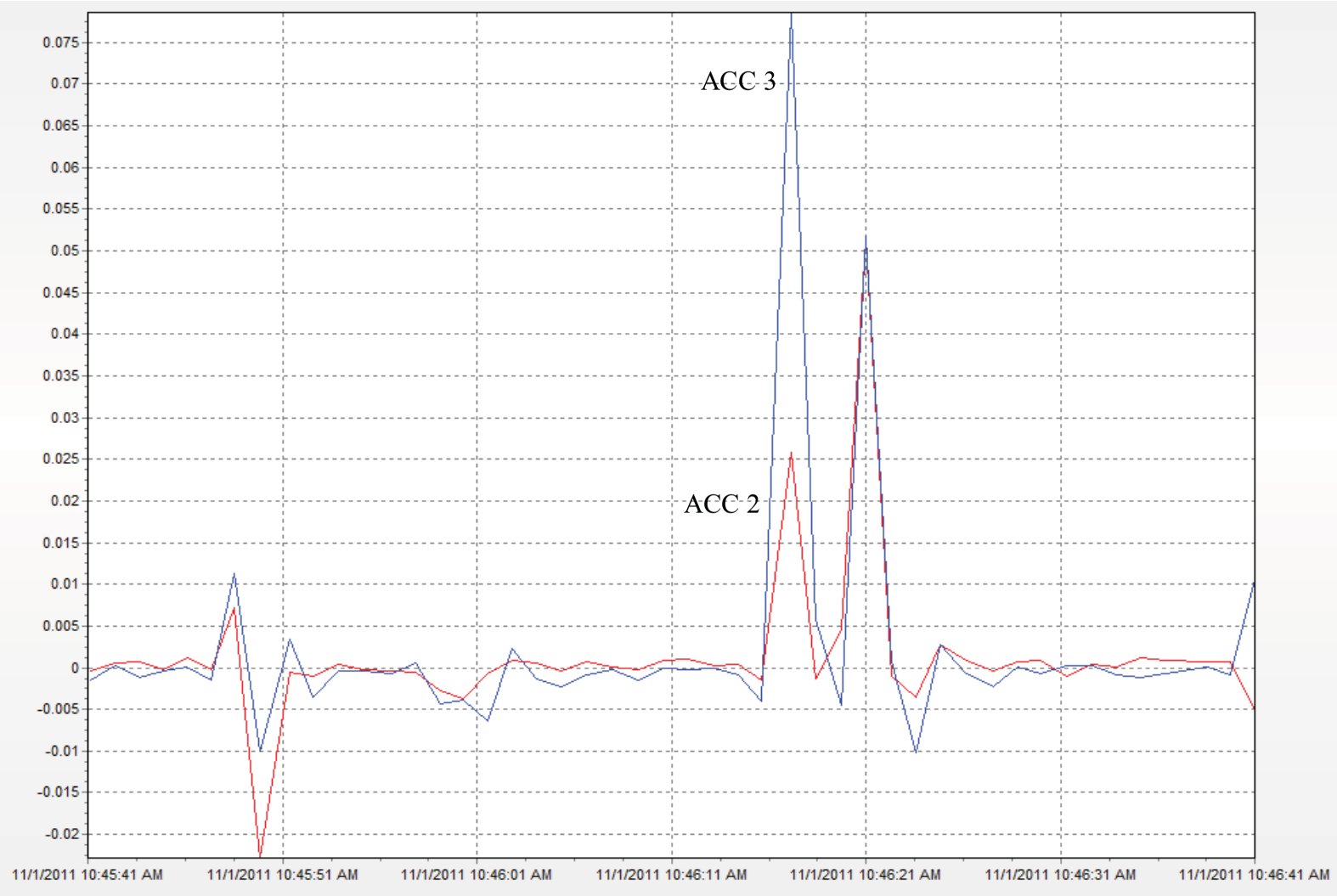

Figure 5.13. Acceleration of 0.078 g at midspan of girder 2 on November 1, 2011

Figure 5.14. Acceleration of -0.074 g at midspan of girder 2 on November 2, 2011

Box Truck weight = 60.98 kips

Truck speed = 48 mph, 3 axles

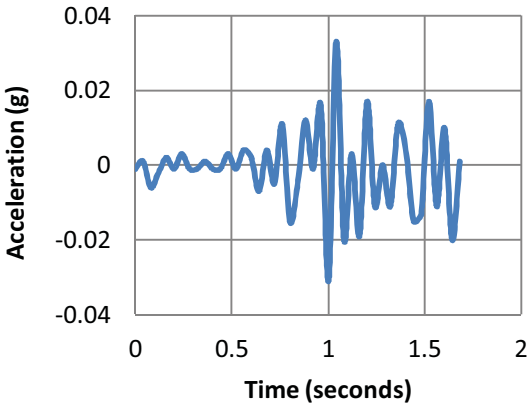

Tank Truck weight = 119.22 kips

Truck speed = 62 mph, 5 axles

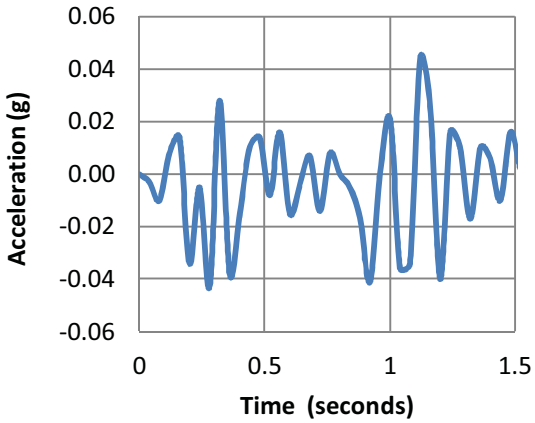

Flatbeds are not weighed

Truck speed = 67 mph, 3 axles

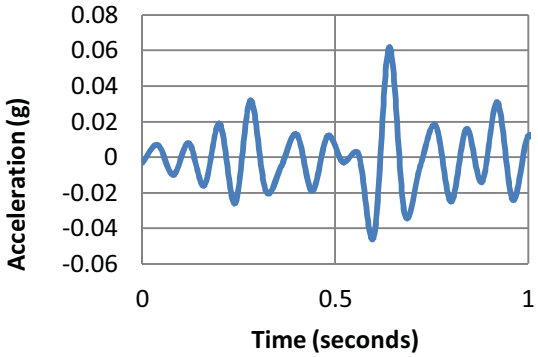

Figure 5.15. Sample of trucks in the data set and
their corresponding acceleration response

5.6 Correlation of Truck Weight, Speed and Girder Acceleration

Of the data set collected on November 21, 2011, 19 of the 90 trucks were able to be matched with a speed, weight, and acceleration signal and the data are shown in Figure 5.16. The acceleration response is compiled in groups of 2.5%-5%g, 5%-7.5%g and 7.5%-10%g.

The heaviest truck was 119.22 kips travelling at 62 mph with a response of 0.088 g. The fastest truck tested was travelling at 68 mph and weighed 60 kips; the corresponding response was 0.053g. The largest response was 0.105g and was triggered by a 62 kip truck traveling at 65 mph; however, there was another truck on the bridge at the same time traveling eastbound that may have added to the acceleration response.

Correlating truck weight to vertical acceleration response provided a baseline data set; however, some trucks were longer than the bridge span and influenced the weight distribution. Additionally, the accelerometers were triggered with multiple trucks on the bridge, making it difficult to know which truck belonged to which response. Ambient truck testing performed on December 5, 2011 collected axle weights from the trucks leaving the port of entry and traveling westbound; speeds were measured and trucks were documented with pictures from east and west bound traffic. Of the total sample size of 196 trucks, 69 trucks were traveling eastbound. For westbound traffic, 73 trucks were weighed; of those 73 trucks, 54 trucks were able to be matched up with speeds, vertical accelerations and pictures. Using the pictures, data were separated into single trucks on the bridge, trailing trucks, trucks in either lane and trucks on the opposite side of the bridge. With this information, vertical acceleration data could be refined. Table 5.2 shows ambient truck observations.

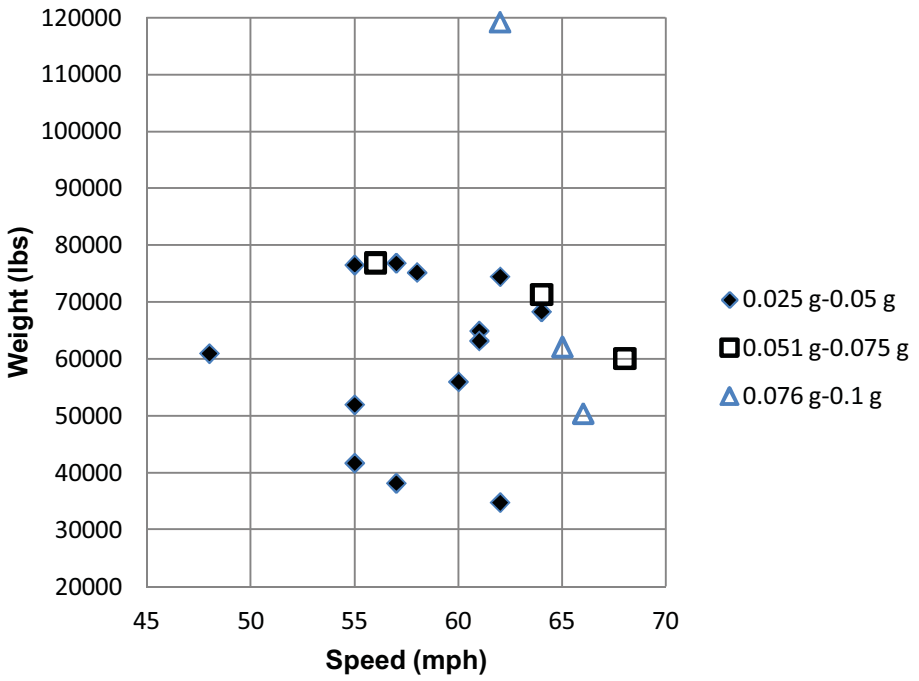

Figure 5.16. Accelerations as a function of weight and speed from Nov. 21, 2011 test

Table 5.2. Ambient truck observations

Date	Traffic Direction	Sample Size	Speed Range (mph)	Weight Range (kips)	Maximum Response (g)
Nov. 21, 2011	West	13	48-64	34.8-76.9	0.050
	West	3	56-68	60.1-76.9	0.072
	West	3	62-66	50.4-119.2	0.105
Dec. 5, 2011	East	69	50-68	--	0.097
	West	47	55-66	30-80	0.064
	West	7	61-68	80-130	0.099

Eastbound traffic speeds were compared to westbound traffic speeds; eastbound trucks were not weighed and there are no accelerometers on the eastbound side of the bridge. If the wheel load was not located on or very near a sensor, the accelerometers triggered similarly for eastbound and westbound traffic, as shown in Figure 5.17. This shows good composite action between both construction phases; the closure pour functioned well and was able to transfer a load path between Phase I and Phase II construction. The two-phase construction at the bridge emulates cast-in-place construction.

When a truck passes over the bridge, the acceleration of the truck load is transferred from the deck to the girders. The accelerometers triggered at 0.025 g; the first set of axles usually triggered the instrument. The double tank truck pictured in Figure 5.18 will be used as an example of axle data analysis. This type of truck gives the highest vertical accelerations in the data set, has the longest length (approximately 95 ft) and has five axles; this type of truck is an exclusion vehicle, meaning it surpasses the 80 kip weight limit for the bridge. Axle weights are plotted with peaks in the acceleration response, shown in Figure 5.19. The accelerometers do not trigger at the same time due to a time lag factor; it takes time to transfer wheel loads through the deck and girders. Additionally, the number of axles give a different response; more axles compound the vertical acceleration due to impulse loads shown in Figure 5.20. It is to be noted that two of the trucks having four axles were empty flatbeds which produces unbalanced impulses. If the truck is traveling at the posted speed of 65 mph; it takes less than a second (95.3 ft/second) to cross the 90 ft bridge. It typically takes 0.3 seconds from the timestamp one axle passes over the sensor until the next axle passes over the sensor. This leaves the first

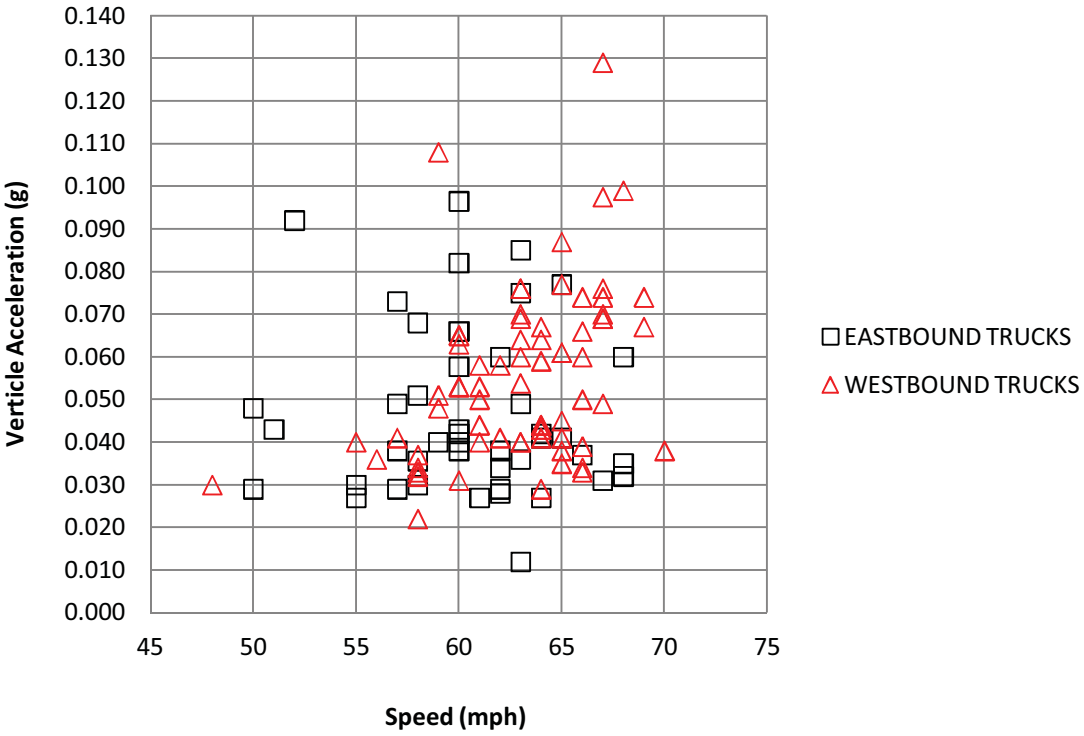

Figure 5.17. Response comparison between eastbound and westbound truck traffic

Figure 5.18. Double tank exclusion vehicle example Truck with five axles and 95 ft long

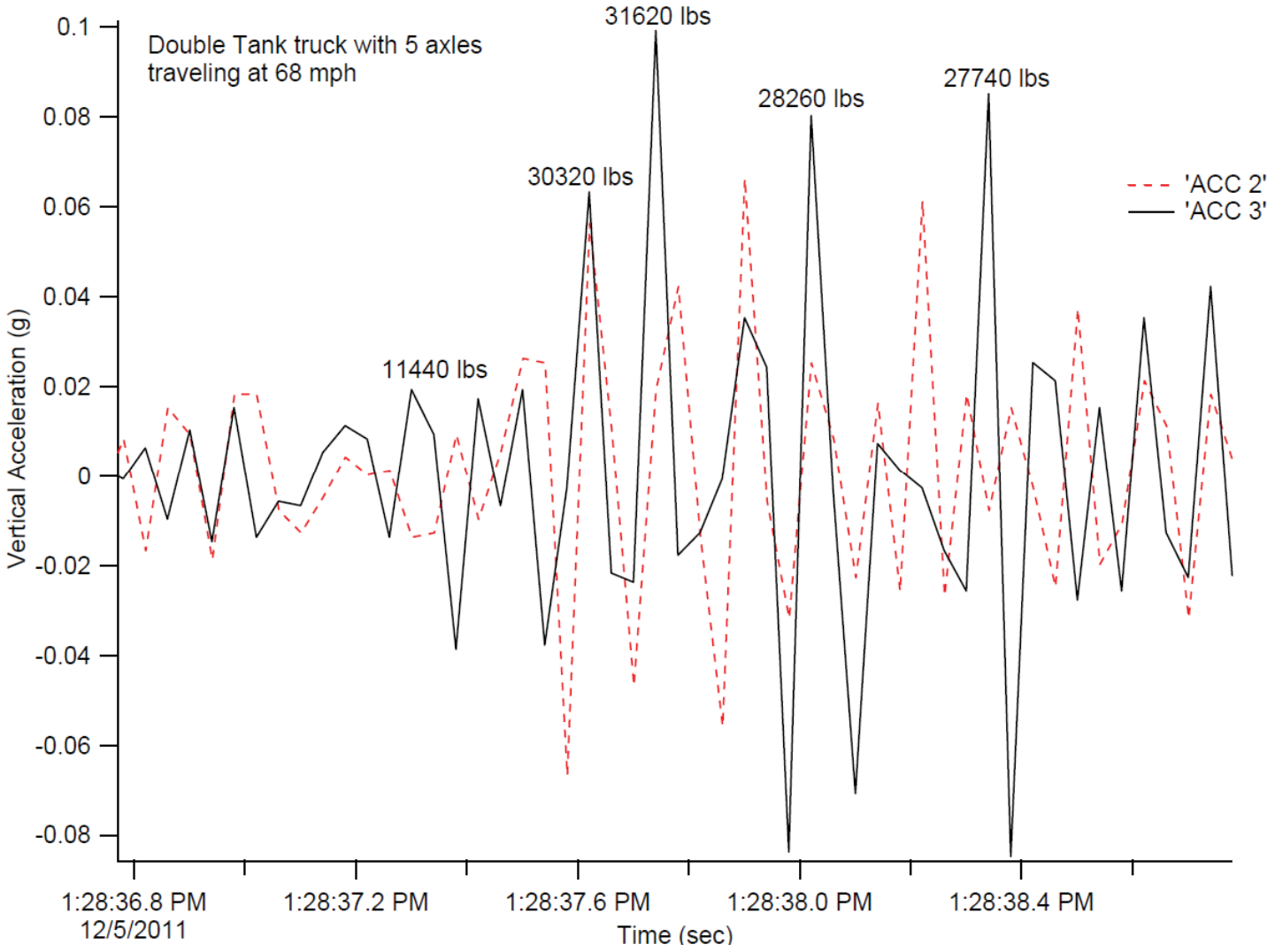

Figure 5.19. Axle weights corresponding to acceleration peaks, total truck weight of 129 kips

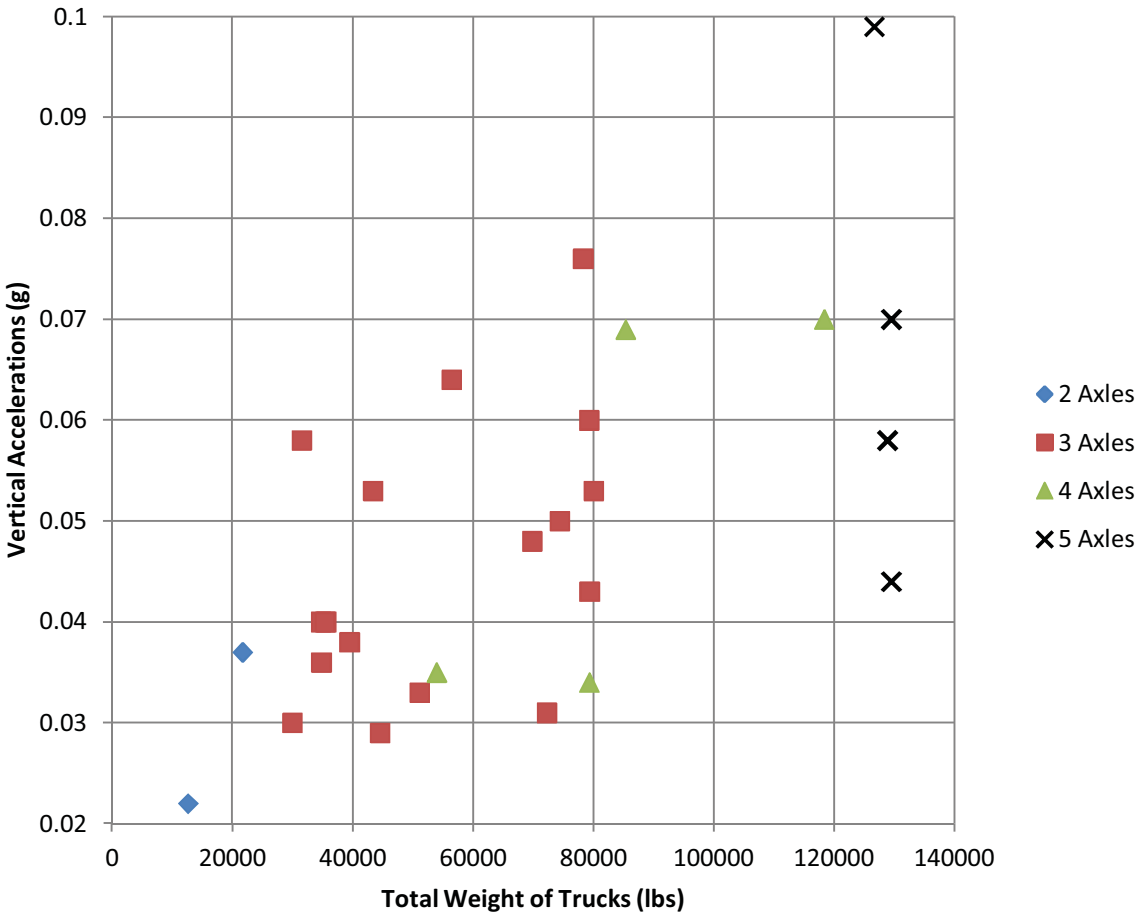

Figure 5.20. Number of axles compared to vertical accelerations

axle response still active when the second set of axles pass over the sensor. By linear superposition in the elastic range, the effects of multiple axles yield a greater vertical acceleration. However, the most significant axles are the first two or three sets. Because the first mode frequency will be shown as 0.125 seconds and the level of damping is 1.47%, the significant effects of the earlier axle loads are damped out. Table 5.3 shows travel time between axles and the cumulative loading effects from Figure 5.18.

A chart comparing the axle weight that gave the largest acceleration with truck speed and vertical accelerations is shown in Figure 5.21. This observation shows that the axle weight, not the total truck weight, influence the peaks in the acceleration records. Axle weight ranges of 25,000 pounds to 35,000 pounds gave vertical accelerations in the range of 0.04 g to 0.09 g. Axle weights below 20,000 pounds gave vertical accelerations below 0.05 g. Similarly, a chart comparing total truck weight and truck speed with vertical accelerations is shown in Figure 5.22. Total truck weight ranges of 80,000 pounds to 130,000 pounds gave vertical accelerations in the range of 0.05 g to 0.09 g. Total truck weights below 80000 pounds gave typical vertical accelerations below 0.05 g. Multiple trucks on the bridge at the same time also skew acceleration data. Only single trucks on the bridge are shown in Figure 5.22 which is a good comparison to Figure 5.21 where multiple trucks were present at times; the data in Figure 5.21 are more clustered than Figure 5.22, which shows an upward trend. This shows that multiple trucks on the bridge at the same time add to the vertical acceleration.

Using typical truck dimensions, accelerometer data can be refined based on axle weight and spacing. It is important to note that a typical axle width per AASHTO is six ft; the girders and sensors on the bridge are spaced at 7 ft-7 in. AASHTO provides some

Table 5.3. Travel time between axles and the cumulative loading effects from exclusion vehicle example truck with five axles and 95 ft long

Speed	Axle Number	Axle Weight (lbs)	Distance Between Axles (ft)	Travel Time Between Axles (seconds)	Total Travel Time (seconds)
68 mph 100 ft/second	1	11440	17	0.25	0.96
	2	30320	30	0.12	
	3	31620	21	0.28	
	4	28260	18	0.31	
	5	27740	-	-	

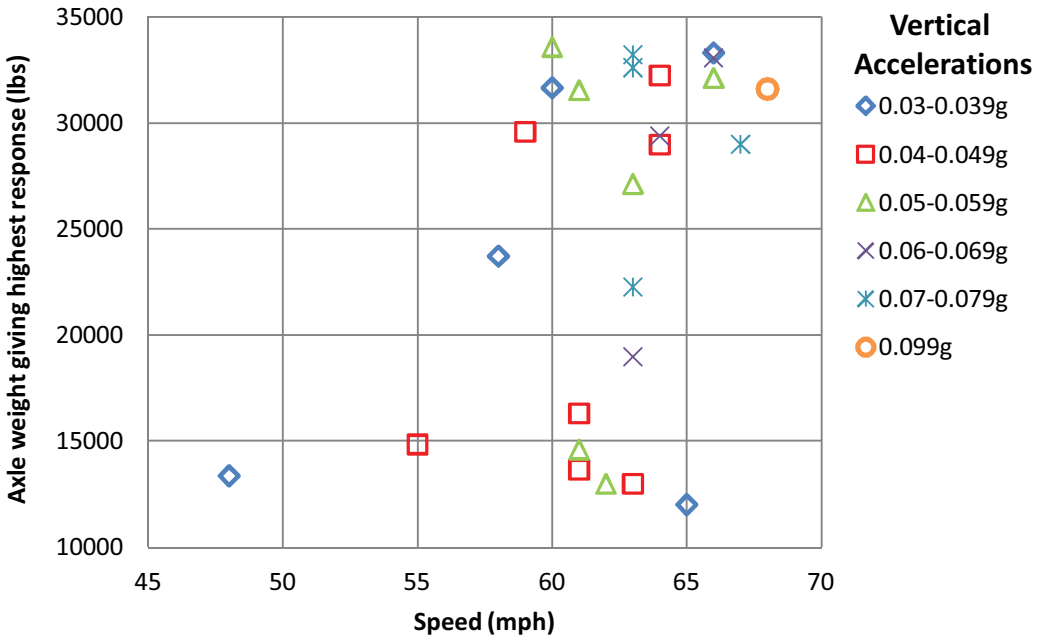

Figure 5.21. Axle weight giving the highest accelerations compared to truck speed

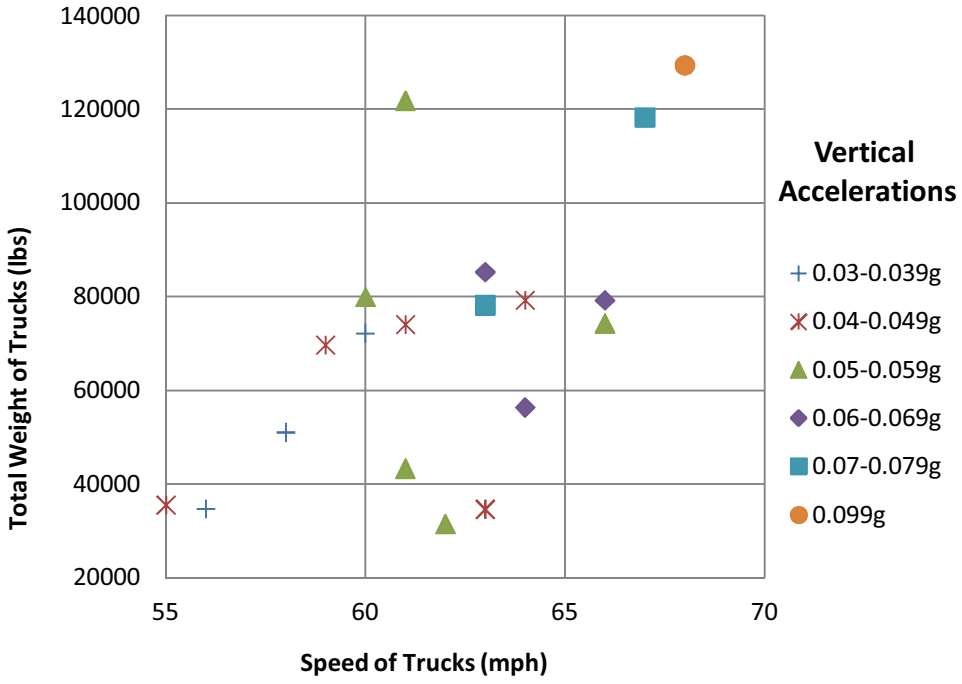

Figure 5.22. Single total truck weight compared to truck speed

standard cab and trailer axle spacing. Most box trucks have a trailer axle spacing of 48 ft; most tank trucks have a trailer axle spacing of 30 ft. The effect of axle spacing was studied by comparing two trucks weighing the same total weight, same number of axles and traveling at approximately the same speed, as shown in Figures 5.23 and 5.24. The box truck with the larger axle spacing gave a larger acceleration (-0.083g) in comparison to the tank truck (0.06g). Therefore, the acceleration magnitude depends on axle weight and spacing.

To observe trends better, ambient data from both November and December 2011 tests were combined for a larger sample size of 74 that included only single trucks on the bridge. Truck speed and truck weight were compared to accelerations separately to discern trends, as shown in Figures 5.25 and 5.26. The posted speed on the bridge is 65 mph and the posted legal weight is 80 kips. The velocity showed a very slight upward trend. However, the sample size of ambient speeds had a narrow range of 48 mph to 75 mph; the sample size needs to be larger to make further conclusions. There are a number of exclusion vehicles that pass over the bridge that are over the legal weight limit of 80 kips. Therefore, weight as well as legal weight was plotted to find any trends. The data showed that the exclusion vehicles consistently triggered accelerations above 0.053g; trucks below 80 kips had a typical range of accelerations from 0.025g to 0.065g.

5.7 Analytical Results

From the collected data, the impact factor and damping coefficients were evaluated. The first truck load test accelerations shown in Figure 5.27 are used in order to compare with the static deflections of the girders before the bridge opened to traffic.

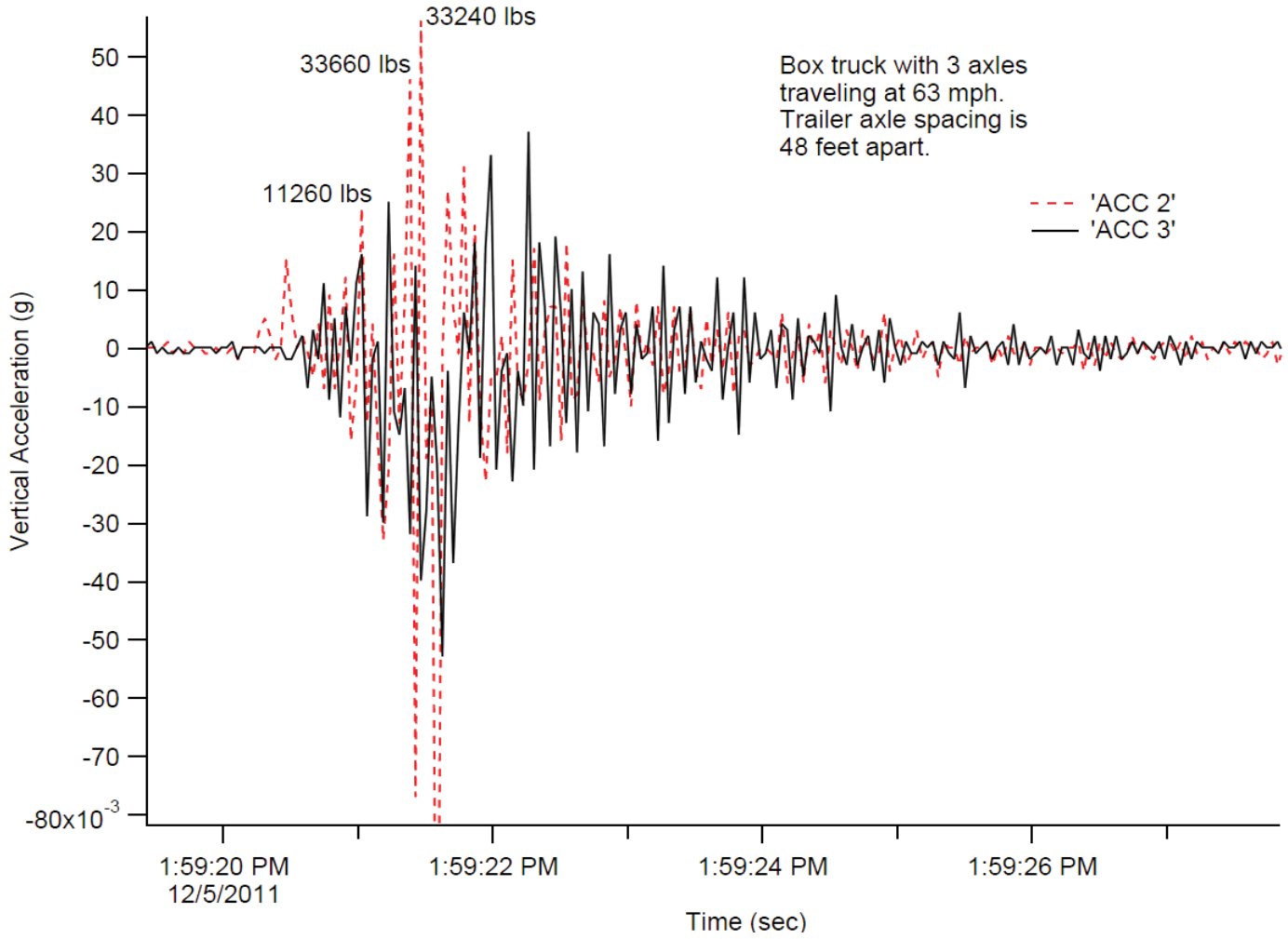

Figure 5.23. Box truck weighing 78 kips with a trailer axle spacing of 48 ft

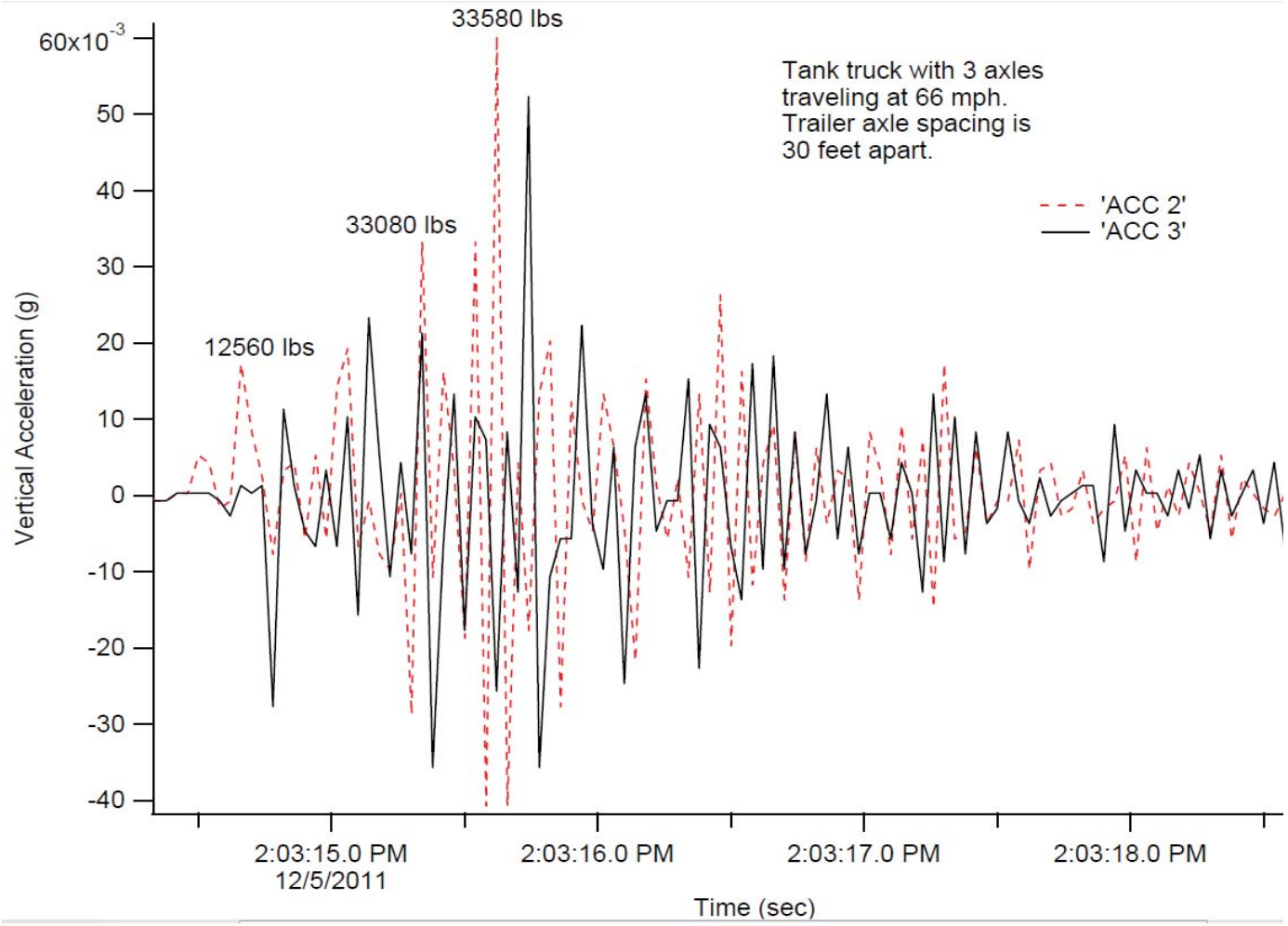

Figure 5.24. Tank truck weighing 79 kips with a trailer axle spacing of 30 ft

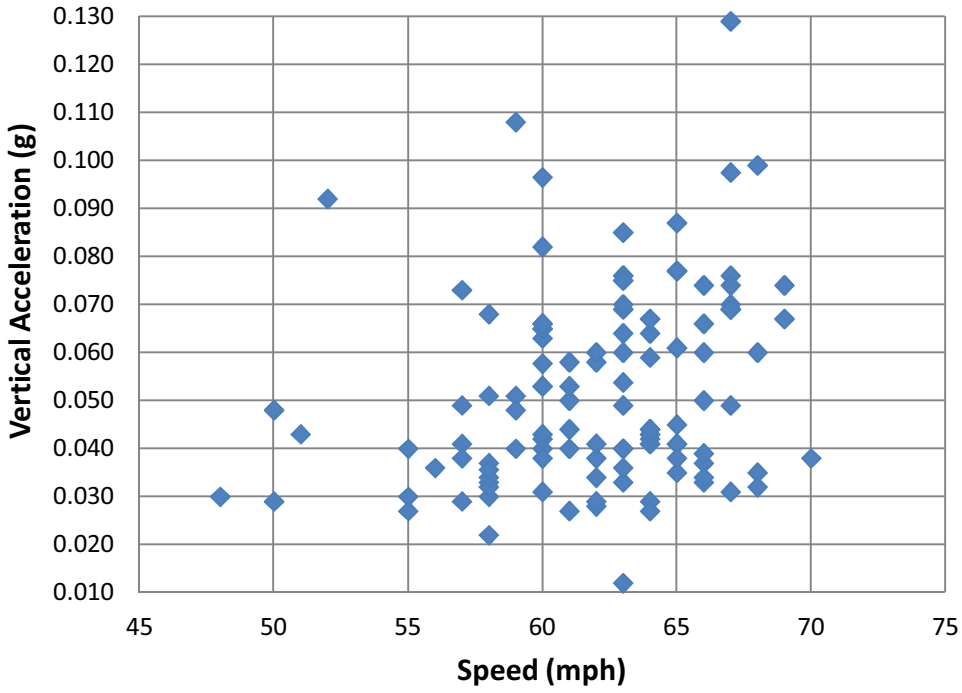

Figure 5.25. Truck Speed compared to vertical accelerations

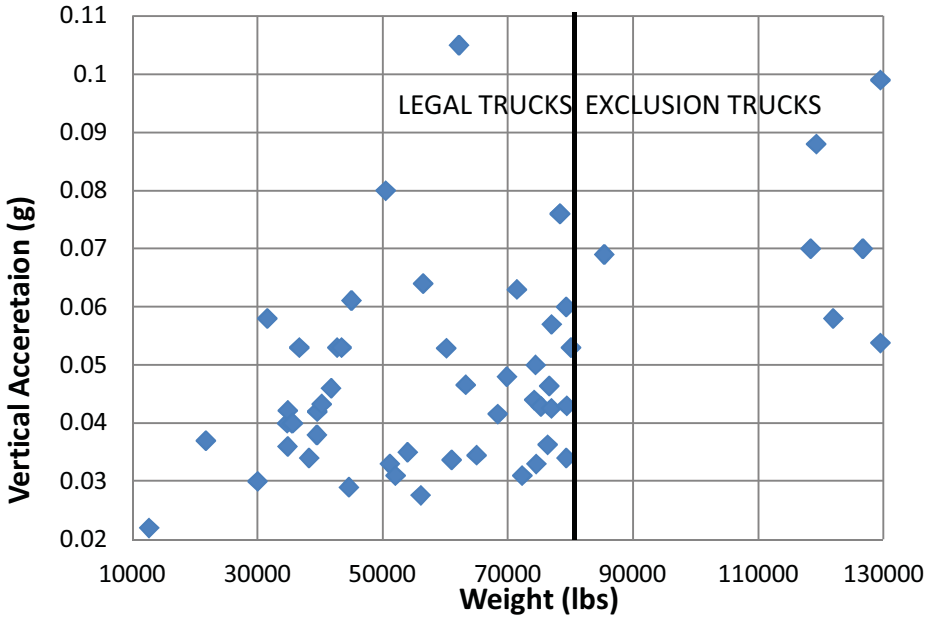

Figure 5.26. Truck Weight compared to vertical accelerations

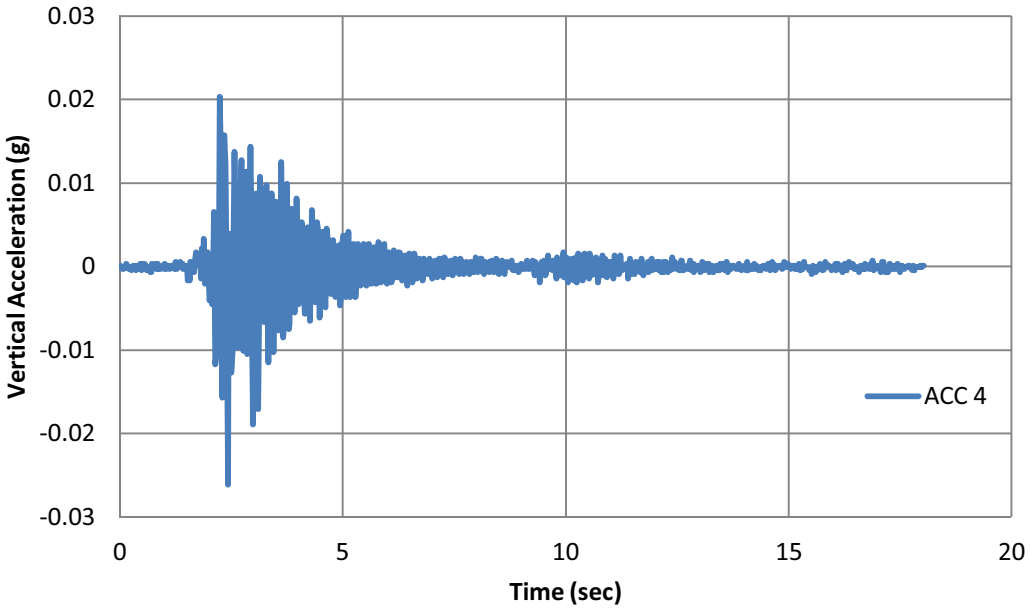

Figure 5.27. Acceleration data for a 43 kip truck traveling at 65 mph from first truck load test, September 2009

From the acceleration data, the damping ratio can be determined using the logarithmic degradation, as shown in Equation (5.1).

$$A(t) = e^{-2\pi * fn * t * \xi} \tag{5.1}$$

where A is the acceleration and t is time. The average peak-to-peak time for vertical acceleration was 0.12 seconds. With a period of 0.12 seconds, the corresponding frequency, fn, is 8.33 Hz. Using this accelerometer data set, the damping ratio is calculated to be ζ=1.47%. Three similar trucks from ambient data weighing 42 to 45 kips and traveling at 60 to 64 mph were analyzed and gave an average damping ratio of ζ=1.45%. The constant average acceleration method can used to determine dynamic displacements in terms of the initial acceleration, velocity and displacement[8], as shown in Equation (5.2).

$$X = Xo + \Delta t(\dot{X}o) + \frac{1}{3}(\ddot{X}o)(\Delta t^2) + \frac{1}{6}(\ddot{X})(\Delta t^2) \tag{5.2}$$

This equation yields a maximum dynamic displacement of 0.014 in. from the 43.16 kip truck during the September 2009 test. This deflection occurred over girder 4 for the truck traveling at 65 mph as shown in Figure 5.28.

To find the dynamic load allowance, or impact factor IM, the most extreme dynamic displacement is divided by the maximum static displacement. Before the bridge was opened to traffic, a survey was completed for the static displacement of the girders using the test trucks. Out of nine tests, the maximum static displacement occurred on girder 4 for the 43.16 kip truck during the September 2009 test and was 0.096 in. This combined

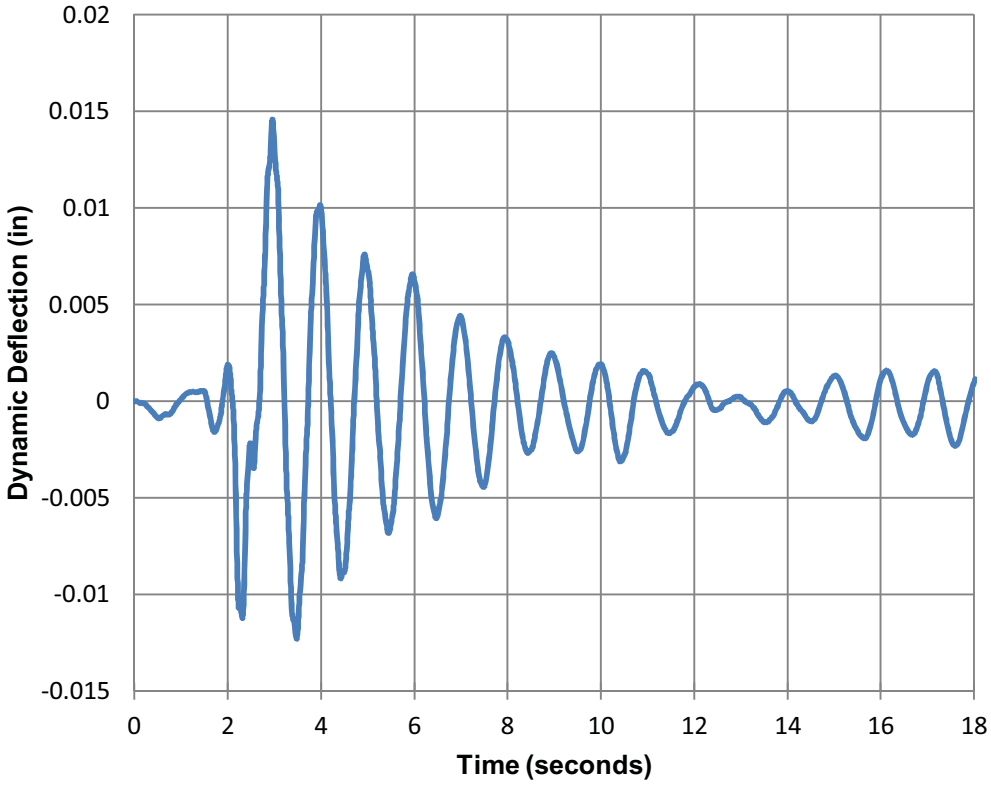

Figure 5.28. Dynamic deflection of 43 kip truck at 65 mph over girder 4

with Figure 5.18 gives an impact factor IM of 1.15. Three similar trucks from ambient data weighing 42 to 45 kips and traveling at 60 to 64 mph were analyzed and gave a dynamic load allowances of 1.20, 1.17 and 1.16. Research has shown that for a similar test using an HS-20 truck (72 kips) traveling at 60 mph on a 140 ft. FRP bridge deck, the impact factor was 1.15.[9] This shows good correlation and for all data, and it is lower than the AASHTO code allowance of 1.33. AASHTO's specification is used for extreme load effects; therefore, extreme events such as exclusion vehicles are analyzed and modeled in this research.

The accelerometers do not trigger evenly due to the fact that truck wheels do not pass over the center of the sensor, as shown in Figure 5.1. The closer the wheel load passes over the accelerometer, the higher the response. If a lighter truck is more centered on the accelerometer, it may give a higher response than that of a heavier truck which is not centered on the accelerometer. This is plausible due to the load sharing effects of multiple girders. A chart representing the relative difference in dynamic deflection of truck wheels between two adjacent sensors, ACC 2 and ACC 3, is shown in Figure 5.29. The figure shows two trucks, one at 0 to 4 seconds (Truck 1) and one at 7 to 10 seconds (Truck 2), giving very different dynamic deflections due to where the wheel load was applied relative to the sensors.

5.8 Model of Bridge

SAP 2000 Bridge[10] was used to generate a finite element model of the bridge. The deck, girders, abutments modeled as springs and prestressed tendons shown in Figure 5.30 were analyzed; area elements were used for the deck and girders, line elements for the prestressing tendons in the girders and spring elements for the abutments. The

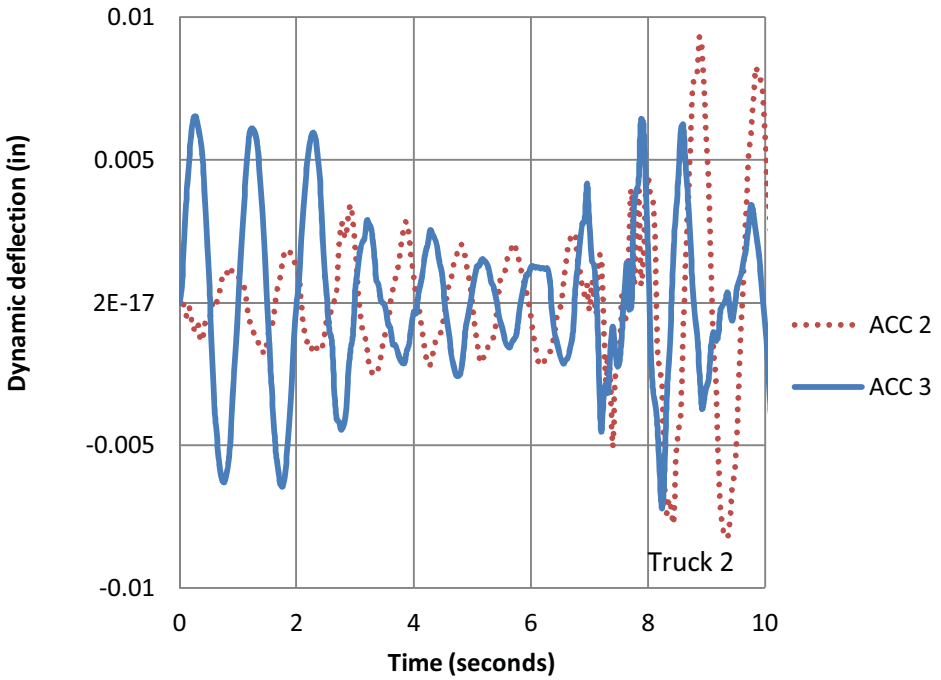

Figure 5.29. Dynamic deflection based on sensor proximity

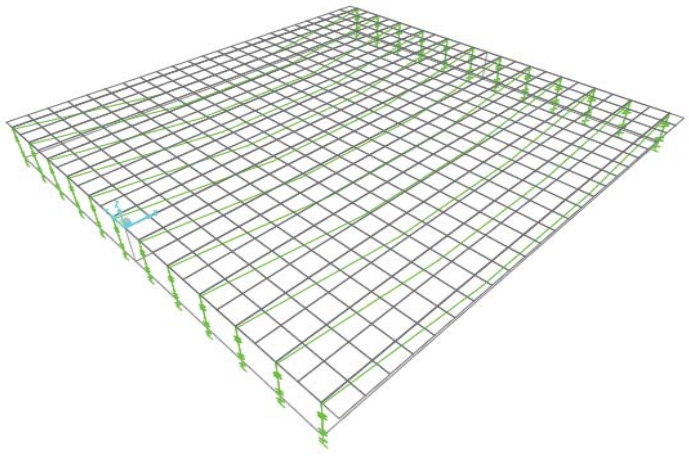

Figure 5.30. Model showing deck, girders and abutments

abutments were modeled as a fixed-fixed integral abutment condition with rotational springs. The connection from the girders to the deck was modeled as a fixed-fixed condition. Material properties used in the model for the compressive concrete strength of the deck and girders were 6200 psi and 7000 psi, respectively. Tendons for the prestressing were modeled as Grade 270 steel and GFRP reinforcement was modeled using #5 bars with an elastic modulus of 5920 ksi and tensile yield strength of 95 ksi. The deck was modeled with GFRP reinforcement at four in. bar spacing. The model contains 52 area elements and 1251 nodes.

The model consisted of area elements that were analyzed using a Hibbler-Hughes time history loading to capture the dynamic effects on the bridge. The model was also used to find static deflections at midspan for various trucks, and to find the impact factor according to Equation 5.2. The 129 kip truck traveling at 68 mph shown in Figure 5.19 was modeled as a time history step function. The modeled truck was placed at midspan in the slow lane. The static deflection shown in Figure 5.31 was 0.225 in.; this occurred over girder 3. Using modeled static deflection information, along with the recorded acceleration data, the impact factor can be calculated for any truck. To find the impact factor, the dynamic displacement is divided by the static displacement. The dynamic displacement for girder 3 for the modeled truck was 0.036 in., giving an impact factor IM of 1.16. This correlates well with the experimental data.

Vertical accelerations can be obtained from the model as well. Using the same model truck and applying a speed and lane location on the bridge, a time history analysis is performed using a direct integration forcing function. Vertical accelerations can then be

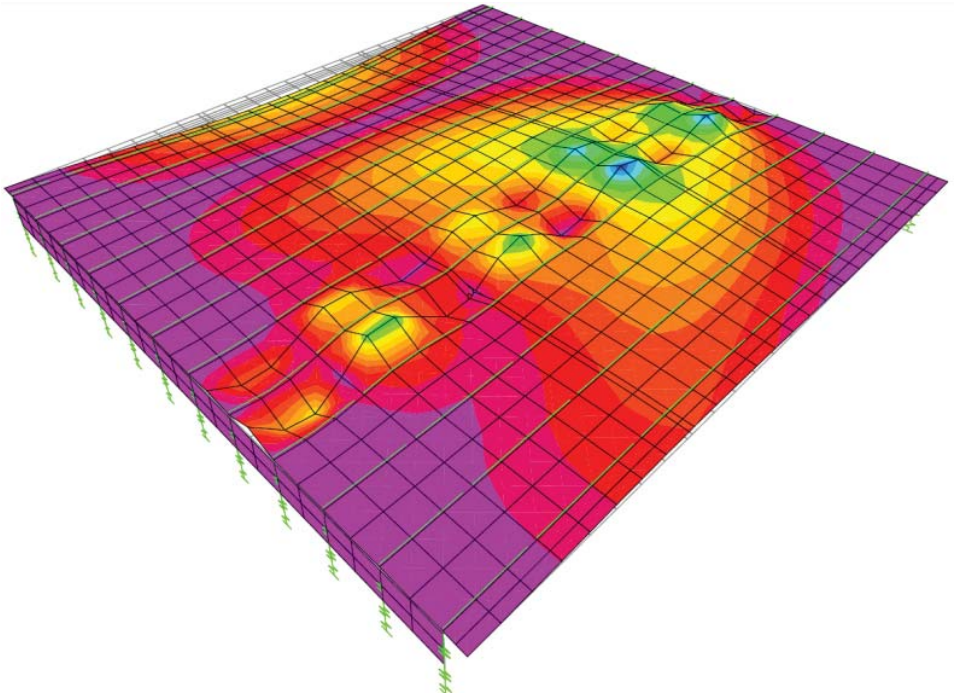

Figure 5.31. Model showing static truck at midspan with 0.225 in. of deflection

plotted at a fixed node against time as shown in Figure 5.32; the response can then be compared to experimental data. The model correlated well with the amplitude of the experimentally obtained acceleration shown in Figure 5.19. This also shows how the accelerometers trigger differently depending on the proximity of the wheel load to the sensor. The time scale in the model is longer compared to the data due to the fact that there is time for the bridge to come to equilibrium in a perfect system; the actual bridge conditions have friction, uneven damping and lateral forces. The model is conservative and predicts on average 25% higher values than the collected data. The collected data and numerical analysis, such as the Newmark-Beta method and logarithmic degradation, did not account for code factors. The collected data are in raw form, whereas the model applies inherent code corrections and phi factors. Additionally, the software does not allow a steel diaphragm between concrete girders; a modular ratio was used for the steel diaphragms to model concrete diaphragms. However, modeled results show a trend and are in a predicted range, as shown in Figure 5.33 comparing experimantal vertical accelerations to modeled vertical accelerations.

Twelve bridge modes were analyzed for the modeled data set and modes 1 and 2 were compared to experimental data. The fundamental period for mode 1 was 0.125 seconds; the period for mode 2 was 0.123 seconds. This period was compared to the period measured during the first truck test, which was approximately 0.12 seconds. Different weights of trucks recorded from ambient tests were modeled; experimental acceleration data were compared to the finite element model shown in Table 5.4 and Figure 5.33. As shown, the single tank truck is similar in weight, number of axles and speed as the box truck, but gives a slightly different response due to axle spacing. These two trucks are

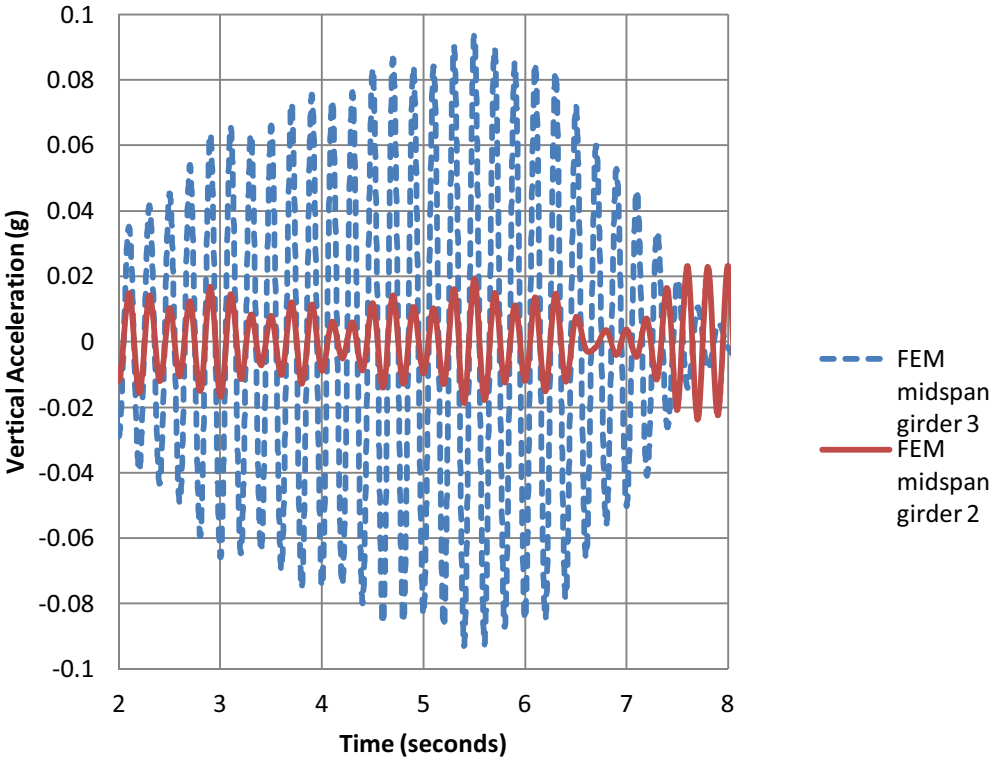

Figure 5.32. Model showing vertical accelerations of the midspan of girder 2 and 3 as a comparison to Figure 5.19

Figure 5.33. Vertical accelerations as a comparison of collected data to the model

Table 5.4. Comparison between experimental accelerations and modeled accelerations

Truck	Length	Speed	Weight	Axles	FEM midspan girder 3	ACC 3	diff	IM
	ft	mph	lbs		g	g	%	
Box Truck	65	64	44480	3	0.023	0.029	20.68966	1.17
Box Truck	65	61	64960	3	0.022	0.034	35.29412	1.11
Single Tank Truck	47	66	79220	3	0.04925	0.06	17.91667	1.04
Box Truck	65	63	78160	3	0.053	0.076	30.26316	1.13
Double Tank Truck	86	68	129380	5	0.0746	0.099	24.64646	1.16

shown also in Table 5.5 to demonstrate the multiple truck effect on the bridge where they are positioned behind each other, in adjacent lanes and on opposite sides of the bridge. When the trucks are trailing each other, the vertical accelerations are high due to sustained inertial forces; when they are on opposite sides of the bridge, the accelerations are low because some of the forces cancel out. A study of axle sequencing was performed and showed that the highest vertical acceleration came from positioning the heaviest axle in the middle of the truck, as shown in Table 5.6.

Statistical modeling was performed to quantify the effects of different variables (speed, total truck weight and axle weight) on the vertical response. More variables in the model yield a higher uncertainty. Two models were developed using STATA/IC 12.0[11] software, one where the axle weight was varied with speed and response held constant and the other where total truck weight was varied with speed and response held constant. The data set included 23 data points and two equations were formed, shown as Equation (5.3) and (5.4).

$$R = 0.0014599S + 5.84E\text{-}7A_1 + 6.04E\text{-}7A_2 - 2.29E\text{-}8A_3 - 1.39E\text{-}7A_4 + 9.66E\text{-}07A_5 - 0.0632924 \quad (5.3)$$

$$R = 0.0013597S + 2.98E\text{-}7W - 0.0534358 \quad (5.4)$$

where R is vertical response, S is speed, A_x is the weight of the xth axle, and W is total truck weight. Equation (5.4) should be used for statistically predicting vertical response; it returned the highest adjusted R-squared value of 0.404. However, the model only considered 23 data points; more research and data would be needed to refine the model.

Table 5.5. Bridge effects with similar weight of trucks traveling at similar speeds

Truck	Length	Bridge position	FEM midspan girder 3	IM
	ft		g	
Box Truck and Single Tank	65 47	Westbound slow lane trailing each other	0.2	1.17
Box Truck and Single Tank	65 47	Westbound slow lane, westbound fast Lane	0.071	1.07
Box Truck and Single Tank	65 47	Westbound slow lane, eastbound slow lane	0.03	1.05

Table 5.6. Box Truck traveling at 64 mph weighing 44 kips with different axle sequence

Axle 1	length 1	Axle 2	length 2	Axle 3	FEM midspan girder 3
lbs	ft	lbs	ft	lbs	g
10860	17	21680	48	11940	0.1
21680	17	10860	48	11940	0.036
11940	17	10860	48	21680	0.012

5.9 Conclusions

Monitoring accelerations is key to understanding the dynamic response and structural health of the bridge. Acceleration data provides insight to truck traffic and dynamic displacements that occurs on the bridge; large displacements may result in dynamic instability and may cause cracking and bridge deterioration. Weight and speed of the trucks, as well as truck axle length and horizontal distance between axles, were correlated with peak accelerations. The maximum accelerations of faster moving trucks traveling between 60 to 70 mph were in general no higher than those at lower speeds of 45 mph to 55 mph. However, the range of speeds for ambient testing in the present research is narrow and more research is needed to observe definitive trends. The research on axle weight and spacing proved that the maximum girder acceleration varied depending on the number of axles and spacing as well as the location of the truck and wheel load in proximity to the sensor. There is a correlation between a greater axle weight of the truck producing greater maximum accelerations at midspan due to impulse forces. It has been shown that trucks weighing 40 kips to 80 kips gave a maximum acceleration of 0.03 g to 0.06 g; however, exception vehicles that are above the legal bridge limit weighing 110 kips to 130 kips consistently gave a maximum acceleration higher than 0.053 g.

From vertical acceleration records, properties of the bridge were found; these include damping, impact factor, period, frequency and dynamic deflections. From the first truck load test, the following characteristic of the bridge are: the fundamental period of 0.12 seconds; the damping ratio of 1.47%; maximum dynamic displacement of 0.031 in. during the September 2009 test over girder 4; and an impact factor in the range of 1.13 to 1.20. The impact factor is below AASHTO code allowance of 1.33, showing that the

loads are within the expected service limit range. Additionally, the bridge and trucks were modeled using finite elements. The model was conservative but correlated with the period of the bridge, dynamic displacements and magnitude of girder accelerations. This study showed that the Beaver Creek Bridge, with precast deck panels reinforced with GFRP, displayed deflections that were within code and design limits. This instrumented bridge could be used to generate more data to refine the understanding of the variables defined in this study.

5.10 Acknowledgments

The author acknowledges the financial assistance of the Utah Department of Transportation, especially Becky Nix. In addition, the author acknowledges Mike Adams from Campbell Scientific. Additional thanks are due to the students, faculty and staff of the University of Utah civil engineering department, especially Jim Ries and Jonathon Wood.

5.11 References

1. American Association of State and Highway Transportation Officials. 2009. *AASHTO LRFD Bridge Design Guide Specifications for GFRP Reinforced Concrete Bridge Decks and Traffic Railings*. 1st Ed. American Association of State Highway Transportation Officials, Washington, DC.

2. Broekhuizen, D. 1996. “Effects of Vertical Accelerations on Prestressed Concrete Bridges.” Thesis. University of Texas at Austin.

3. Lynch J., Wang, Y., Loh, K., Yi, J., and Yun, C. 2006. “Performance monitoring of the Geumdang Bridge Using a Dense Network of High-Resolution Wireless Sensors.” *Smart Mater* 15: 1561–1575.

4. Lau, D., Cheung, M. and Li, W. “Dynamic Monitoring of the Confederation Bridge.” Proceedings *12WCCE 2000* pp.1257.

5. DeWolf, J., Lauzon, R., and Culmo, M. 2002. “Monitoring Bridge Performance.” *Structural Health Monitoring* 1:129.

6. Gangone, M. V., Whelan, M. J., Janoyan, K. D., Minnetyan, L., and Qiu, T. 2010. "Wireless Sensor Performance Monitoring of an Innovative Bridge Design in New York State." *Bridge Maintenance, Safety, Management and Life-cycle Optimization* 420-426.

7. American Concrete Institute Committee 440. 2006. *Guide for the Design and Construction of Structural Concrete Reinforced with FRP Bars (ACI 440.1R-06).* American Concrete Institute, Farmington Hills, MI.

8. Hart, G., and Wong, K., 2000. Structural Dynamics for Structural Engineers. New York, NY.

9. Hag-Elsafi, O., Albers, W. F., and Alampalli, S. 2012. "Dynamic Analysis of the Bentley Creek Bridge with FRP Deck." *Journal of Bridge Engineering* 17(2): 318-333.

10. *SAP 2000*. 2011. Computer software. Vers. 14.2. Computers and Structures Inc. Web.

11. STATA/IC. 2012. Computer software. Vers. 12.0. STATA Inc. Web.

CHAPTER 6

CONCLUSIONS AND FUTURE RESEARCH

6.1 Conclusions

Health monitoring the Beaver Creek Bridge, for more than two years, revealed new knowledge in the area of GRFP applications. The goal of the research was to study if GFRP is an acceptable substitute for steel reinforcement in bridge decks. GFRP bars are noncorrosive but also have a low modulus of elasticity making deflections a concern. At the conclusion of the research, it has been shown that the deflections of the GFRP deck panels and bridge as a whole were well below code limits. Additionally, strains and dynamic deflections were below acceptable code limits as explained by the following statements.

First, the GFRP precast deck panels were evaluated during lifting for stress, strain and deflection. Panels were lifted by straps and cables at four points from below to reduce the shear concentration on the GFRP bars had embeds been used. This lifting layout proved a success; strains were below ACI code limit of 138 με and no cracking was observed. A finite element model was used to analyze the lifting. Results matched well with the collected data and deflections were able to be plotted; analyzed deflections were less than 0.13 in. and below AASHTO code limit of span/800 or 0.62 inches. Various two point lifting configurations were analyzed in the model, which exceeded code deflection limits.

Secondly, programs were developed in conjunction with a vendor that allowed for the quick assessment of the critical elements of the bridge for inspection. The application of the vendor's software was used to assess how changes in the responses of the elements of the bridge lead to a better and quicker assessment of the "health" of the bridge by converting raw collected data into strains, deflections and accelerations that could be compared to code limits and design assumptions. Additionally, the bridge was instrumented in a way that remote data could be acquired to monitor critical elements of the bridge that would indicate the condition of the structure, specifically the inclusion of real time dynamic responses. Software was used for remote monitoring through a secure IP address from the bridge to the University of Utah research laptop. By monitoring remotely, collected data were assessed to determine the influence of weather conditions and truck traffic. Truck traffic was able to be captured real time on screen as well as an event triggering traffic camera.

Over the course of 2 years strains, static deflections and dynamic deflections were found to be within code limits and live load distribution factors were below AASHTO's recommendations. The maximum strain recorded was 121 με; this is below that tensile cracking limit 138 με. The maximum deflection on the bridge was 0.17 inches which is below the allowable deflection of span/800 or 1.32 inches.

Third, the dynamic properties of the structure were determined with the instrumentation that was operational at the bridge. From collected data structural damping, dynamic displacements and impact factors were calculated. Damping was calculated by logarithmic degradation and showed a damping of less than 2%. Vertical accelerations were transformed to dynamic displacements using the Newmark-Beta

method. Dynamic displacements obtained from the Newmark-Beta method and the SAP 2000 model were significantly lower than the static displacements that were obtained by survey data before the bridge opened to traffic and by the SAP 2000 model. Dynamic displacements were approximately 0.02 in.; static displacements were less than 0.2 in. and below code requirements. Impact factors were calculated to be in the range of 1.15-1.2, compared to AASHTO's code allowance of 1.33. This showed the bridge to be dynamically stable and AASHTO to be conservative.

Fourth, from collected acceleration data, hypotheses were formed regarding the weight and speed of a particular truck and the impact if there are multiple trucks on either side of the bridge. From acceleration data, the speed variation was too narrow to draw conclusive trends. The maximum girder acceleration varied depending on the number of axles and spacing as well as the location of the truck and wheel load in proximity to the sensor. There is a correlation between a greater weight of the truck producing greater maximum accelerations at midspan due to impulse forces. However, most responses above 0.06g come from special permit vehicles that typically weigh 120 kips. Trucks with similar weight on opposite sides of the bridge or even adjacent lanes produced a very different response than those similar weight trucks trailing each other in the same lane. Multiple trucks in the same lane prolong impulse loading and generated a higher response.

Fifth, from the collected data a finite element model was produced. From the model, improvements for future construction were made in terms of number of girders and deck thickness. By checking deflection and stresses, the modeled bridge could be built using ten AASHTO III girders with an 8 in. deck. However, service limits were checked only

for stresses and deflection and a full analysis would need to be made for construction. Analysis was performed to demonstrate the effects of multiple trucks on the bridge, those going in the same direction and those going in the opposite direction, by the use of a finite element model confirm the coupling effect from the closure pour. Selected trucks were modeled as finite elements in various positions on the bridge to check the stability of the cast-in-place closure. Twelve significant mode shapes were found for the model. Mode 1 in the vertical direction dominated and showed strong composite action between the deck and girders. Mode 2 and 4 in the horizontal direction showed strong force transfer at the closure pour linking both phases. Accelerations from the finite element model were compared to collected data. The model showed, in general, a 20-35% consistent difference from the collected data. The model has built-in code factors for a margin of safety; the raw data and numerical analysis, such as the Newmark-Beta method and logarithmic degradation, did not account for code factors.

6.2 Future Research

This research monitored GFRP corrosion by tensile cracking limits; if the bridge deck was not cracked, by assumption there was no pathway for corrosion. In the future, monitoring corrosion in the deck bars with chemical testing over time would provided better reassurance in GFRP noncorrosive attributes.

As stated, vertical accelerations are important to monitor because of the motion in the girder seat. This research monitors the accelerations but does not test or monitor the girder seat movement. Future research should monitor the girder seat for slippage at the haunch due to vertical accelerations.

Additionally, a statistical program using probability to ascertain where the truck is, lane wise, and how many trucks are present from the acceleration signatures would be very useful for department of transportation agencies. The program could also be developed in a way that could predict the weight and speed of the trucks by the vertical acceleration signal given off by the accelerometers. For future research, an expansion of the collected speed range would have to occur to make definite conclusions.

Lastly, by using impact factors and accelerometer axle data, pavement analysis may be researched. Impact factors may give insight into the longevity of the pavements and future wear and tear of the bridge surface.